

# **Mt Holland Earl Grey TSF2**

## **Groundwater Model**

---

Prepared for Covalent Lithium

May 2025

# Mt Holland Earl Grey TSF2

## Groundwater Model

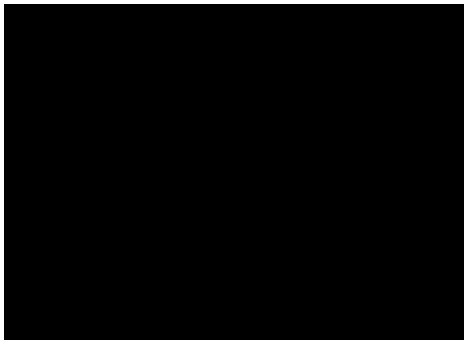
Covalent Lithium

E240786 RP1

May 2025

Version	Date	Prepared by	Reviewed by	Comments
1	12 May 2025			Final
2	19 May 2025			Final

Approved by



Suite 3.03  
111 St Georges Terrace  
Perth WA 6000  
ABN: 28 141 736 558

This report has been prepared in accordance with the brief provided by Covalent Lithium and, in its preparation, EMM has relied upon the information collected at the times and under the conditions specified in this report. All findings, conclusions or recommendations contained in this report are based on those aforementioned circumstances. This report is to only be used for the purpose for which it has been provided. Except as permitted by the *Copyright Act 1968* (Cth) and only to the extent incapable of exclusion, any other use (including use or reproduction of this report for resale or other commercial purposes) is prohibited without EMM's prior written consent. Except where expressly agreed to by EMM in writing, and to the extent permitted by law, EMM will have no liability (and assumes no duty of care) to any person in relation to this document, other than to Covalent Lithium (and subject to the terms of EMM's agreement with Covalent Lithium).

© EMM Consulting Pty Ltd, Ground Floor Suite 01, 20 Chandos Street, St Leonards NSW 2065. 2025.  
ABN: 28 141 736 558

## Executive Summary

Covalent Lithium Pty Ltd (Covalent), as part of its Revised Proposal under the *Environmental Protection Act 1986*, commissioned the development of a numerical groundwater model to assess the impacts of expanded mining activities and the addition of a second tailings storage facility (TSF2) at the Mt Holland site. The modelling was required to inform the environmental impact assessment process and respond to the Office of the Environmental Protection Authority's (oEPA) request for additional information on potential inland water impacts, particularly from TSF seepage and pit dewatering.

The groundwater model was developed using MODFLOW-USG, supported by Groundwater Vistas graphical user interface, and constructed in accordance with the Australian Groundwater Modelling Guidelines (Barnett et al. 2012). The model incorporated site-specific geological, hydrological, and operational data, with a particular focus on evaluating predictive head drawdown from the Earl Grey Lithium pit, seepage fate from TSF1 and western and eastern sides of TSF2, and long-term recovery behaviour post-mining. A probabilistic uncertainty analysis (PUA) was employed to account for data limitations and conceptual uncertainties.

Model history matching performance for the modelled groundwater levels showed a SRMS of 0.76%, a residual mean of 0.02 metres (m) and a mean absolute error of 0.06 m. The model has been classified as Class 1 under the Australian Groundwater Modelling Guidelines reflecting the duration of monitoring data, spatial coverage and assumptions. Consequently, the model has been classified as Class 1 under the Australian Groundwater Modelling Guidelines—indicating low predictive confidence, suitable for early-stage assessments in data-scarce environments.

Key findings are that groundwater drawdown is expected to extend north-south, aligned with a structurally-controlled Shear zone, that is inferred to have relatively higher permeability in contrast to surrounding lithology. TSF seepage-induced mounding of up to 70 m primarily occurs beneath TSF2 east, and to a lesser extent beneath TSF1 and TSF2 west, 50 m and 30 m respectively, mainly due to the presence of a thick and relatively higher-conductive Saprock unit beneath them.

At the end of the 100-year post-closure period, a Earl Grey Lithium pit is predicted with a water level that stabilises at 264 m Australian Height Datum (AHD), resulting in a permanent terminal sink. Mounding beneath TSF1 persists, influenced by its location within a low-permeability zone, while mounding beneath TSF2 dissipates over time due to the presence of Saprock unit which accelerates the vertical water movement.

Modelling confidence will be further improved with expanding the groundwater monitoring network, particularly around TSF1 and residual mounding zones; conducting site-specific hydrogeological investigations to refine parameter estimates; expand the model domain to better capture regional-scale processes; enhancing geological and hydrogeological mapping of the ore body, especially of structural features such as the Shear zone; and revisiting predictions as new post-mining data becomes available.

This model serves as a vital decision-support tool for assessing groundwater risks and informing future management strategies, particularly around long-term groundwater levels.

# TABLE OF CONTENTS

---

<b>Executive Summary</b>	<b>ES.1</b>
<b>1 Introduction</b>	<b>1</b>
1.1 Background and context	1
1.2 Modelling objectives	1
1.3 Modelling scope	2
1.4 Model confidence classification and adherence to best practice guidelines	2
<b>2 Hydrogeological conceptual model</b>	<b>4</b>
2.1 Environmental setting	4
2.2 Regional geology	6
2.3 Hydrogeology	10
2.4 Groundwater quality	17
2.5 Groundwater discharge	17
2.6 Groundwater sensitive receptors	17
<b>3 Model design</b>	<b>18</b>
3.1 Software	18
3.2 Domain and spatial discretisation	18
3.3 Temporal discretisation	21
3.4 Regional groundwater flow	21
3.5 Existing mine-related activities	22
<b>4 History-matching</b>	<b>24</b>
4.1 Approach	24
4.2 Results	29
4.3 Adopted parameters	33
<b>5 Predictions</b>	<b>39</b>
5.1 Overview and objectives	39
5.2 Scenario definition and representation	39
5.3 Results	40
<b>6 Limitations</b>	<b>51</b>
<b>7 Summary and recommendations</b>	<b>52</b>
<b>References</b>	<b>53</b>

## Appendices

Appendix A	Hydrographs	A.1
------------	-------------	-----

### Tables

Table 1.1	Evaluation of model confidence level classification (after Barnett et al. 2012)	3
Table 2.1	Estimated hydraulic conductivity of local lithology	14
Table 2.2	Water level variability between December 2024 to March 2025	16
Table 3.1	Model stress periods	21
Table 4.1	Monitoring bore details	24
Table 4.3	Conceptual hydraulic parameter values	27

### Figures

Figure 2.1	Monthly rainfall and evaporation for years January 1960 to December 2024	4
Figure 2.2	Mean annual rainfall and cumulative deviation from mean	5
Figure 2.3	Interpreted basement geology (after GSWA 1:100,000 scale mapping)	7
Figure 2.4	Simplified regolith (after GSWA 1:500000 scale regolith map)	9
Figure 2.5	Groundwater bore network and aquifer testing sites	12
Figure 2.6	Pre Lithium mining conceptual potentiometric heads	13
Figure 2.7	Groundwater levels against SILO gridded rainfall for Mt Holland	16
Figure 3.1	Model domain (vertical exaggeration x 5)	18
Figure 3.2	Model mesh (vertical exaggeration x 1)	19
Figure 3.3	Model layers and hydrostratigraphic units (vertical exaggeration x 10)	20
Figure 3.4	Constant head boundary conditions (vertical exaggeration x 5)	22
Figure 3.5	Current mine plan – DRN cells (vertical exaggeration x5)	22
Figure 4.1	Target locations (vertical exaggeration x 5)	26
Figure 4.2	Pilot points distribution (vertical exaggeration x 10)	28
Figure 4.3	Comparison between simulated potentiometric heads and conceptual contours for steady-state	30
Figure 4.4	Average measured head compared and the simulated ensemble	31
Figure 4.5	Modelled posterior distribution of total dewatered void volumes.	32
Figure 4.6	Water balance during history matching period	32
Figure 4.7	Parameter distributions – Horizontal conductivity – Whole ensemble	34
Figure 4.8	Parameter distributions – Specific storage – Whole ensemble	35
Figure 4.9	Parameter distributions – Specific yield – Whole ensemble	36
Figure 4.10	Spatial distribution of adopted hydraulic conductivity – percentile 50 of the total of realisations (vertical exaggeration x 5)	37
Figure 4.11	Spatial distribution of adopted specific storage – percentile 50 of the total of realisations (vertical exaggeration x 5)	37

Figure 4.12	Spatial distribution of adopted specific yield – percentile 50 of the total of realisations (vertical exaggeration x 5)	38
Figure 5.1	Updated mine plan – DRN cells (vertical exaggeration x 5)	39
Figure 5.2	Water balance during predictive period	40
Figure 5.3	Predicted seepage from the TSF1 during the operation	42
Figure 5.4	Predicted modelled dewatering to Earl Grey	43
Figure 5.5	Potentiometric heads change (drawdown/mounding) at the end of the operations (P10)	45
Figure 5.6	Potentiometric heads change (drawdown/mounding) at the end of the operations (P50)	46
Figure 5.7	Potentiometric heads change (drawdown/mounding) at the end of the operations (P90)	47
Figure 5.8	Potentiometric heads change (drawdown/mounding) 100 years after mine closure (P50)	49
Figure 5.9	Potentiometric heads 100 years after mine closure (P50) – particle tracking	50

# 1 Introduction

## 1.1 Background and context

Covalent Lithium Pty Ltd (Covalent) is the manager appointed by a joint venture between subsidiaries of Sociedad Química y Minera de Chile S.A. (SQM) and Wesfarmers Limited to develop and operate the Earl Grey Lithium Project (the Project) via mining and processing lithium at the Mt Holland mine site, located approximately 380 kilometres (km) directly (or 445 km by road) east of Perth.

The Project was granted environmental approval in November 2019 under the *Western Australian Environmental Protection Act 1986* (EP Act) through Ministerial Statement 1118, and in February 2020 was granted approval under the *Environment Protection and Biodiversity Conservation Act 1999* (EPBC Act) through EPBC Decision 2017/7950. Following these initial environmental approvals, the Project has been amended under the EP Act through Ministerial Statement 1167 (change to implementation conditions), Ministerial Statement 1199 (change to Proposal), and under the EPBC Act through EPBC Decision 2017/7950 approval variations (change to Proposal and implementation conditions).

Covalent is currently seeking approval to expand the current operations to accommodate Life of Mine (LOM) infrastructure and to duplicate processing infrastructure to increase nameplate capacity to 4 million tonnes per annum (Mtpa) and with debottlenecking expansion, up to 4.4 Mtpa. In accordance with Section 38 of the EP Act, Covalent submitted a Referral for the proposed changes as a 'Revised Proposal' (Significant Amendment) for the purpose of an environmental impact assessment. On receipt of this referral the Office of Environmental Protection Authority (oEPA) have requested further Information from Covalent on the potential for impacts to inland waters before assessment of the 'Revised Proposal' can proceed.

As part of the further information, the oEPA requested among other aspects, the development of a hydrogeological numerical model to include the tailings storage facility 2 (TSF2), and the discussion of any potential impacts to inland waters that would result from brine disposal.

The groundwater numerical modelling exercise was conducted in accordance with:

- Barnett et al 2012, *Australian groundwater modelling guidelines*.

## 1.2 Modelling objectives

To address potential impacts associated with the implementation of TSF2 and the updated mining plan, the following modelling objectives were established:

- Evaluate the historic and future changes on the water balance of the groundwater system, including the following:
  - Seepage from TSF1 and proposed TSF2.
  - Groundwater inflows to the Earl Grey Lithium mine void.
  - Lateral groundwater flow at the boundaries of the model domain.
- Assess the cumulative impacts to groundwater levels from proposed water management activities, specifically derived from TSF seepage and groundwater inflows to the Earl Grey Lithium mine void.

### 1.3 Modelling scope

The modelling scope of this project included:

- Model build:
  - Provide a conceptual site model for the hydrogeology.
  - Build a groundwater numerical model that reflects the above conceptualisation.
  - Consider the geometry of the geological features, boundary conditions, mining dewatering and TSFs.
- History matching:
  - History matching performance (SRMS, residuals, absolute residual) against the measured water levels at monitoring bores and dewatering volumes from the Earl Grey pit.
  - Parameterise the hydraulic parameters in the hydrostratigraphic units and assess the posterior distributions compared the conceptual ranges.
  - Water balance during the history matching phase.
- Predictions:
  - Water balance during the operations and recovery period.
  - Timeseries of seepage from modelled facilities: TSF1 and TSF2.
  - Timeseries of total modelled inflow (dewatering) to Earl Grey for percentiles (p) of p10, p33, p50 p67 and p90.
  - Timeseries of seepage from modelled facilities: TSF1 and TSF2 (west and east sides).
  - Modelled drawdown, in plain view, at the end of the project of p10, p50 and p90 case and 100 year recovery period post operations for the water table.
  - Modelled hydrographs, in an appendix, for all bores that have sufficient temporal record.
  - Water balance during the operations and recovery period.

### 1.4 Model confidence classification and adherence to best practice guidelines

The groundwater model was conducted in accordance with the *Australian Groundwater Modelling Guidelines* (Barnett et al. 2012). In this regard, the modelling objectives outlined in Section 1.2 require prediction of impacts from the Project, as well as predictions of leakage from the TSFs, groundwater level change and groundwater inflows into the open pit locally as a result of operation of the Project. To achieve this outcome, the following technical aspects related to model complexity have been considered:

- Regional simplicity of the main hydrostratigraphic units with simplified mesh discretisation.
- Simpler model layering in areas distant from the project infrastructure to capture main hydrostratigraphic units only.
- Local detail in and around Project components such as the open pit and the TSFs.

- Because of the remote nature of the site and lack of temporal groundwater level data for the history matching period, the groundwater modelling workflow has embraced probabilistic predictive uncertainty analysis (PUA) to accommodate some of the limitations in the spatial and temporal baseline data and conceptual understanding. The PUA was implemented to explore the potential uncertainty envelope of predictions of temporal groundwater level change including drawdown/mounding, leakage from the TSFs, and inflows into the open pit.

The *Australian Groundwater Modelling Guidelines* (Barnett et al. 2012) developed a system to classify the confidence level for groundwater models. Models are classified as Class 1, Class 2 or Class 3 in order of increasing confidence based on key indicators such as available data, calibration procedures, consistency between calibration and predictive analysis and level of stresses. The three classes of model are defined as:

- Class 1 – low confidence in model predictions, suitable for use in low value resource or low risk developments.
- Class 2 – medium confidence in model predictions, suitable for use in projects with medium to high risk developments.
- Class 3 – high confidence in model predictions, suitable for use in high value resources and projects such as regional sustainable yield assessments.

Groundwater modelling conducted for the Project aligns best with the criteria for a low confidence level (Class 1), with the majority of the features being low confidence. The following key indicators, based on Table 2-1 of Barnett et al. (2012), are summarised in Table 1.1.

**Table 1.1 Evaluation of model confidence level classification (after Barnett et al. 2012)**

Data	Class	Calibration/ History-matching	Class	Prediction	Class	Key indicator	Class
Few or poorly distributed existing wells from which to obtain reliable groundwater and geological information. The new bores are well distributed however, the temporal data is very limited. The other existing bores shown very variable levels without and lack of construction details.	1	Calibration is based on an inadequate distribution of data. Not enough temporal data.	1	Predictive model time frame far exceeds that of calibration.	1	Model predictive time frame is more than 10 times longer than transient calibration period.	1
Records of groundwater extraction.	2	No calibration was possible in many points as they did not align with the conceptual heads.	1	Transient predictions were conducted without enough temporal data for the calibration.	1	Stresses in predictions are more than 5 times higher than those in calibration (increase of the area and depth of the open pit).	1

## 2 Hydrogeological conceptual model

The hydrogeological conceptual model for the Covalent Lithium Project defines the primary geological layers, hydrostratigraphic units, aquifer characteristics, groundwater flow behaviour, boundary conditions, and key assumptions. This model is essential for the development of a numerical groundwater model that will assess groundwater conditions pre-mining and potential operational and post-mining impacts.

The project area is divided into two hydrographic catchments, separated by a surface water sub-catchment divide. The northwestern catchment exhibits a topographic gradient towards the north, with inferred hydraulic gradients following a north-westward direction in the upper section and an east-north-eastward direction in the lower southern section.

### 2.1 Environmental setting

#### 2.1.1 Climate

Precipitation gauge records are available from three sites located near the study area (Surface water solutions, 2023):

- Mulgara (ID 12298) – 49 km NW of the Study Area, 37 years of data between 1984 and 2021.
- Lake Carmody (ID 10670) – 54 km SW of the Study Area, 114 years of data between 1906 and 2021.
- King Rocks (ID 10581) – 62 km WSW of the Study Area, 89 years of data between 1930 and 2019.

The available local rainfall records are limited in terms of proximity and continuity of record over the recorded period. Therefore, rainfall and associated climate data for the study area was downloaded from the Queensland government’s Scientific Information for Land Owners (SILO) database (Queensland DES 2023). The SILO database provides spatial and temporal interpolation of gauge records to estimate local precipitation and pan evaporation (Jeffrey et al., 2000). Based on SILO grid data for the Earl Grey site from January 1960 to December 2023, the average annual precipitation is 351 millimetres per year (mm/yr), and average annual pan evaporation is 2,007 mm/yr (i.e. annual evaporation greatly exceeds annual rainfall).

Class A pan evaporation and monthly rainfalls for January 1960 to December 2023 are presented in Figure 2.1.

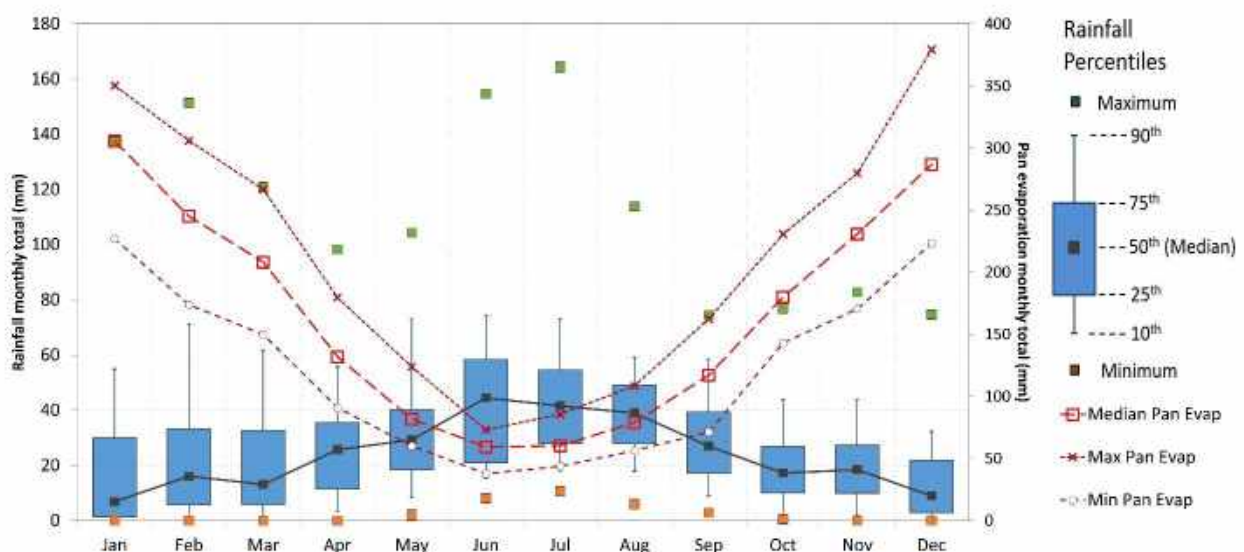
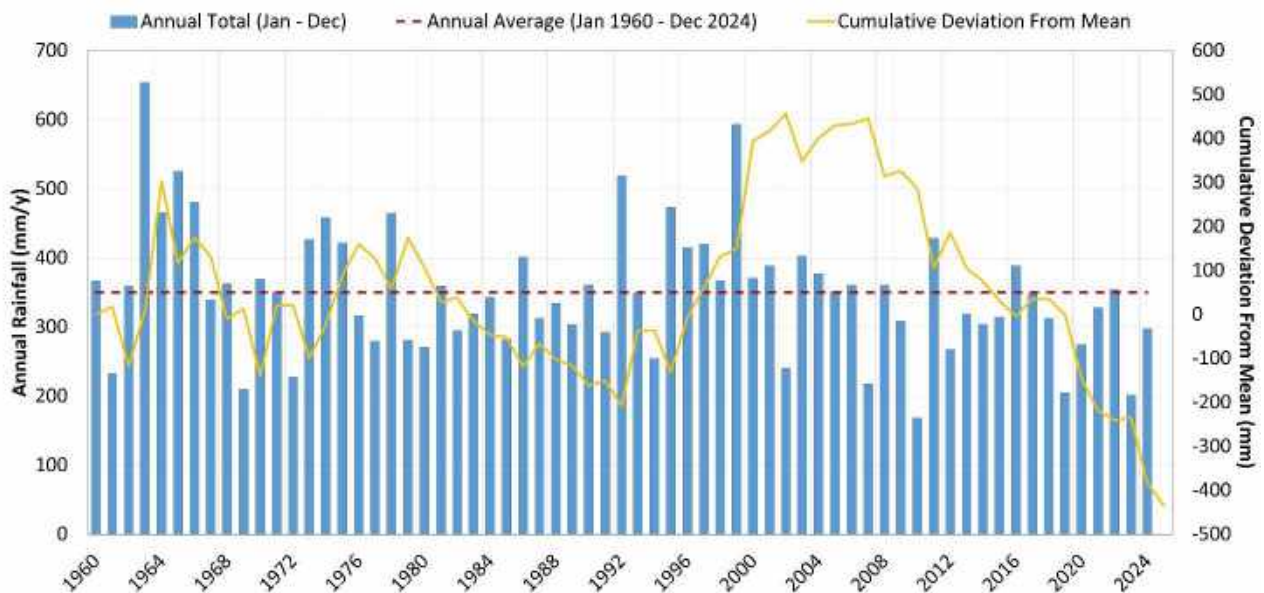


Figure 2.1 Monthly rainfall and evaporation for years January 1960 to December 2024

Long-term SILO data extracted at the project area indicates the median annual rainfall from 1960 to 2024 is 349 mm, very similar to the mean, and shows a moderate level of inter annual variability ranging from a minimum of 169 mm (2010) to a maximum of 654 mm (1963). The wettest months are the winter months, between June and July, although monthly average rainfall is relatively low throughout the year. Surface runoff flows are intermittent and generally of short duration, following large rainfall events only.

Mean monthly Class A pan evaporation exceeds mean monthly rainfall for all months except for June to August. Over the summer months pan evaporation exceeds mean monthly rainfall by an order of magnitude, and as such perennial surface water bodies in the area are uncommon. The high rate of evaporation plays a major role in the formation of salt lakes and saline groundwater within the wider area.

Annual rainfall totals and the cumulative deviation from mean (CDFM) rainfall from 1960–2024 are presented in Figure 2.2. The CDFM curve provides a summary of the deviation of annual rainfalls relative to the annual average rainfall for the period (1960–2024). This slope helps characterise periods of drought (decreasing CDFM trend) and wet conditions (increasing CDFM trend). Note that the CDFM approach assumes a level of stationarity and consistency of both the rainfall average and rainfall distribution (i.e. the prevailing climate regime) across the assessment period. The annual rainfall summary indicates the trend since the mid-2000s to the present has been one of a drying climate. The rainfall record highlights a relatively high level of natural year on year rainfall variability.



**Figure 2.2 Mean annual rainfall and cumulative deviation from mean**

### 2.1.2 Regional hydrology

The Earl Grey site is located within the Swan Avon – Yilgarn River catchment in the Avon River Basin as mapped by the WA Department of Water and Environmental Regulation (DWER). The Project site spans a sub-catchment divide, with the western portion of the site located within the 4,094 km<sup>2</sup> Yellowdine sub-catchment and the eastern portion located within the 7,582 km<sup>2</sup> Lake Eva sub-catchment. Both sub-catchments drain to the north and are characterised by discontinuous chains of salt lakes along valley floors.

Owing to the semi-arid climate both sub catchments are ephemeral and only flow after rare, significant rainfall events. Further information on rainfall intensity and flood frequency is provided within Surface Water Solutions (2023).

## 2.2 Regional geology

The Project is located within the Youanmi Terrane, of the Yilgarn Craton (Doublier et al, 2012). It comprises an elongated, north striking (in the south) belt of Archean greenstones between granitoid and gneissic dome complexes (Keats 1991). The regional structure is dominated by east-northeast compressional deformation associated with the emplacement of the granitoid rocks with resultant shear zones cross cutting and displacing the north trending greenstone belt.

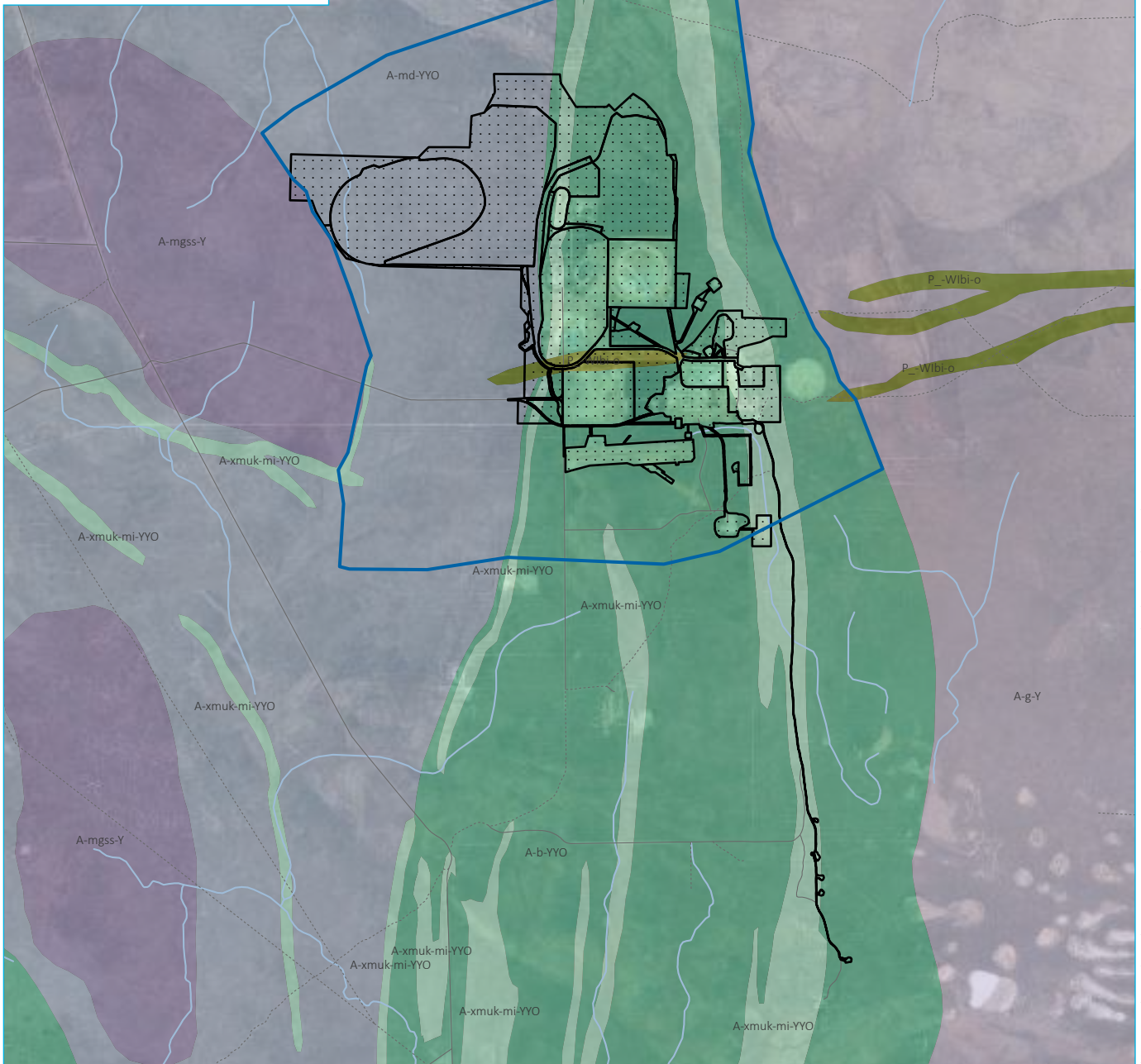
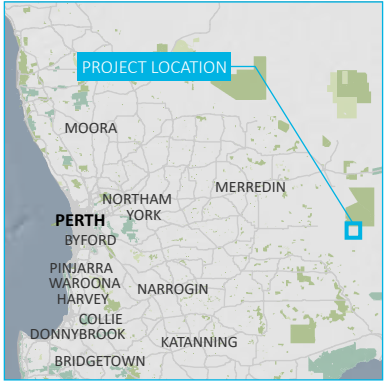
Local arcuate greenstone belts wrap around granitoid domes to the north of Earl Grey as a direct consequence of granitoid intrusions (Keats 1991). The Archean basement rocks have been intruded by numerous west-southwest trending dolerite dykes of Proterozoic age.

The Youanmi Terrane has undergone amphibolite facies metamorphism, which has commonly caused total loss of original rock textures. This, coupled with the poor outcrop in the area, means detailed stratigraphic reconstruction is problematic (Keats 1991). The greenstone comprises an upper and lower sequence separated by a major unconformity. The lower sequence comprises a volcanic succession up to 5 km thick consisting of tholeiitic and komatiitic basalt, the latter dominating the upper part of the volcanic succession (Doublier et al. 2012). Two north south trending semi continuous zones of banded iron formation (BIF) occur within the lower volcanic sequence associated with ultramafic volcanics in the area (Keats 1991; Doublier et al. 2012).

The upper sequence of the greenstone belt comprises clastic sedimentary rocks up to 2 km thick (Doublier et al, 2012). The sedimentary sequence is represented by basal black shale overlain by a mixed sequence of psammitic and pelitic units with minor quartzite and meta-conglomerate (Doublier et al, 2012).

The dominant structural controls in the region include north-northwest trending shear zones, which have played a significant role in both the emplacement of pegmatites and post-mineralization deformation. These structures have also influenced groundwater flow and secondary porosity development in fractured rock aquifers.

The simplified regional basement geology is presented in Figure 2.3.



Source: EMM (2025); Landgate (2021, 2025); Esri (2025); GA (2009)

- KEY**
- Model extent
  - Mine layout
  - Existing environment
  - Minor road
  - Vehicular track
  - Named watercourse

State interpreted bedrock geology (1:500,000)

- Binneringie Dyke; Dolerite and gabbro; includes cumulate and granophyric differentiates (P\_-Wibi-o)
- Yilgarn Craton granites; Foliated metagranite, locally gneissic; may include amphibolite lenses; includes deeply weathered rock (A-mgss-Y)
- Yilgarn Craton granites; Granitic rock, undivided; metamorphosed (A-g-Y)

- Youanmi Terrane greenstones; Metakomatiite, metachert, and metamorphosed banded iron-formation (A-xmuk-mi-YYO)
- Youanmi Terrane greenstones; Mafic volcanic rock with minor mafic and ultramafic intrusive rocks; subordinate felsic rocks; metamorphosed (A-b-YYO)
- Youanmi Terrane greenstones; Metasedimentary rock, undivided; includes metamorphosed sandstone, siltstone, shale, and chert; commonly deeply weathered (A-md-YYO)

### Interpreted basement geology (after GSWA 1:100,000 scale mapping)

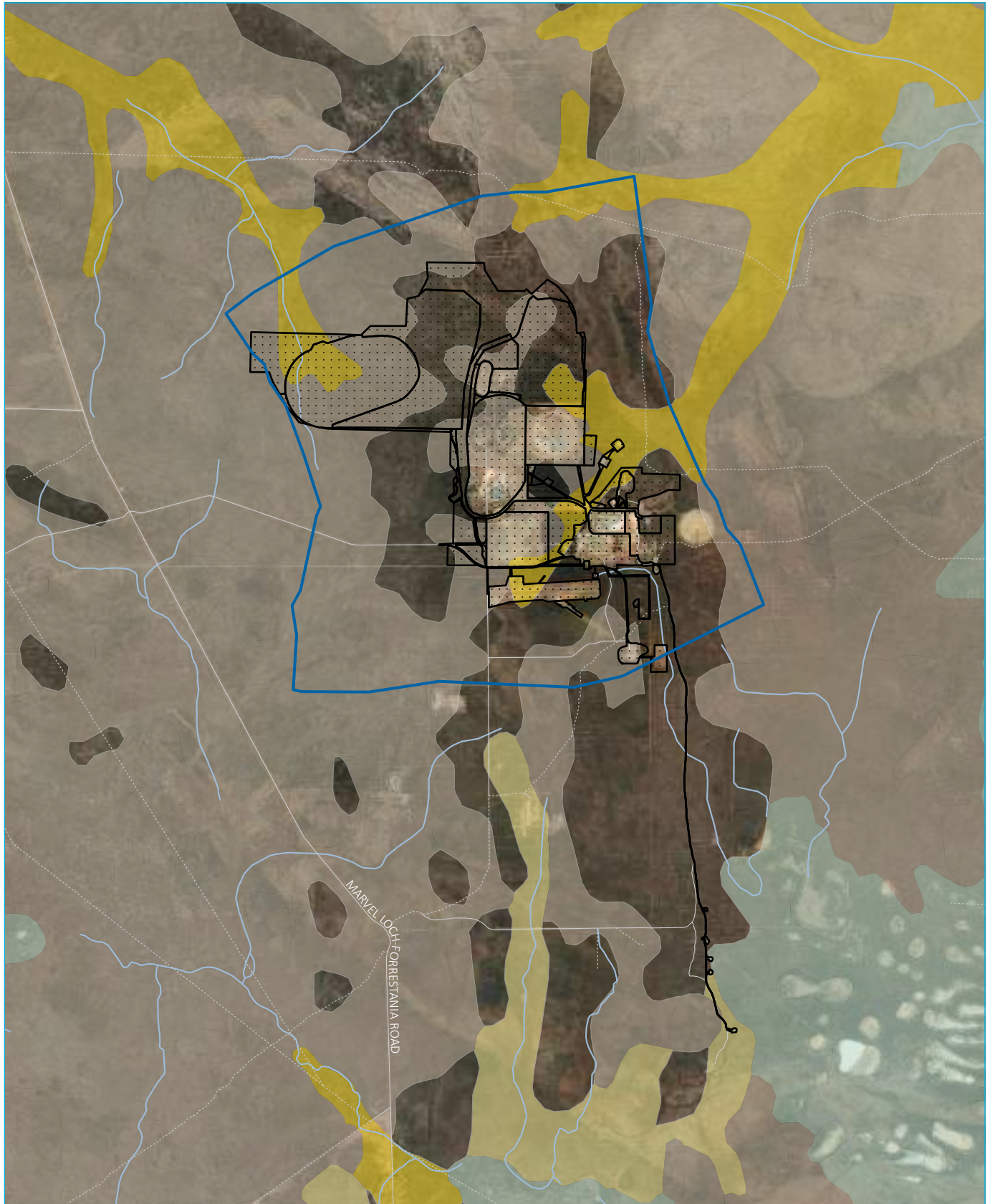
Covalent Lithium  
Mt Holland Earl Grey TSF2 Groundwater Model  
Figure 2.3



\\emmm.local\vdrrive\2024\E240786 - Mt Holland Earl Grey TSF2 groundwater model\GIS\02\_Maps\GWM\GWM007\_InterpretedBasementGeology\_20250512\_01.aprx\_16/05/2025

The Archean basement rocks are transgressed by palaeo-drainage features comprising valley and channel landforms that have been in existence since the Mesozoic era (252 to 66 million years ago) (Magee 2009). Playas with thin evaporite covers have developed in many palaeovalleys in response to increasing aridity and evolution of saline groundwater. The playas and salt lakes are active landscape elements and are considered sites of significant groundwater discharge with negligible sediment accumulation. Modern, poorly defined, ephemeral drainage connects some playas, but these only flow in extreme rainfall events.

An extensive deep weathering profile within the Archean basement rock occurs adjacent to the Cenozoic filled palaeovalleys (Commander *et al* 1992). The weathering profile, referred to as the regolith, comprises extensively leached, white saprolitic clay overlaying deeply weathered saprock with relict rock textures, particularly over granitic weathering profiles. The weathered profile can be up to 80 m deep beneath overlying Quaternary cover. The simplified regolith cover overlying the interpreted basement rock is provided in Figure 2.4. It is noted that most of the development envelop is over exposed bedrock with poorly developed drainage.



Source: EMM (2025); Landgate (2021, 2025); Esri (2025); GA (2009)

KEY

- |                           |                                    |
|---------------------------|------------------------------------|
| Model extent              | 1:500k State regolith geology      |
| Mine layout               | Colluvial unit (Quaternary)        |
| Existing environment      | Alluvial/fluvial unit (Cenozoic)   |
| Minor road                | Lacustrine unit (Cenozoic)         |
| Vehicular track           | Residual or relict unit (Cenozoic) |
| Watercourse/drainage line | Exposed unit (Archean-Proterozoic) |

Simplified regolith  
(after GSWA 1:500000 scale regolith map)

Covalent Lithium  
Mt Holland Earl Grey TSF2 Groundwater Model  
Figure 2.4



\\emml.local\drive\2024\E240786 - Mt Holland Earl Grey TSF2 groundwater model\GIS\02\_Maps\_GWM\GWM008\_SimplifiedRegolith\_20250512\_01.aprx 16/05/2025

## 2.3 Hydrogeology

### 2.3.1 Aquifer Types

The project lies within the eastern Yilgarn Palaeovalley designated as the Watsonia Groundwater Management Subarea of the Watsonia Groundwater Management Area (GMA). The DWER Water Register recognises four principal aquifer types within the Watsonia Groundwater Management Subarea: alluvium, calcrete, palaeochannel and fractured rock aquifers. DWER split these four aquifer types within the Watsonia subarea across two districts, the “Combined Fractured Rock West” and “Palaeochannel” districts.

The main groundwater sources in the region are derived from:

- Regional, topographic catchment-controlled systems in fresh and weathered fractured rock.
- Cenozoic filled paleochannel sands (not identified within the development envelop).
- Carbonate or siliceous caprock units that commonly overlie palaeovalleys or develop over deep saprolitic weathering profiles.
- Shallow alluvium.

Based on RC exploration drilling and bore installations across Earl Grey there is between 2–10 m of colluvium cover. Given the location of the project at a surface water sub-catchment divide, there is no evidence of groundwater within the colluvium and it is assumed to be unsaturated. Beneath the colluvium cover there is a deeply weathered, saprolite clay derived from the in-situ weathered parent fractured rock. The saprolite is of variable thickness contingent on the weathering and weathering products of the parent rock types.

Beneath the saprolite is a saprock with relict texture of the parent rock associated with either greenstone or granitic rock types. The saprock is more developed in the northwest catchment and is somewhat absent in the east. Groundwater was found towards the base of the saprock profile, first water strikes and intersects were generally 30 to 40 m lower than the eventual potentiometric head at roughly 60 m below ground level (bgl) or within fractured bedrock where weathering profiles were shallow.

Fractured rock aquifers tend to be limited in extent with water supplies generally contained in localised structurally controlled zones with limited storage. Yields from fractured rock aquifers can decrease rapidly and are generally less reliable and less sustainable than those obtained from palaeochannel sands. Within greenstone rocks of the Youanmi Terrane, groundwater has been found close to major lineaments, shear zones, deeply oxidised zones, within the saprock profile, and where fractures occur in competent quartzites and BIF (Aquaterra, 2008).

The deep weathering profile of the ultramafic and basaltic sequences, characteristic of the region, results in a thick siliceous caprock. Modest supplies of groundwater can be derived from this weathered zone. The historic Bounty water supply borefield draws from such an aquifer, located around 7 km to the south-southeast of the Earl Grey pit area (GRM, 2017; URS, 2002). The storativity and hydraulic conductivity of these aquifers is largely related to the degree of fracture intensity.

Proterozoic dolerite dykes have been shown to exhibit low permeability or hydraulic barriers to groundwater flow across the Yilgarn and Pilbara provinces (Golder, 2017). The dykes can effectively partition permeable basement units such as fractured BIF. GRM (2023) infer some permeability may be aligned parallel with the chill margins of emplaced dolerite/gabbroic dykes.

### 2.3.2 Groundwater occurrence

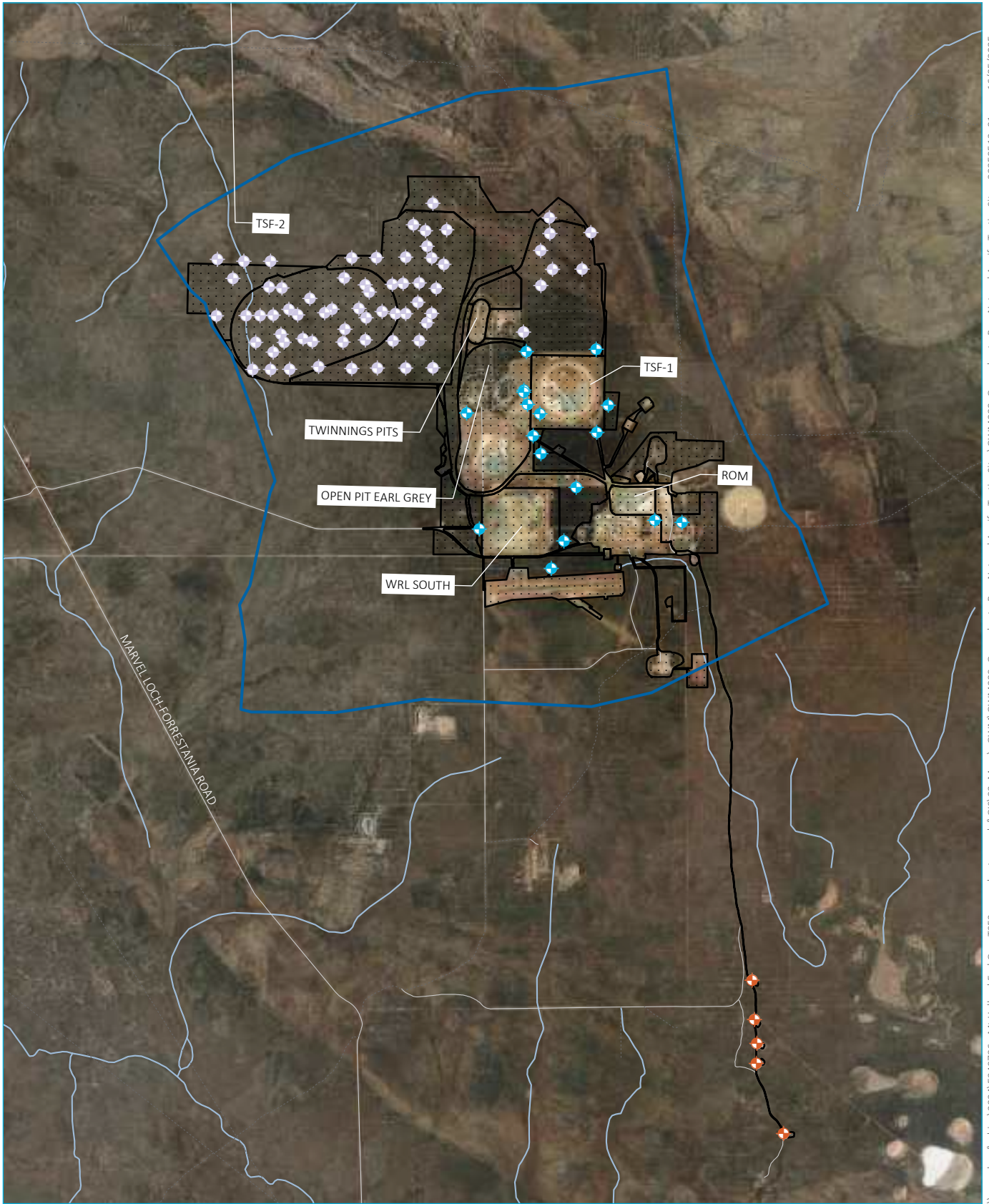
Hydrogeological investigation holes (EGH series completed in February 2017), and monitoring bores (MB series, completed in October 2017 and December 2024) have been installed around the perimeter of TSF-1, proposed TSF-2 and the Earl Grey mine void (Figure 2.5). There are historic water supply production bores associated with Bounty Goldmine borefield to the south (not shown) that help constrain the groundwater level interpretation presented within Figure 2.6.

The hydrogeological investigations prior to 2024 have been conducted over the lower greenstone sequence comprising mafic and ultramafic rock suites. The hydrogeological investigation conducted in December 2024 was over the upper meta volcanic-clastic and sedimentary rock sequence of the greenstones where TSF-2 is proposed.

Groundwater level data has been collected at disparate time frames associated with various investigations and is incomplete across the nominal model domain, given the need for this domain to extend beyond the footprint of the Site. To address this, these existing holes were used to develop a relative topographic level versus depth to water relationship. This relationship was then used to infer the conceptual potentiometric heads presented in Figure 2.6 given a digital elevation model. Within most observation locations, depths to groundwater are in the order of 60 to 100 m bgl.









The conceptual potentiometric heads indicate hydraulic gradients are to the north in northwest corner, to the south in the southwest and the remainder of the model domain has a general east to northeasterly trend consistent with the main palaeodrainage trend of the Lake Lefroy surface water catchment.

Groundwater is assumed to discharge via upward hydraulic gradients beneath salt lakes of Lake Lefroy further east. The salt lakes and playas are the only nearby classified high potential groundwater dependent ecosystems within the Bureau of Meteorology groundwater dependent ecosystem atlas. There are no groundwater dependent ecosystems within the development envelope.



Source: EMM (2025); Landgate (2021, 2025); Esri (2025); GA (2009)

KEY

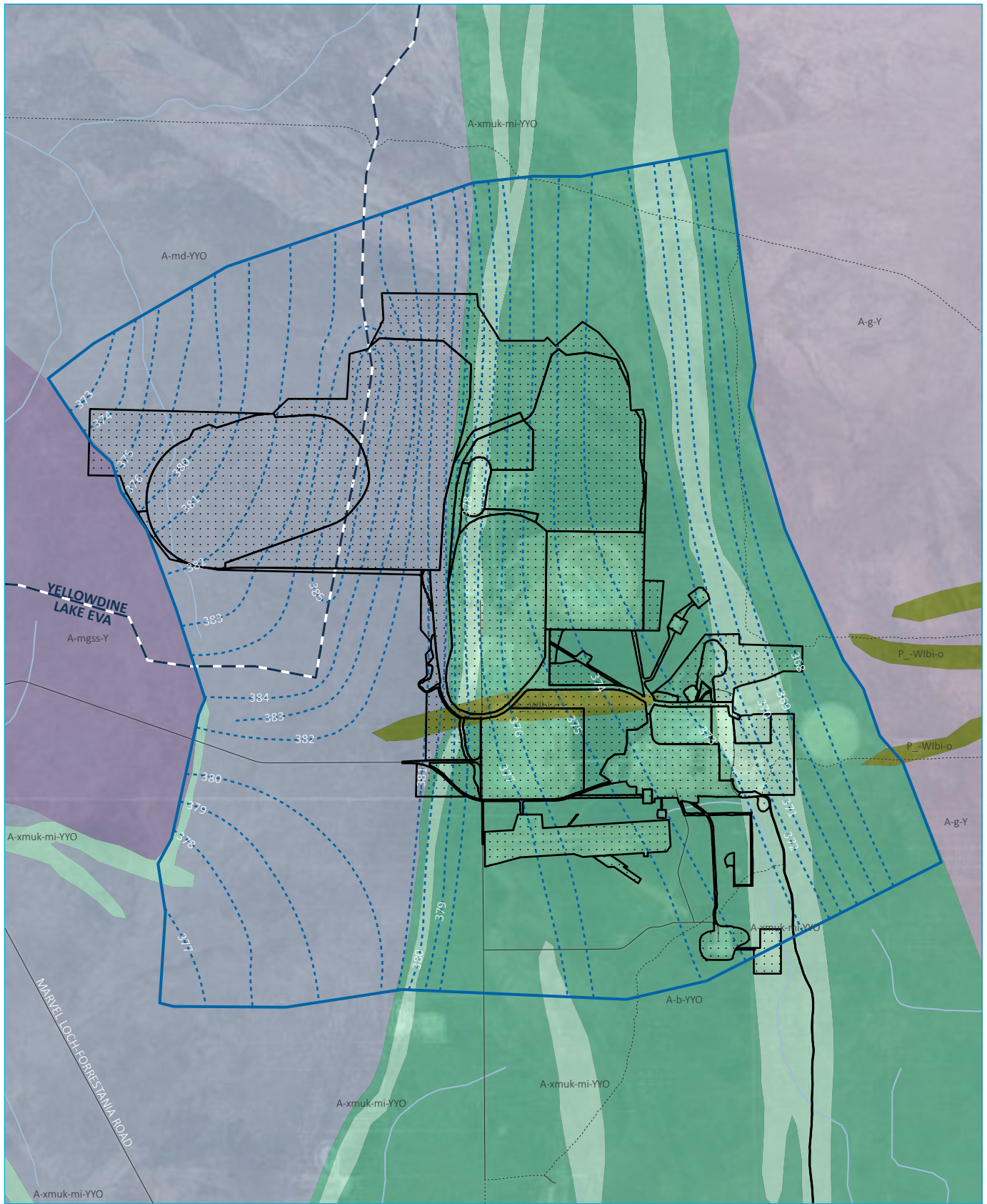
- |   |   |
|---|---|
|  Model extent            | Existing environment  |
|  Mine layout             |  Minor road                |
| Groundwater bore network  |  Vehicular track           |
|  Bounty production bore  |  Watercourse/drainage line |
|  Groundwater sample site |   |
|  TSF2 monitoring bore    |   |

Groundwater bore network and aquifer testing sites

Covalent Lithium  
Mt Holland Earl Grey TSF2 Groundwater Model  
Figure 2.5



\\emml.local\drive\2024\E240786 - Mt Holland Earl Grey TSF2 groundwater model\GIS\02\_Maps\GWM\GWM009\_GroundwaterBoreNetworkAquiferTestingSites\_20250512\_01.aprx 16/05/2025



Source: EMM (2025); Landgate (2021, 2025); Esri (2025); GA (2009)



- KEY**
- Model extent
  - Mine layout
  - Surface water sub-catchment
  - Groundwater Level (mAHD)
- Existing environment
- Minor road
  - Vehicular track
  - Watercourse/drainage line

- State interpreted bedrock geology (1:500,000)
- Binneringie Dyke; Dolerite and gabbro; includes cumulate and granophyric differentiates (P\_-Wibi-o)
  - Yilgarn Craton granites; Foliated metagranite, locally gneissic; may include amphibolite lenses; includes deeply weathered rock (A-mgss-Y)
  - Yilgarn Craton granites; Granitic rock, undivided; metamorphosed (A-g-Y)
  - Youanmi Terrane greenstones; Metakomatiite, metachert, and

Pre lithium mining conceptual potentiometric heads

Covalent Lithium  
Mt Holland Earl Grey TSF2 Groundwater Model  
Figure 2.6



\\emmm.local\vdrive\2024\E240786 - Mt Holland Earl Grey TSF2 groundwater model\GIS\02\_Maps\GWM\GWM010\_PrelithiumMiningConceptualHeads\_20250512\_01\_aprx\_16/05/2025

### 2.3.3 Aquifer parameters

Aquifer parameters have been derived from a combination of airlift testing of angled exploration holes and slug testing of select EGH series bores (GRM, 2017). A total of 26 hydraulic conductivities were determined from 16 individual bores using multiple analysis methods over different time series (i.e., early and late time data). The mean hydraulic conductivity (K) was  $2 \times 10^{-2}$  m/day, with values ranging over four orders of magnitude, from  $10^{-1}$  to  $10^{-4}$  m/day. The results are skewed towards the higher end of the range, likely due to multiple tests on individual bores and selection bias favouring more productive holes, excluding very low-yielding or dry boreholes.

Storativity (S) values of  $1 \times 10^{-3}$  were only calculated for bores EGH01 and EGH07 (GRM, 2017), confirming assumed low storage and permeability of the fractured rock aquifer system, with significant depth to groundwater.

A summary of estimated hydrogeological parameters for each unit is provided below, incorporating values from literature and the GRM model (Table 2.1).

**Table 2.1 Estimated hydraulic conductivity of local lithology**

Hydraulic conductivity (m/d)	Metasediments	Meta Basalt	Fractured Metasediment/ Metabasalt	Dolerite dykes	Pegmatite/Granite
Saprolite	$10^{-4} - 10^{-6}$	$10^{-3} - 10^{-5}$	$10^{-3} - 10^{-5}$	$10^{-3} - 10^{-4}$	$10^{-6} - 10^{-5}$
Saprock	$10^{-2}$	$10^{-3} - 10^{-4}$	$10^{-2} - 10^{-4}$	$10^{-3} - 10^{-5}$	$10^{-4} - 10^{-5}$
Fresh rock	$10^{-4} - 10^{-6}$	$10^{-5} - 10^{-7}$	$10^{-4} - 10^{-6}$	$10^{-5} - 10^{-7}$	$10^{-6} - 10^{-8}$

### 2.3.4 Geological description of the hydrostratigraphic units

It is generally established that the bedrock, fractured rock aquifers of the Yilgarn are low permeability, and that permeability and storage may be enhanced by weathering. Hence, hydrostratigraphic units for the groundwater modelling have been derived given the degree of weathering, regardless of the primary lithology, i.e. ultramafic and mafic volcanic rocks, felsic volcanic and metasedimentary rocks and granitic bodies, except for a north trending shear zone which abuts the western wall of the orebody. This unit was included to history match current observed dewatering which is higher than anticipated from earlier modelling. Four other primary hydrostratigraphic units, one of overlying colluvium, and three based on weathering: that is, Saprolite, Saprock, and Fresh Rock:

- Colluvium (Superficial Cover) – The Colluvium consists of unconsolidated sediments deposited by surface processes, forming a thin veneer across the project area. It is composed of clay, silt, and fine gravel, with a friable texture and oxidation-related alteration. It includes fragments of duricrust and laterite, which contribute to its heterogeneous composition and low to medium permeability. Around Earl Grey the Colluvium is unsaturated and mainly acts as a conduit for rainwater infiltration, with water movement largely controlled by underlying geological structures.
- Saprolite (Highly Weathered Zone) – The Saprolite is the upper portion of the deep weathering, formed by in-situ chemical leaching of the underlying bedrock. Primarily composed of clay-rich materials, including kaolinite, smectite, and secondary quartz, with relict textures of the original rock destroyed. Derived from a range of parent rocks, including basalt, pegmatite, iron formations, and metasediments. It commonly displays brown to grey coloration, influenced by iron oxidation and leaching processes. The thickness is highly variable across the project area, ranging from a few meters to a maximum of 70 m, increasing towards the northwest. The majority of the saprolite is likely unsaturated.

- Saprocks (Main Aquifer) – The Saprocks is a partially weathered bedrock, where primary minerals and texture are still present, but the rock mass has undergone significant weathering, opening of fractures or bedding and development of secondary porosity. Relative to the other units this represents the higher permeability, but overall, still low permeability, with groundwater movement controlled by fractures and secondary porosity. The parent rock comprises basalt, pegmatite, iron formations, and metasediments. The saprock ranges from a few meters to 75 m, generally increasing towards the northern part of the project area. The hydraulic conductivity is likely highly heterogeneous, with permeability depending on fracture density and degree of weathering. Groundwater strikes around TSF2 area were generally around 100 m bgl, indicating that the saprock is confined beneath the overlying saprolite.
- Fresh Rock (Basement Unit) – The Fresh Rock represents the unaltered bedrock, composed of basaltic and komatiitic rocks, meta-sediments, banded iron formation and localized pegmatites from the Archaean greenstone sequence. A low-permeability basement unit, except where fracturing and structural discontinuities enhance groundwater movement. The basement is continuous at depth and represents a confined aquifer.

The hydrogeological properties of different rock types and weathering extents are summarized in Table 2.1, which provides estimated hydraulic conductivity (K), storativity (S), and thickness ranges for each hydrostratigraphic unit based on field falling head tests (GRM, 2017), literature review, and previous groundwater model parameters (GRM, 2017, 2023). This table serves as a reference for understanding groundwater movement and aquifer characteristics within the project area.

### 2.3.5 Recharge

Groundwater recharge can be described as the deep percolation of rainfall or surface water to the water table. Ongoing groundwater level monitoring at Earl Grey commenced in 2020. The monitoring of depth to water across eleven bores and the southern vent raise (SVR) from the Bounty underground is presented in Figure 2.7 against monthly rainfall from the SILO gridded data point for Earl Grey.

Owing to the depth to groundwater there is no obvious correlation between rainfall and groundwater levels, although this may also reflect the frequency of monitoring to date. That lack of correlation also reflects the semi-arid environment within which the Project lies. The December 2024 depth to groundwater are from the new TSF2 area bores which have a greater depth to the potentiometric head. Automated pressure transducer data loggers have been installed within the 2024 series of nine monitoring bores set to daily recording to help better define the potential for groundwater recharge and temporal data calibration. On the 12–13 March 2025 after 2.5 months of continuous monitoring, the data showed no significant recharge, and the water level behaviour is summarised in Table 2.2.

At this stage, the trends in Table 2.2 are descriptive only and may not be indicative of long-term aquifer dynamics or seasonal influences, hence the significance of the datalogger in providing these invaluable spatially distributed and long-term datasets with frequent monitoring intervals.

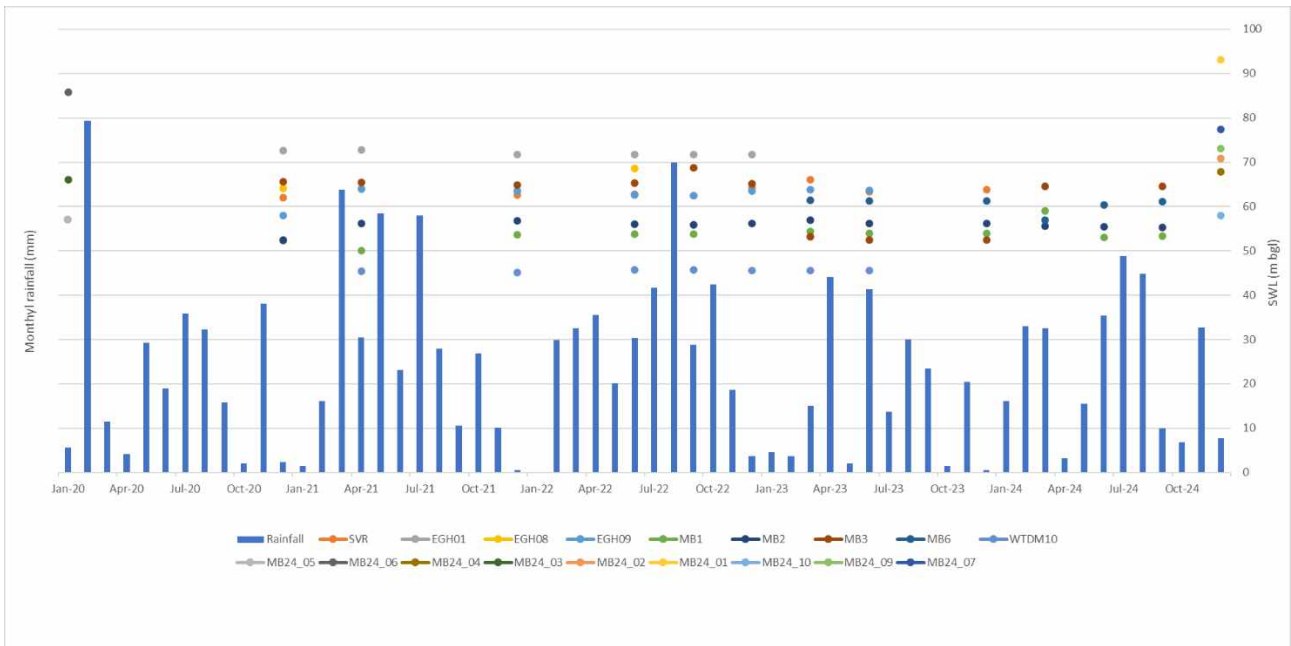


**Figure 2.7** Groundwater levels against SILO gridded rainfall for Mt Holland

**Table 2.2** Water level variability between December 2024 to March 2025

Hole ID	Water level behaviour
MB24_01	Slightly rising, minor daily oscillations (93.73 to 93.67 m bgl)
MB24_02	Fluctuating with general downward trend (71.43 to 71.55 m bgl)
MB24_03	Stable, fluctuations within ~ 0.10 m (57.5 to 57.6 m bgl)
MB24_04	Short-term fluctuations (58.28 to 58.42 m bgl)
MB24_05	Cyclical variations, range of 0.14 m bgl
MB24_06	Stable, steady water table (86.67 to 86.56 m bgl)
MB24_07	Gradual but small rise from 78.62 to 78.5 m bgl
MB24_09	Gradual rise of about 59 cm (between 73.3 and 73.89 m bgl)
MB24_10	Declining trend of about 1.12 m (from 58.77 to 59.89 m bgl)

Johnson et. al. (1999) suggests fractured rock aquifers of the Northern goldfields are recharged infrequently by rainfall and run-off from ephemeral drainages into open fractures and weathered zones. Given the location of Earl Grey at a sub-catchment divide and lack of well-developed drainage, groundwater recharge to the saprock is likely to occur via rainfall infiltration. It is likely that only very high intensity/duration rainfall events would induce infiltration recharge, with rainfall from lesser events evaporating prior to infiltration. On current evidence recharge from rainfall is practically negligible.

## 2.4 Groundwater quality

Groundwater within the study area is hypersaline, with salinity levels reaching up to three times that of seawater. However, salinity distribution is highly variable, suggesting the influence of localized preferential flow paths and dilution processes. Key findings include:

- No clear regional trend in salinity variation across the Site.
- Northeast bores exhibit lower salinity levels, but the pattern remains inconsistent.
- Hypersaline conditions suggest limited groundwater circulation and a dominance of evaporative concentration processes over recharge dilution.

## 2.5 Groundwater discharge

Groundwater discharge primarily occurs through:

- Natural evaporation: From salt lakes and playas in low-lying areas.
- Groundwater throughflow: Albeit limited by low permeability units.
- Mining Dewatering: Localized removal of groundwater from pegmatite units.

Due to low hydraulic conductivity and steep hydraulic gradients, groundwater discharge rates remain low.

## 2.6 Groundwater sensitive receptors

Potentially sensitive groundwater receptors include:

- Salt Lakes and Playas: Areas of natural discharge classified as aquatic and terrestrial groundwater dependent ecosystems in the BoM Groundwater Dependent Ecosystem Atlas (<http://www.bom.gov.au/water/groundwater/gde/map.shtml>).
- .
- Future Water Supply Bores: Monitoring required for potential impacts.

Mining dewatering activities have not yet demonstrated significant regional groundwater depletion, though ongoing monitoring is required.

## 3 Model design

### 3.1 Software

The model was run using MODFLOW-USG (Panday et al., 2013) version 2.4.0 (Panday, 2024) through the Groundwater Vistas V8 Pro graphical user interface (ESI, 2021). MODFLOW-USG represents a major revision of the standard MODFLOW code, in that it uses a different underlying numerical scheme comprising control volume finite difference (CVFD), rather than traditional MODFLOW's finite difference (FD) scheme. 'USG' is an acronym for Un-Structured Grid, meaning that MODFLOW-USG supports a variety of structured and unstructured model grids, including those based on cell shapes (Panday et al., 2013). The CVFD method also means that a model cell can be connected to an arbitrary number of adjacent cells, which is not the case with a standard FD scheme.

In contrast with structured rectangular finite-difference grids, flexible meshes have the advantages of a finer mesh resolution to be focused solely in areas of a model that require it as opposed to refinement over the entire mesh, significantly decreasing cell count and consequently model run times and file sizes; and spatial areas not required in the model may be omitted rather than deactivating cells or retaining "dummy" layers (i.e. layer pinch-outs). The flexible meshes allow cell boundaries to follow important geographical or geological features, such as watercourses or outcrop traces, more accurately modelling the geometry of the physical system. Finally, the orientation of the flow interfaces between cells may vary, allowing preferential flow directions to be modelled with higher accuracy.

### 3.2 Domain and spatial discretisation

#### 3.2.1 Model domain

The model domain is located within the Swan Avon – Yilgarn River catchment. The domain spans a sub-catchment divide, with the western portion of the site located within the 4,094 km<sup>2</sup> Yellowdine sub-catchment and the eastern portion located within the 7,582 km<sup>2</sup> Lake Eva sub-catchment. Both sub-catchments drain to the north and are characterised by discontinuous chains of salt lakes along valley floors.

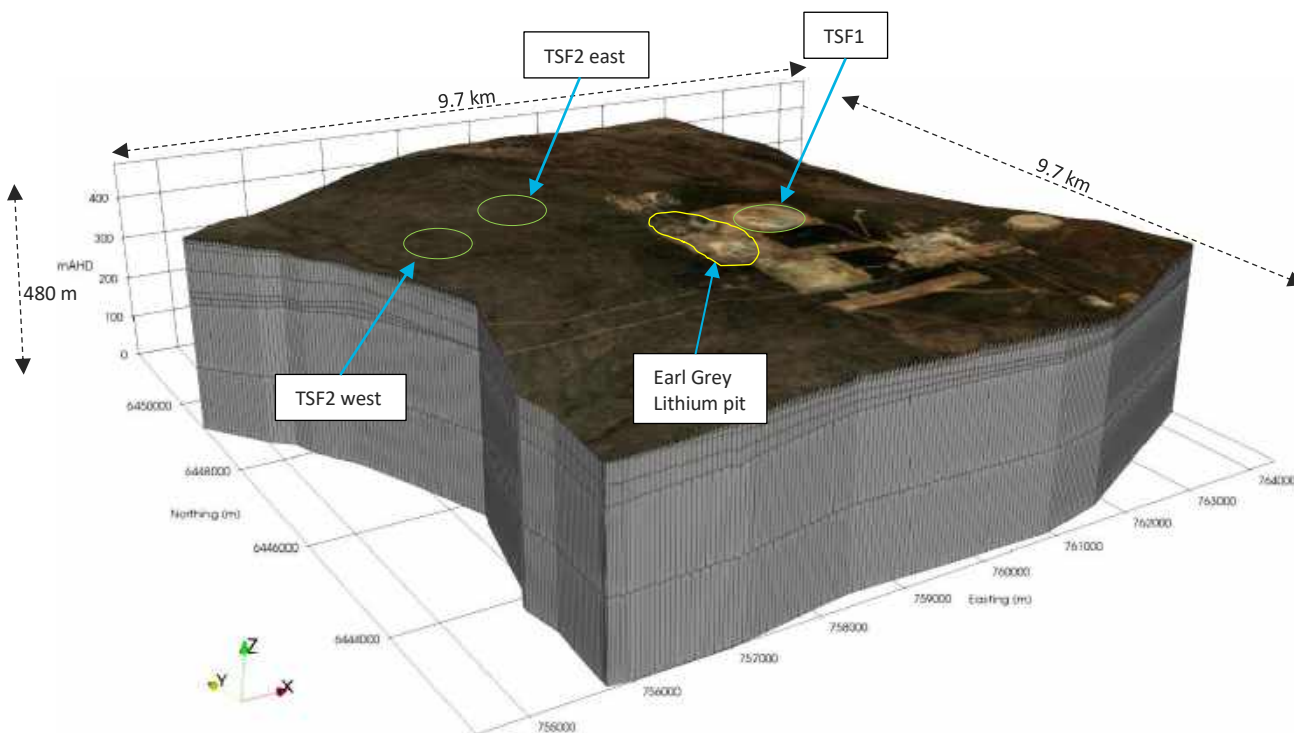
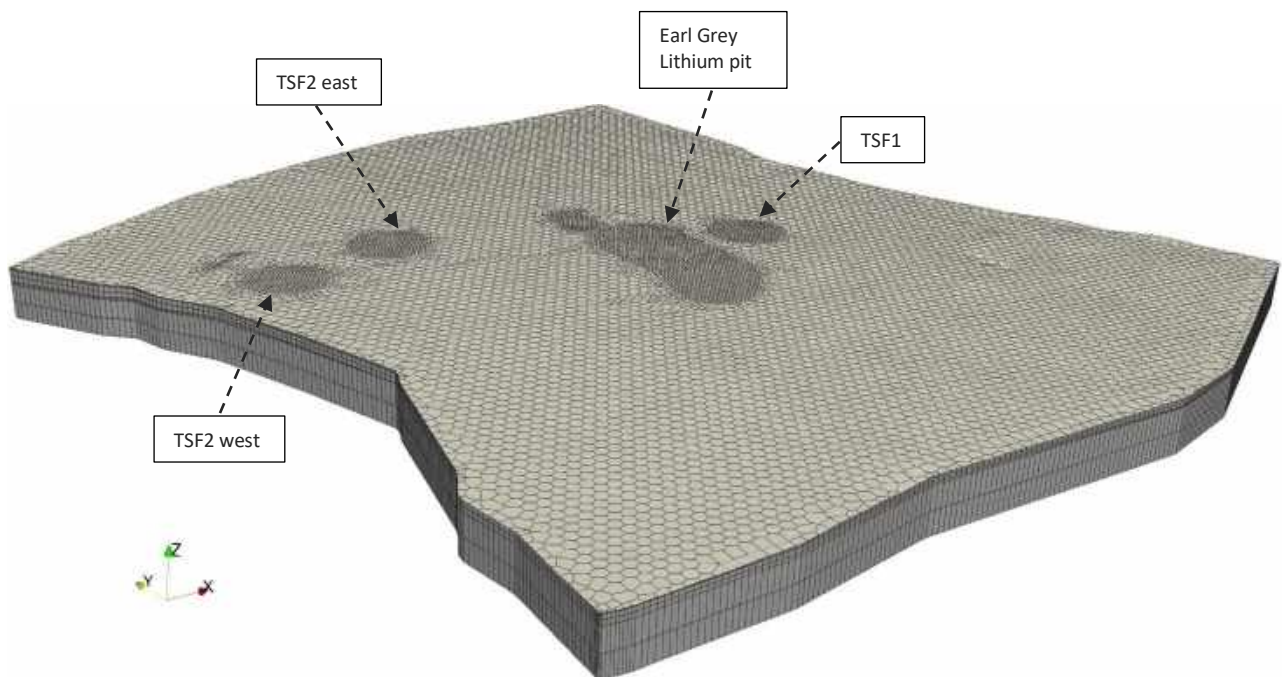


Figure 3.1 Model domain (vertical exaggeration x 5)

### 3.2.2 Mesh

The model domain in plan view was discretised into 95,552 Voronoi cells, specifically tailored to encompass areas significant to the project's goals and components (see Figure 3.2). The dimensions assigned to various element cell sizes within the domain were as follows:

- Earl Grey Pit void received a node spacing of 30 m.
- TSF1 and TSF2 were allocated a node spacing of 30 m.
- Twinning pits received a maximum node spacing of 30 m.
- The remainder of the model's domain was designated a maximum node spacing of 100 m.



**Figure 3.2** Model mesh (vertical exaggeration x 1)

### 3.2.3 Layers and hydrostratigraphic units

There are eight layers, two for each HSU (see Figure 3.3). They are distributed as follows:

- Layers 1 and 2: comprise by the Colluvium unit, with thickness varies from 0 to 78 m (Figure 3.3E).
- Layers 3 and 4: comprise by the Saprolite unit, its thickness varies from 5 to 101 m (Figure 3.3D), the Saprolite displays a regional extent across the entire model, overlying the Saprock.
- Layers 5 and 6: contains the Saprock and Shear zone units. The thickness of the Saprock unit ranges from 0 to 86 m. As shown in Figure 3.3C, the Saprock does not extend across the entire model domain, pinching out towards the east and south.
- Layers 7 and 8: form the basement of Fresh rock and the inferred Shear zone, varying from 296 to 410 m. As observed in Figure 3.3A, the Shear zone intersects the Fresh rock from north to south, as shown in Figure 3.3B, facilitating regional groundwater transfer.

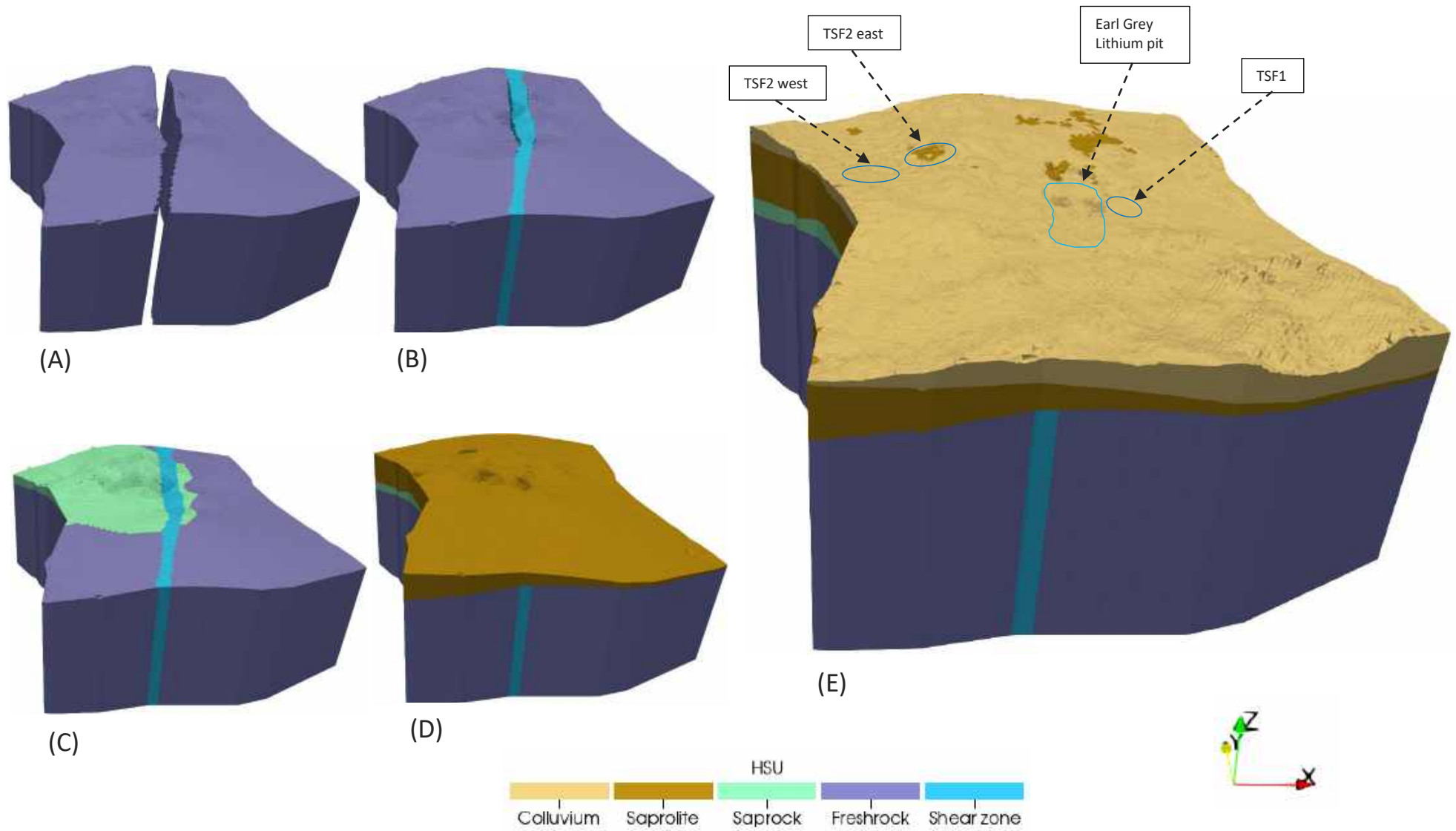


**Figure 3.3** Model layers and hydrostratigraphic units (vertical exaggeration x 10)

### 3.3 Temporal discretisation

The following table shows the periods considered for temporal discretisation.

**Table 3.1 Model stress periods**

Stress period	Start	End	Stress period duration	Description
1	31 December 2019	1 January 2020	Steady state	Develops baseline steady-state conditions in response to modelled hydraulic properties and boundary conditions. Single time step.
2 to 5	1 January 2020	31 December 2023	Yearly	History matching period. Dewatering from Earl Grey Lithium pit started in August 2024. Adaptative time steps with a multiplier of 1.2.
6	1 January 2024	31 July 2024	Monthly	
7	1 August 2024	31 December 2024	Monthly	
8 to 32	1 January 2025	31 December 2049	Yearly	Prediction scenario: Dewatering volumes from the Earl Grey Lithium pit, leakage volumes from the TSFs, drawdown and mounding in the water table, groundwater level changes across the monitoring bores, flow direction from the TFs. Adaptative time steps with a multiplier of 1.2.
33	1 January 2050	1 January 20150	100 years	Recovery period run. Adaptative time steps with a multiplier of 1.2.

### 3.4 Regional groundwater flow

Constant head boundary condition cells were implemented along the entire perimeter of the model domain to represent lateral groundwater flow entering and leaving the model domain owing to its position straddling a surface water catchment divide. To establish the hydraulic heads at each edge node, existing boreholes were utilised to develop a relationship between relative topographic elevation and depth to the water table. This relationship was then used to infer the conceptual groundwater level at these nodes. The boundary condition was applied to the cells at the edges of the model corresponding to weathered layers HSUs (Saprolite, Saprock and Fresh rock), which are below the superficial HSU.

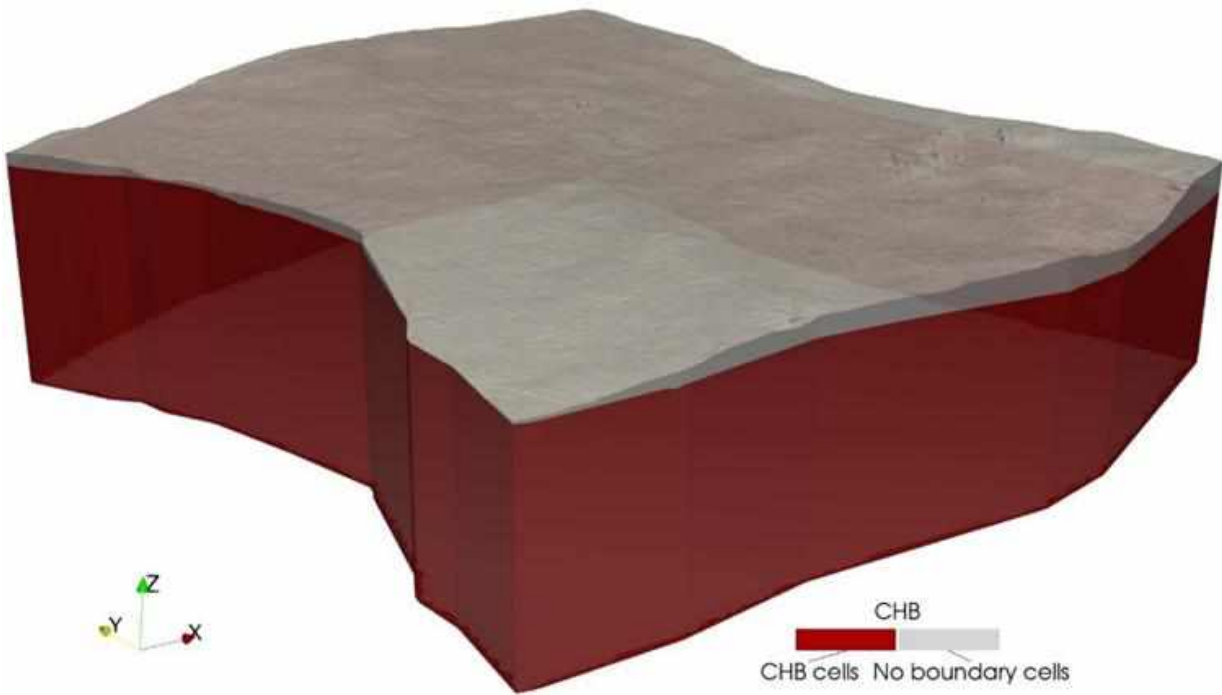


**Figure 3.4** Constant head boundary conditions (vertical exaggeration x 5)

### 3.5 Existing mine-related activities

#### 3.5.1 Current Earl Grey Lithium mine void

The dewatering of the Earl Grey pit was simulated using the MODFLOW Drain (DRN) package. The drain stage elevation was set at the base of the pit void for each model cell and stress period, with a conductance value of 1,000 m<sup>2</sup>/d. The modelled drain cells are shown in Figure 3.5, along with the intersection of HSUs within the Earl Grey pit. As of December 2024, the existing mine void intersects all HSUs. The current pit has an area of 451,750 m<sup>2</sup> and goes to 360 mAHD.

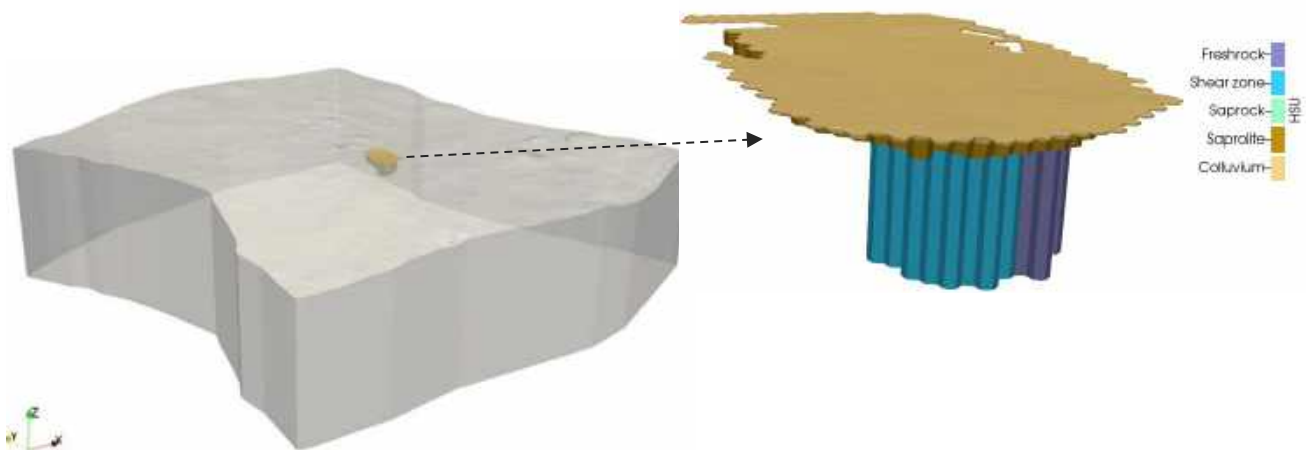


**Figure 3.5** Current mine plan – DRN cells (vertical exaggeration x5)

### 3.5.2 Tailing storage facilities

The existing Tailings Storage Facility (TSF1) was represented in a simplified manner using the MODFLOW River (RIV) package, which enables indirect simulation of the tailings accumulation. This package calculates head-dependent fluxes, as described by Panday et al. (2013), based on a conductance term that is calculated as follows:

$$C_{ij} = \frac{KA_i}{L_{ij}} \left[ \frac{m^2}{d} \right]$$

Where

- $C_{ij}$ : Conductance ( $m^2/d$ ) of the riverbed at cell  $i$  at stress period  $j$ .
- $K$ : Conductivity ( $m/d$ ) of the riverbed, which was calculated from the average conductivity of the tailing materials.
- $A_i$ : Area ( $m^2$ ) of the cell  $i$ .
- $L_{ij}$ : The thickness ( $m$ ) of the riverbed at cell  $i$  during stress period  $j$  is denoted as  $L_{ij}$ : . Historical tailings relative elevations were provided and extrapolated across the stress periods used for history matching. The variable  $L_{ij}$  was then obtained by calculating the difference between these extrapolated elevations and the relative elevation of cell  $i$  in layer 1.

The flux is calculated as the product of the calculated conductance ( $C_{ij}$ ) and the conductivity (horizontal and vertical) of the different realisations.

As the tailings grow over time,  $L_{ij}$  increases and therefore  $C_{ij}$  gets reduced. This results in more flow resistance from tailings to the groundwater system. In contrast, the head difference between the prescribed tailings heads and the groundwater heads may increase, as a result of the TSF growth, increasing the potential for vertical seepage.

## 4 History-matching

### 4.1 Approach

PESTPP-IES was employed in this model to history-match the groundwater model, offering a robust and computationally efficient solution for calibrating complex systems. Its iterative ensemble smoother approach enables the integration of diverse observational datasets, including hydraulic heads and volumetric inflows, facilitating a more comprehensive representation of the system's behaviour. The method's capacity to handle high-dimensional parameter spaces without relying on gradient-based optimisation proved particularly valuable, especially under conditions of data scarcity or model nonlinearity. By leveraging ensemble-based data assimilation, PESTPP-IES allowed for improved uncertainty quantification and model performance, supporting more reliable groundwater management outcomes (White et al., 2020).

#### 4.1.1 History matching targets

##### i Targets

Two target types are described as follows:

- Hydraulic heads: Hydraulic heads were measured at four monitoring bores (refer to Table 4.1). As groundwater levels at these bores remained stable over time, the average level was calculated and used to evaluate the history matching performance.

**Table 4.1** Monitoring bore details

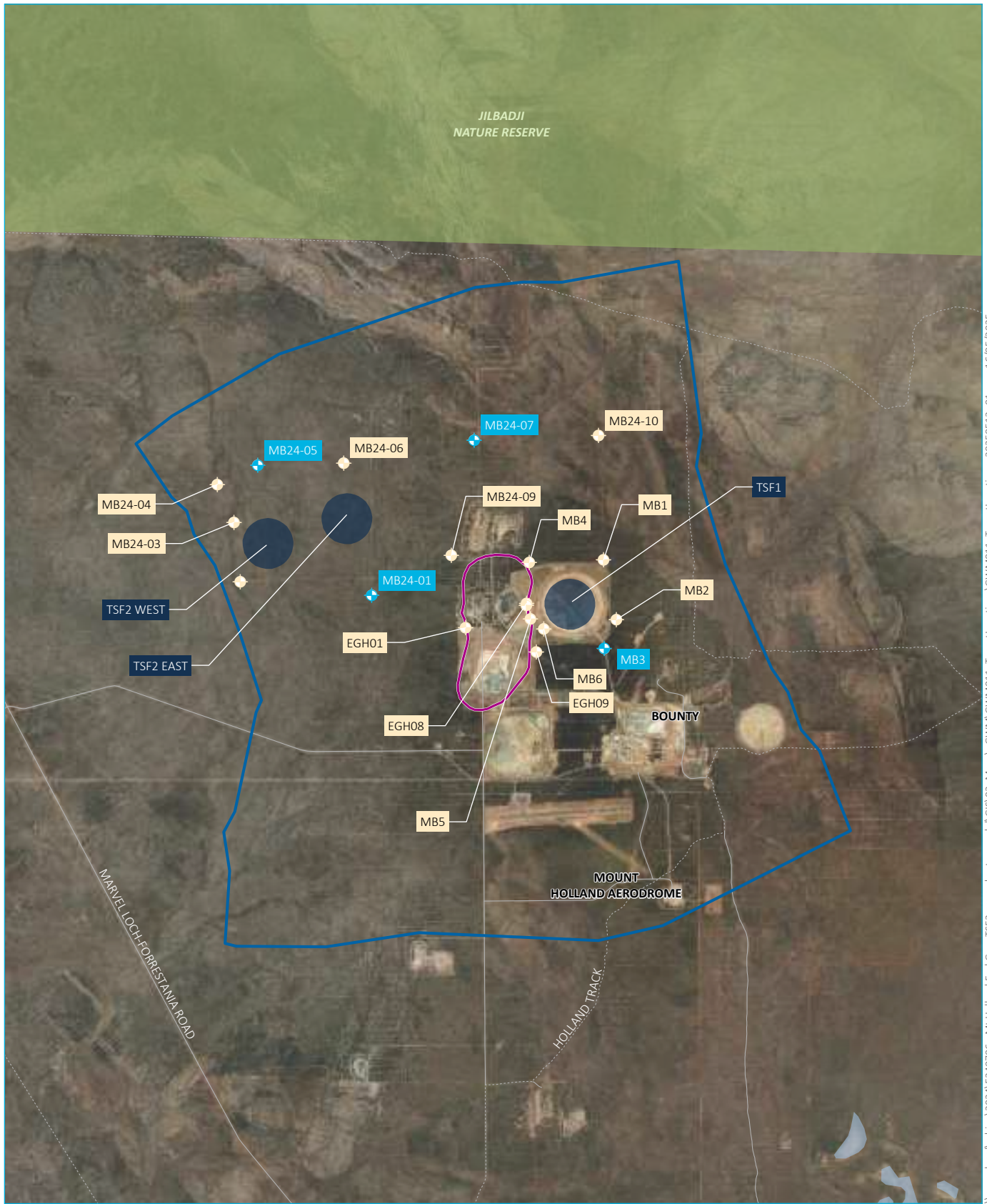
Bore	Type	East (m)	North (m)	HSU	Monitoring period	Monitoring frequency
MB3	Manual	761,025	6,446,380	Fresh rock	31/12/2020 – 30/09/2024	Quarterly
MB24-01	Logger	757,796	6,447,118	Fresh rock	31/12/2020 – 10/09/2023	Daily
MB24-05	Logger	756,213	6,448,924	Fresh rock	17/12/2024 – 31/12/2024	Daily
MB24-07	Logger	759,219	6,449,273	Fresh rock	17/12/2024 – 31/12/2024	Daily

- Dewatering volumes recorded between August 2024 and December 2024 totalled 97,775 kL, as presented in Table 4.2. This total volume was considered the dewatered amount during Stress Period 7 and used as a target for the history matching.

**Table 4.2** Dewatering volumes

Component	Period	Volume (kL)
Earl Grey pit	01/08/2024 – 31/08/2024	699
	01/09/2024 – 30/09/2024	24,132
	01/10/2024 – 31/10/2024	14,951
	01/11/2024 – 30/11/2024	29,553
	01/12/2024 – 31/12/2024	27,805

While most groundwater levels from the manual monitoring bores were reviewed, not all were included in the history-matching dataset. Historical data from the logger bores is also limited, with records only available from the second half of December 2024. Consequently, only bores MB3, MB24-01, MB24-05, and MB24-07 were considered. Due to the absence of seasonality or temporal changes in the measured groundwater levels, average groundwater levels were calculated for each of these bores to facilitate comparison with the simulated results.



Source: EMM (2025); Landgate (2021, 2025); Esri (2025); GA (2009)

**KEY**

- Earl Grey pit boundary
- Model extent
- Tailings storage facility (TSF)
- Target location
- + Used
- + Not used
- Existing environment
- Minor road
- Vehicular track
- Waterbody
- Reserve

DRAFT

Target locations

Covalent Lithium  
Mt Holland Earle Grey TSF2 Groundwater Model  
Figure 4.1



\\emmlocal\drive\2024\E240786 - Mt Holland Earle Grey TSF2 Groundwater Model\GIS\02\_Maps\_GWMM\GWMM011\_TargetLocations\_20250512\_01.aprx 16/05/2025

## ii Measurement noise and target weighting scheme

Each groundwater level observation was perturbed adding measurement noise derived from a Gaussian distribution centred around the observation and with a standard deviation equal to 0.1 m. The same was applied to measured dewatering volumes, with a standard deviation of 10 kL.

An objective function was defined combining observation residuals with weights defined for each observation point. In this case, observation weights initially set to 1.0 and were internally calculated by PESTPP-IES at the first iteration using the mean objective function of the ensemble, so that 75% of the total objective function was allocated to groundwater levels at the four monitoring bores mentioned above, while the remaining 25% was assigned to the total volume of water dewatered from the pit between August and December 2024.

### 4.1.2 Parameterisation

To parameterise the model, a stochastic but spatially invariant property field for each HSU was generated based on the parameter ranges presented in Table 4.3. This field was combined with a spatially variant field generated with kriging interpolation of pilot points to introduce heterogeneity. In this approach, the values assigned to the pilot points acted as multipliers rather than direct hydraulic property values. These multipliers are applied to the hydraulic parameters derived from the stochastic property field.

#### i Prior parameter distribution

The conceptual ranges of the hydraulic parameters across each HSU are presented in Table 4.3.

**Table 4.3 Conceptual hydraulic parameter values**

Parameter	HSU	Geometric mean (initial value)	Minimum	Maximum	Vertical anisotropy (kz/kh)	Horizontal anisotropy (kx/ky)
Horizontal hydraulic conductivity (m/d)	Colluvium	$10^{-1}$	$10^{-2}$	$10^0$	1	1
	Saprolite	$10^{-3}$	$10^{-4}$	$10^{-2}$	$10^{-2}$	100
	Saprock	$10^{-2}$	$10^{-3}$	$10^{-1}$	1	1
	Fresh rock	$10^{-3}$	$10^{-4}$	$10^0$	$10^{-2}$	100
	Shear zone	$10^{-1}$	$10^{-2}$	$10^0$	1	1
Specific storage (1/m)	Colluvium	$10^{-6}$	$3.2 \times 10^{-5}$	$10^{-3}$	-	-
	Saprolite	$10^{-6}$	$3.2 \times 10^{-5}$	$10^{-3}$	-	-
	Saprock	$10^{-8}$	$3.2 \times 10^{-7}$	$10^{-5}$	-	-
	Fresh rock	$10^{-9}$	$3.2 \times 10^{-8}$	$10^{-6}$	-	-
	Shear zone	$10^{-6}$	$3.2 \times 10^{-5}$	$10^{-3}$	-	-
Specific yield (-)	Colluvium	$10^{-3}$	$10^{-2}$	$10^{-1}$	-	-
	Saprolite	$5 \times 10^{-2}$	$7.1 \times 10^{-2}$	$10^{-1}$	-	-
	Saprock	$2 \times 10^{-3}$	$4.5 \times 10^{-3}$	$10^{-2}$	-	-
	Fresh rock	$10^{-4}$	$3.2 \times 10^{-4}$	$10^{-3}$	-	-
	Shear zone	$10^{-3}$	$10^{-2}$	$10^{-1}$	-	-

## ii Pilot points

Pilot points were uniformly distributed across each hydrostratigraphic unit (HSU) for all hydraulic properties. Each point was assigned a lower multiplier bound of 0.1, an upper bound of 10, and an initial value of 1. These pilot points were positioned at the top layer of each HSU (refer to Figure 4.2) and were then extrapolated laterally in the X–Y plane. As a result, no vertical variation was applied within each HSU.

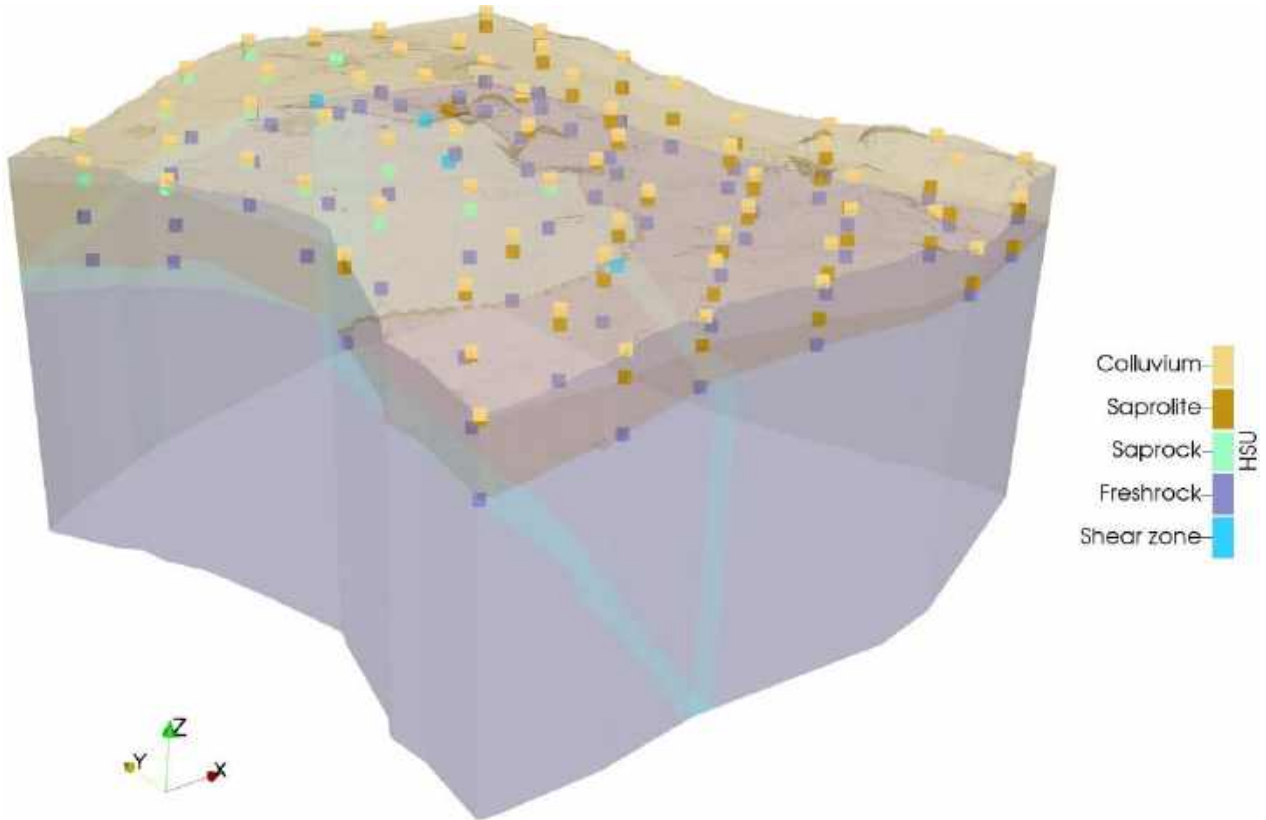


**Figure 4.2** Pilot points distribution (vertical exaggeration x 10)

### 4.1.3 Model performance

History-match performance was statistically quantified using scaled root mean square (SRMS) error for hydraulic head, given as a percentage:

$$SRMS = \frac{100}{\Delta H} \sqrt{\frac{1}{n} \sum_{i=1}^n [W_i(z_{hi} - h_i)]^2}$$

Where:

- $\Delta H$  is the range of measured hydraulic heads across the model domain.
- $n$  is the number of measurements used in the history-matching dataset.
- $W_i$  is the statistical weight of 1 applied to measurement  $i$ .
- $z_{hi}$  is the modelled hydraulic head at location  $i$ .

- $h_i$  is the measured hydraulic head at location  $i$ .

## 4.2 Results

Following the completion of 10 PESTPP-IES iterations, Iteration 2 was selected as the accepted posterior distribution of parameters to be used in the predictive scenario.

### 4.2.1 Simulated hydraulic heads

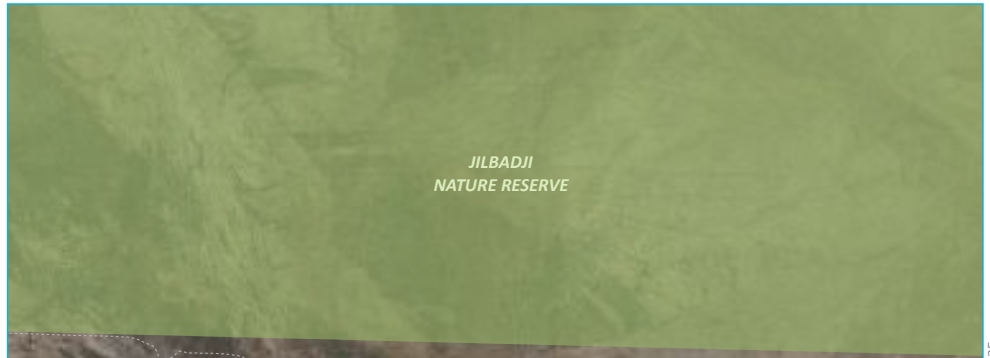
The modelled hydraulic heads showed a SRMS of 0.76%, a residual mean of 0.02 m and a mean absolute error of 0.06 m. This value is considered relatively high and indicates a suboptimal fit to the observed data. The elevated SRMS is attributed to limitations in both the spatial and temporal coverage of available data, as well as uncertainties in the conceptual understanding of the HSUs across the broader model domain.

The comparison between simulated and conceptual potentiometric head contours is presented in Figure 4.3. One of the most notable aspects is the good fit of the simulated head with the conceptual contours in the eastern portion of the model domain. In this area, particularly around bores MB1, MB2, MB3, and SVR, the simulated heads closely reflect the conceptual contours, both regarding gradient and flow direction. This suggests that, despite the limited data availability, the model effectively captures the hydraulic behaviour in this sector, likely due to the presence of consistent topographic and hydrogeological features and better-defined boundary gradients.

In contrast, within the central area around the Earl Grey pit and TSF1, the model appears to slightly underrepresent the localised variations evident in the conceptual model. While the general north-south alignment of contours is preserved, the simulated heads show a smoother gradient compared to the conceptual contours, which display more abrupt transitions. Moreover, the sparse bore coverage reduce the ability of the model to replicate fine-scale variations near infrastructure.

In the western part of the model, particularly around TSF2 west and TSF2 east, larger discrepancies are evident. The simulated head contours appear flatter and do not replicate the sharp gradients of the conceptual contours, especially across the 385 mAHD catchment divide. This suggests that the model's boundary conditions, and local hydraulic parameters, may not fully capture the natural hydrological controls in this area. This discrepancy is also reflected in the measured versus simulated ensemble results for MB24 series bores, where Figure 4.4 shows that while bores such as MB24-01 and MB24-05 are reasonably centred around the observed values, there is still some deviation—potentially stemming from the limitations in local geological understanding and the absence of pumping test data.

Figure 4.4 further demonstrate the varying calibration performance across bores. For example, MB3 and MB24-05 show strong agreement between the observed hydraulic head and the centre of the simulated ensemble, suggesting a good model fit at those points. Meanwhile, MB24-07 shows a slight underestimation, with the modelled ensemble peaking just below the measured average. These patterns generally support the visual interpretation from the contour map – indicating that while some areas are well-represented, others would benefit from improved data or refinement of hydrogeological assumptions.



Source: EMM (2025); Landgate (2021, 2025); Esri (2025); GA (2009)



**KEY**

- ▭ Earl Grey pit boundary
- ▭ Model extent
- ▭ Tailings storage facility (TSF)
- Simulated contour (mAHD)
- - - Conceptual contour (mAHD)
- Existing environment
- Minor road
- - - Vehicular track
- ▭ Waterbody
- ▭ Reserve

**INSET KEY**

- Major road
- ▭ National Park
- ▭ Reserve
- ▭ Other conservation/management area

Comparison between simulated potentiometric heads and conceptual contours for steady-state

Covalent Lithium  
Mt Holland Earl Grey TSF2 Groundwater Model  
Figure 4.3



\\emmlocal\drive\2024\E240786- Mt Holland Earl Grey TSF2 groundwater model\GIS\02\_Maps\GWM\GWM001\_ SteadyStateComparison\GWM001\_ SteadyStateComparison\_20250422\_01.aprx.12/05/2025

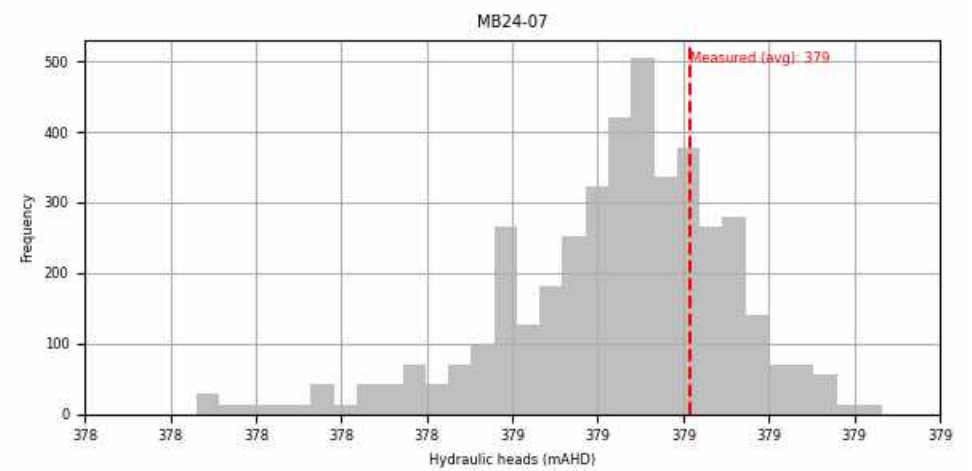
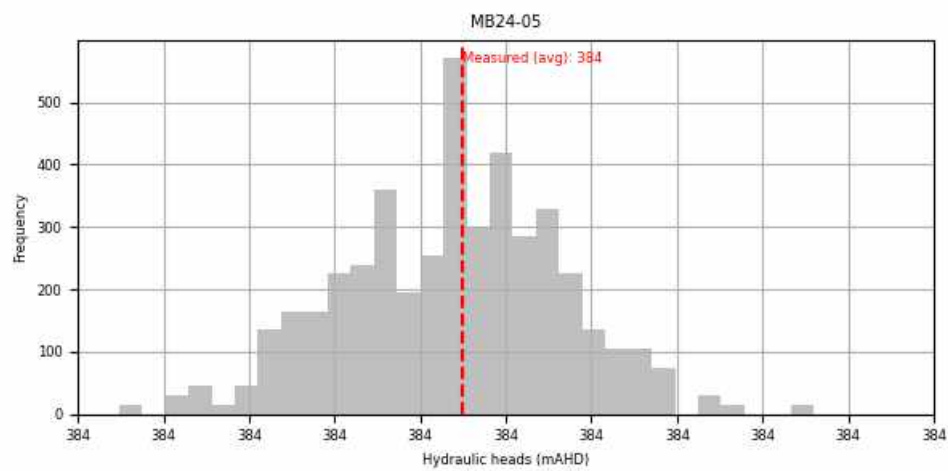
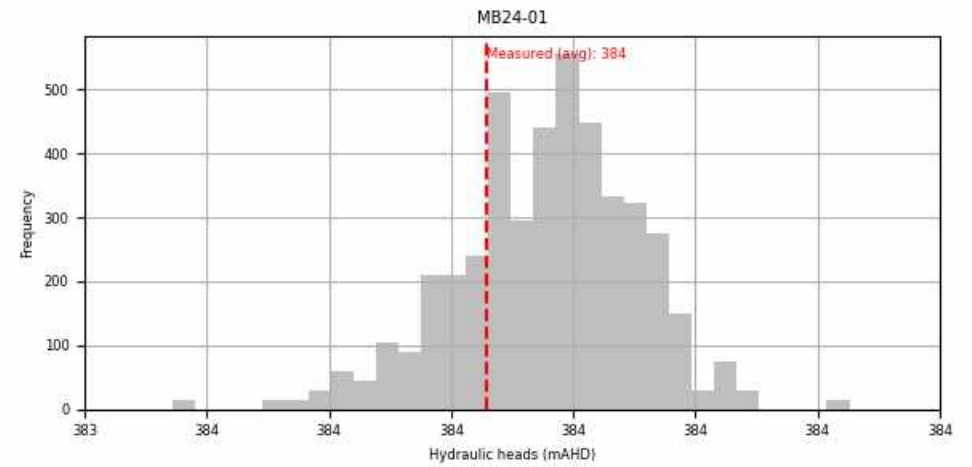
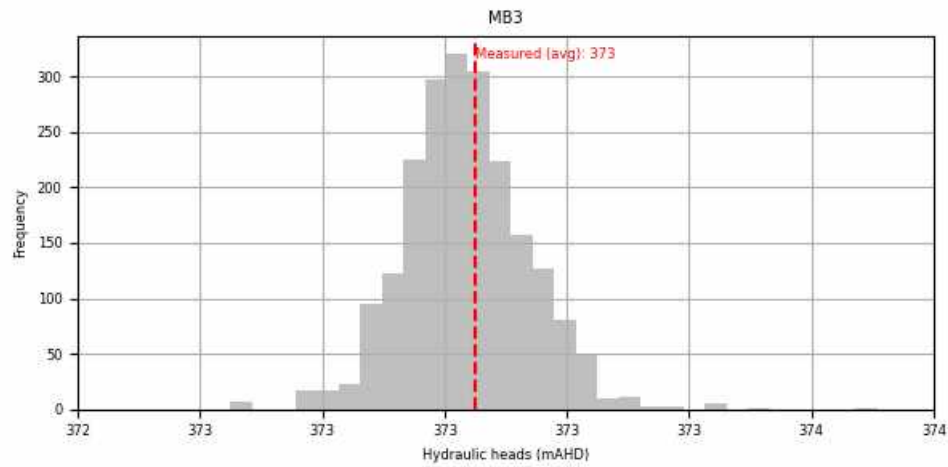


**Figure 4.4** Average measured head compared and the simulated ensemble

### 4.2.2 Simulated dewatering volumes

As previously mentioned, the total dewatered volume for the period August to December 2024 (Stress Period 7) was 97,775 kL. This value lies approximately at the centre of the ensemble of realisations, indicating that the observed volume is well captured within the model's uncertainty range.

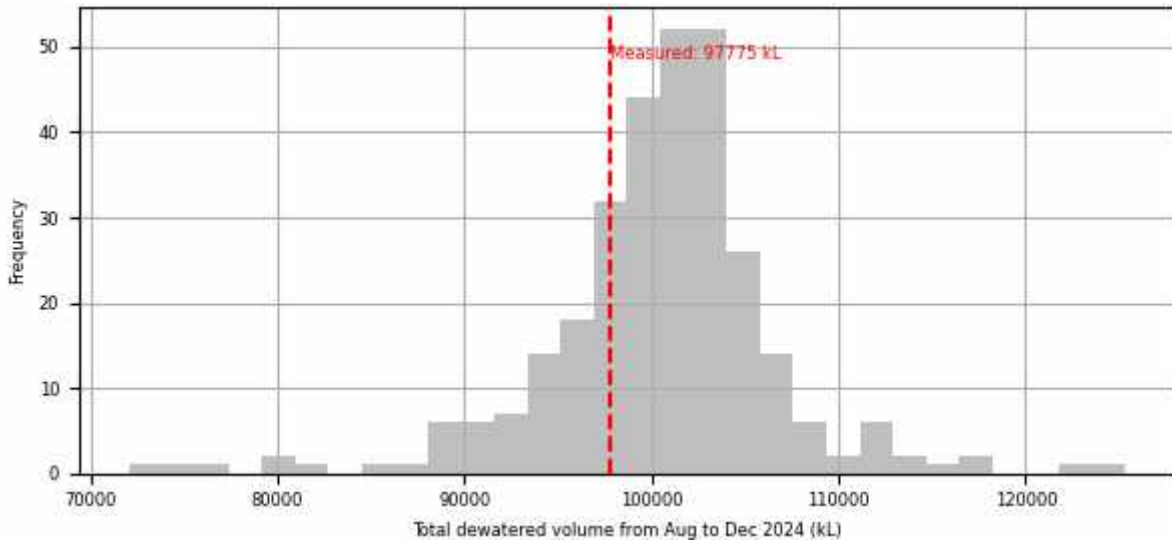


Figure 4.5 Modelled posterior distribution of total dewatered void volumes.

### 4.2.3 Water balance

During the initial part of the history matching period (January 2020 to December 2023), the hydrogeological system remains relatively stable (see Figure 4.6 for reference), with water fluxes predominantly governed by the constant head boundary condition. Inflows and outflows from these boundaries are nearly balanced, both averaging around 68 kL/day, indicating a quasi-steady state. There is no contribution from TSF1 seepage or operational pumping. However, from August 2024 onwards, the system experiences a marked shift. Inflows are recorded, particularly from TSF1 seepage and increased storage entry. Corresponding outflows rise sharply, with notable increases in storage outflow and the commencement of pumping activities Earl Grey pit sump. These changes highlight a transition to dynamic conditions, where seepage from TSF1 and dewatering operations become the dominant driver of the water balance.

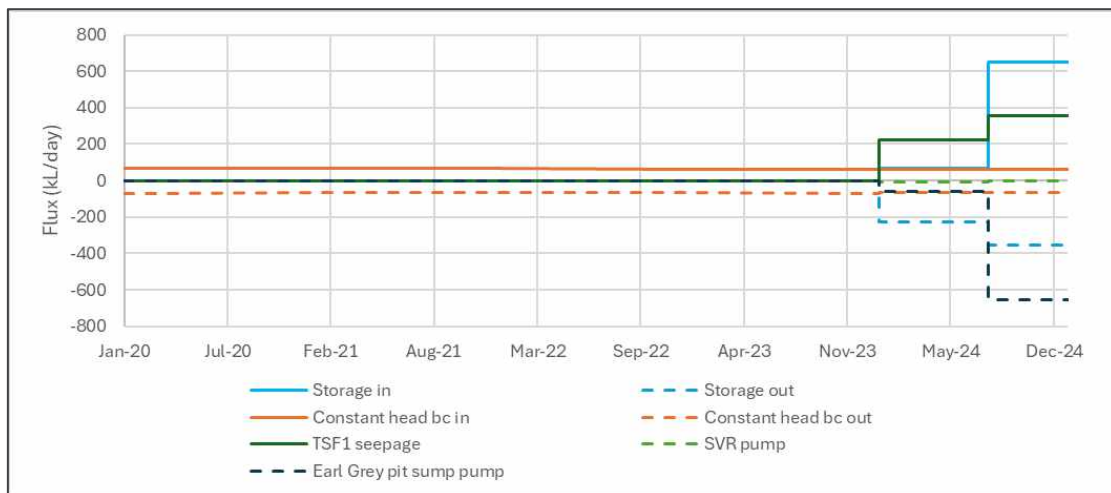


Figure 4.6 Water balance during history matching period

### 4.3 Adopted parameters

The prior and posterior parameter distributions are presented below. To characterise the complete ensemble of realisations and their impact on each model node, the whole ensemble (all nodes for each HSU) histograms are presented. As illustrated in Figure 4.7, the Saprock unit consistently exhibits the highest hydraulic conductivity values, aligning with expectations from the conceptual model. Notably, the western portion of this unit shows the highest values (refer to Figure 4.10). The Shear zone follows as the second most conductive zone, with an average hydraulic conductivity of approximately  $10^{-2}$  m/d. In contrast, the Saprolite and Fresh rock units exhibit the lowest conductivity values, indicating that most water is conveyed into the pit via the Shear zone. The spatial distribution of conductivity in both the Shear zone and Fresh rock units appears consistent across the model domain, with no distinct patterns emerging.

Upon history matching (iteration 2 of PESTpp-IES), the posterior parameter distributions reveal several important shifts from their prior counterparts. In terms of hydraulic conductivity (Figure 4.7), the posterior distributions across most units are narrower and more peaked, suggesting that the parameterisation reduced uncertainty and favoured a more constrained range of values. For instance, the Saprock, Fresh rock and Shear zone units show a marked reduction in variance, confirming their dominant hydraulic roles while enhancing model confidence in those properties. The Saprolite and Colluvium units also exhibit posterior narrowing, with slight shifts in the mode, suggesting adjustments to better align with observed heads and fluxes.

In specific storage (Figure 4.8), the posterior distributions generally maintain the same central tendencies as their priors but exhibit clear reductions in spread – most notably in the Shear zone and Saprock units. Only the Shear zone unit shows an upward shift to values around  $10^{-4}$  m<sup>-1</sup>. Regarding specific yield (Figure 4.9), as specific storage, the distribution maintains similar central tendencies, showing lightly downward changes in Colluvium, Saprolite and Saprock units, while increasing values in Fresh rock and Shear zone units. Figure 4.11 and Figure 4.12 illustrate the spatial distribution of specific storage and specific yield, respectively. As shown, the parameter values are generally well distributed within each unit.

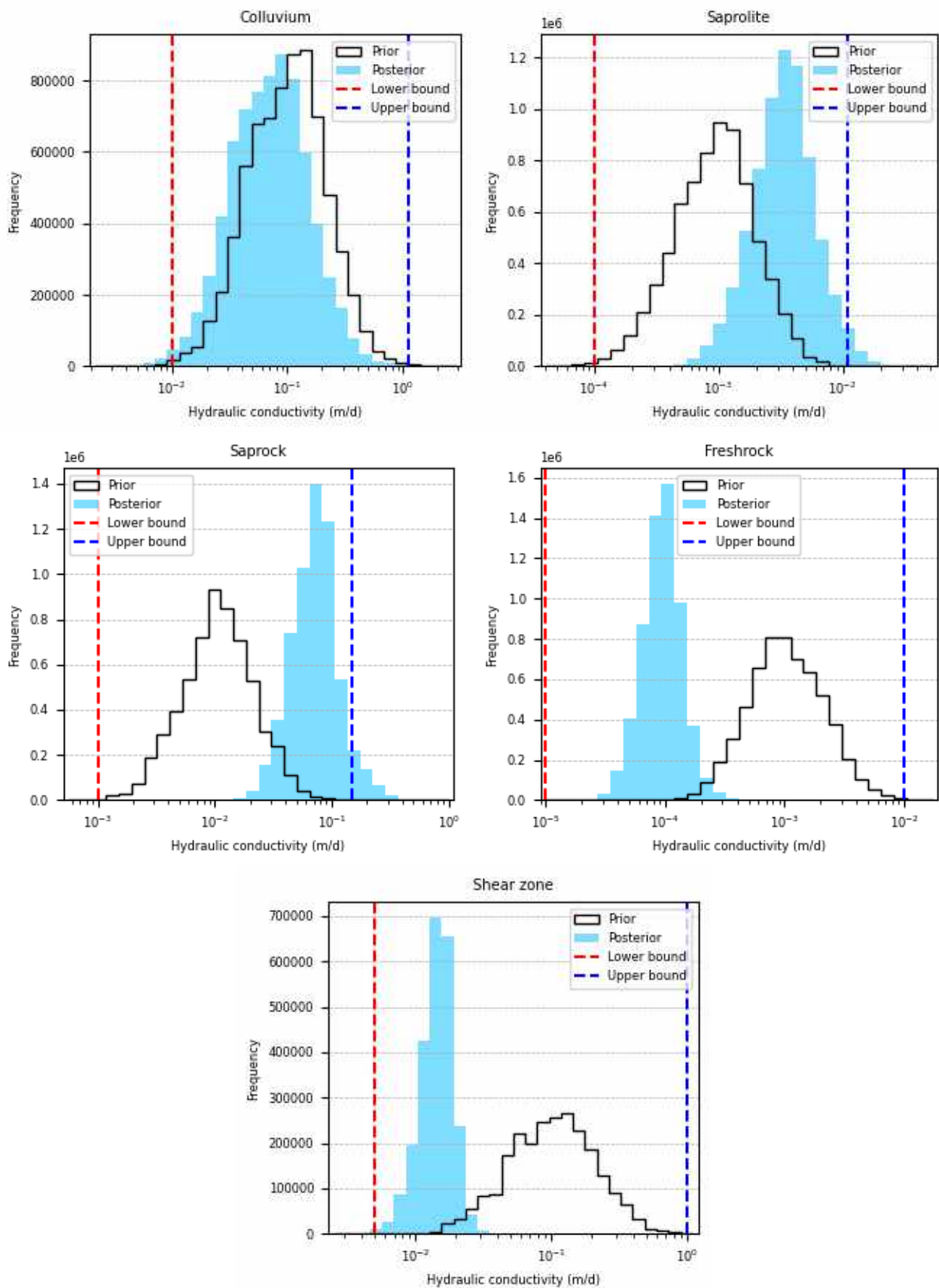


Figure 4.7 Parameter distributions – Horizontal conductivity – Whole ensemble

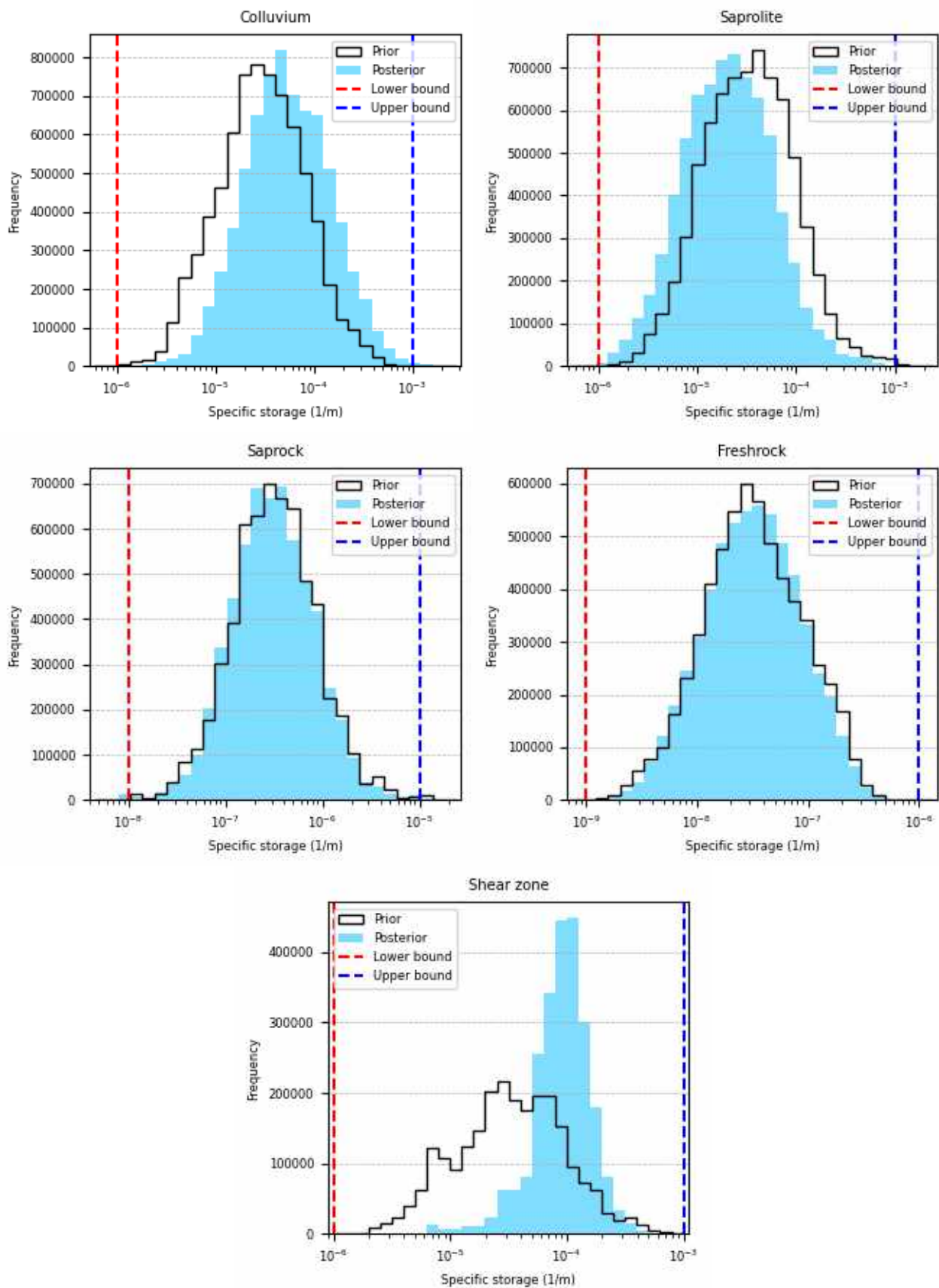


Figure 4.8 Parameter distributions – Specific storage – Whole ensemble

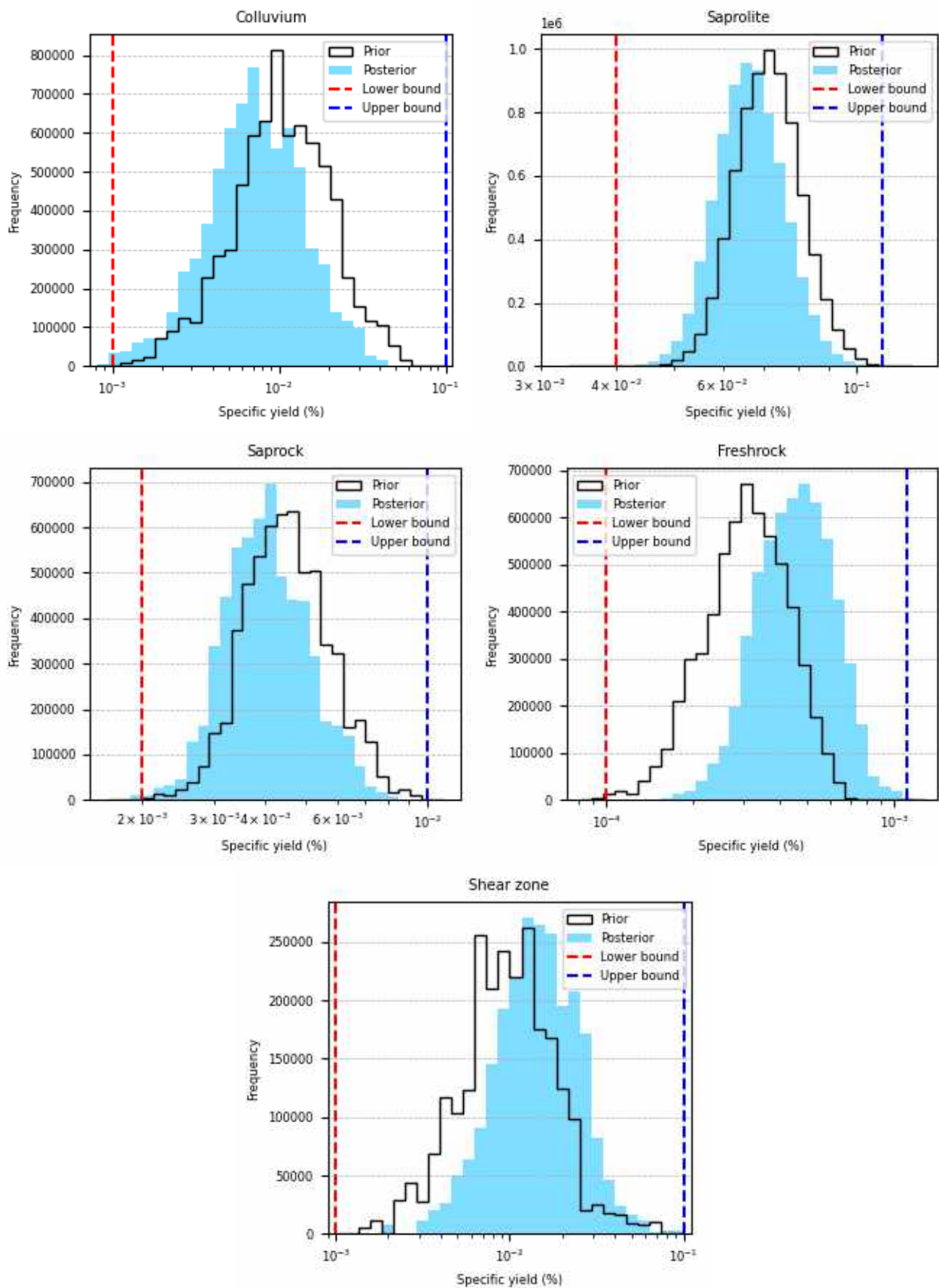


Figure 4.9 Parameter distributions – Specific yield – Whole ensemble

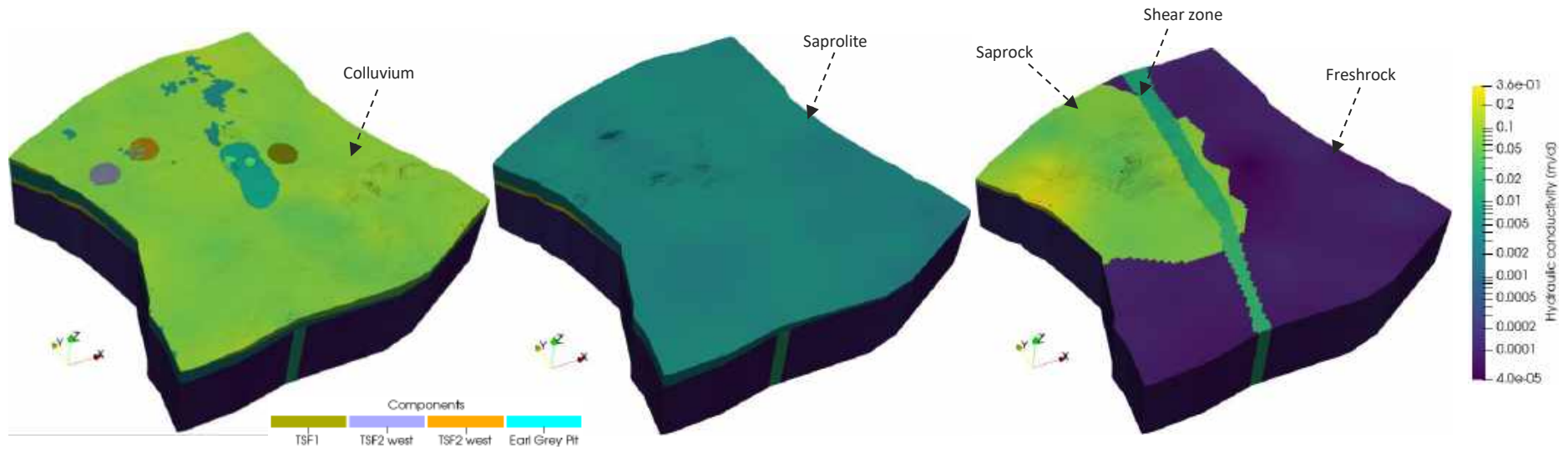


Figure 4.10 Spatial distribution of adopted hydraulic conductivity – percentile 50 of the total of realisations (vertical exaggeration x 5)

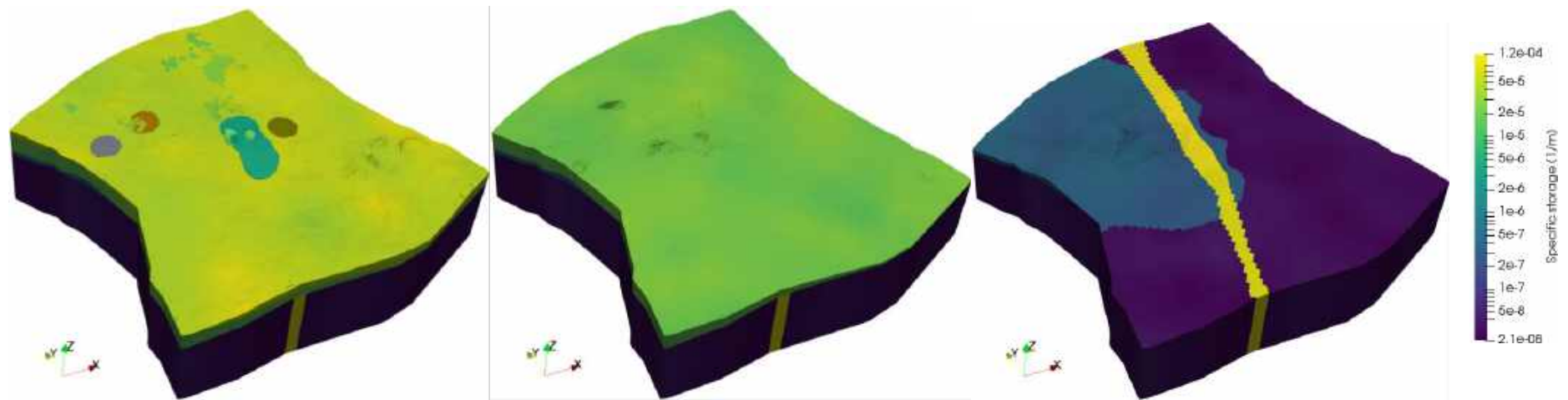


Figure 4.11 Spatial distribution of adopted specific storage – percentile 50 of the total of realisations (vertical exaggeration x 5)

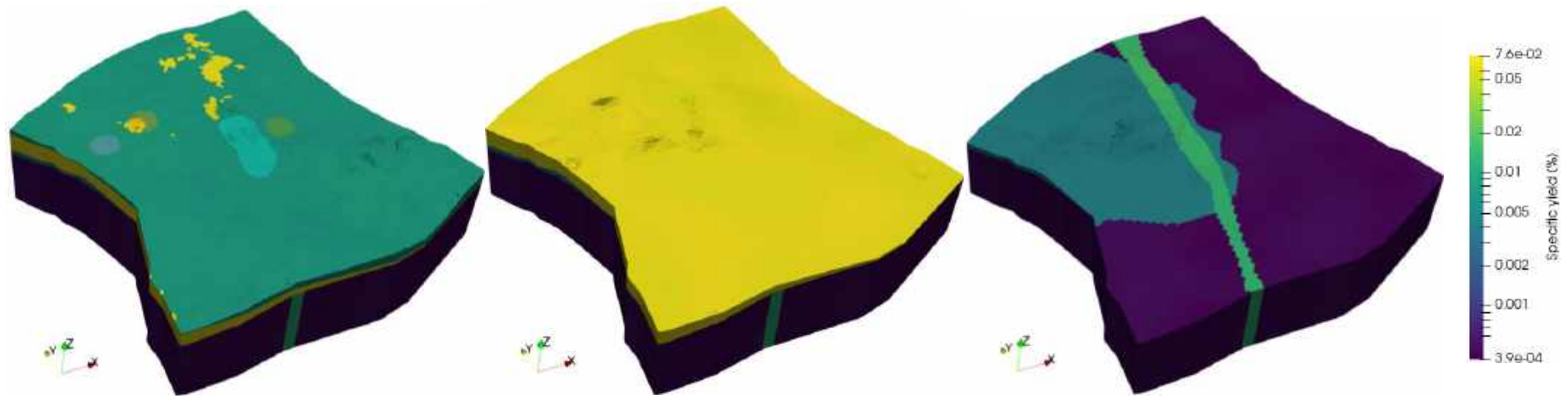


Figure 4.12 Spatial distribution of adopted specific yield – percentile 50 of the total of realisations (vertical exaggeration x 5)

## 5 Predictions

### 5.1 Overview and objectives

The first objective of the current model is to simulate fate and transport of seepage from TSF2, with the western section scheduled from November 2028 to December 2048 and the eastern section from September 2030 to January 2050. Second, the model also incorporates the updated mining plan for the Earl Grey pit, alongside the current and future operations of TSF1, to assess their combined impacts on the groundwater system. Specifically, the model predicts the seepage from the TSFs, dewatering rates, groundwater drawdown, and groundwater levels in the monitoring bores throughout both the predictive and recovery periods. The recovery phase extends for 100 years following mine closure.

### 5.2 Scenario definition and representation

#### 5.2.1 Updated Earl Grey Lithium mine plan

The updated mining plan for the Earl Grey Lithium pit was simulated using the DRN package, consistent with the methodology outlined in Section 3.5.1. Compared to the current configuration, the future pit is significantly larger—with an area of 1,777,581 m<sup>2</sup> approximately four times greater—and deeper, extending from 360 mAHD down to 91 mAHD.

During the 100-year recovery period (from the end of operations, December 2049, to December 2150), a water balance was conducted accounting for inflows into the pit void. Given that groundwater will be exposed, both evapotranspiration and recharge were considered as part of the pit-lake dynamics. The stage at which the water balance is achieved – where inflows plus recharge equal evapotranspiration – was determined through analytic calculations. This equilibrium level was used to define the General Head Boundary (GHB) condition within the pit shell cells. These cells were assigned transient stage values until the system reached equilibrium, at which point the final stage values were applied to represent long-term conditions.

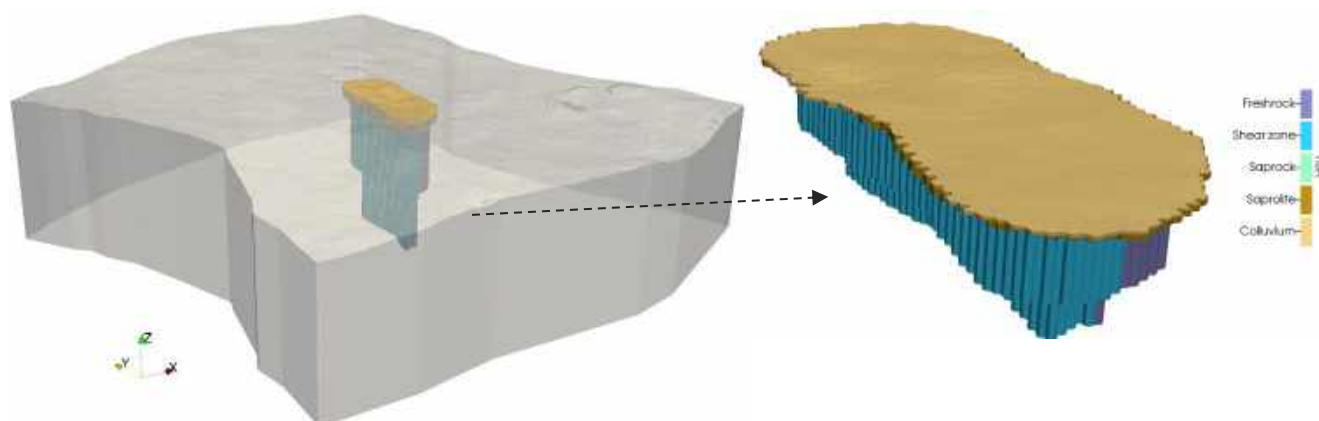


**Figure 5.1** Updated mine plan – DRN cells (vertical exaggeration x 5)

#### 5.2.3 TSFs

The TSF2 (west and east sides) seepage was simulated with the river boundary condition as explained in Section 3.5.2. Each of the sides cover an approximate area of 388,950 of m<sup>2</sup>. The western side will operate from November 2028 to December 2048, while the eastern side will operate from September 2030 to January 2050. The growth of both sides was implemented using yearly stress periods; the end of the eastern side marks the end of the operation and the beginning of the recovery period. For the recovery period the TSFs boundary conditions were removed from the numerical model, effectively eliminating seepage. The TSF1 operations was extended until December 2033 with the same methodology.

## 5.3 Results

### 5.3.1 Water balance

The percentile 50 of the total of realisations water balance for the whole model during the predictive period (operations and recovery phases) is presented in Figure 5.2. During the operations (2025–2050), the system undergoes a marked shift from a groundwater-dominated regime to one increasingly influenced by operational dynamics associated with the dewatering from the Earl Grey pit and TSFs seepage, which impact the storage. Initially, system inflows are primarily driven by storage increases, TSF seepage, and constant head boundary inflows, while the Earl Grey pit sump pump represents the dominant outflow, with discharges exceeding 3,500 kL/day. From 2046 onward, pit lake recharge begins to impact the water balance, with rainfall and surface runoff accumulation in the pit area. Concurrently, evapotranspiration from the pit surface introduces a new outflow pathway, gradually offsetting the gains from recharge.

In the recovery period (2051–2150), the system transitions into a more stable, passive hydrological state. Active pumping ceases, and storage inflows gradually decline, reflecting reduced recharge and system adjustment post-mining. Constant head boundary inflows remain steady, while storage outflows decrease over time, suggesting a decline in system drainage. The pit lake emerges as the primary hydrological feature, with its recharge progressively decreasing and evapotranspiration maintaining relatively consistent outflow levels of around -480 kL/day. This balance between rainfall-driven inflow and atmospheric losses suggests the pit lake reaches a long-term equilibrium, becoming the dominant mechanism controlling the system's water balance.

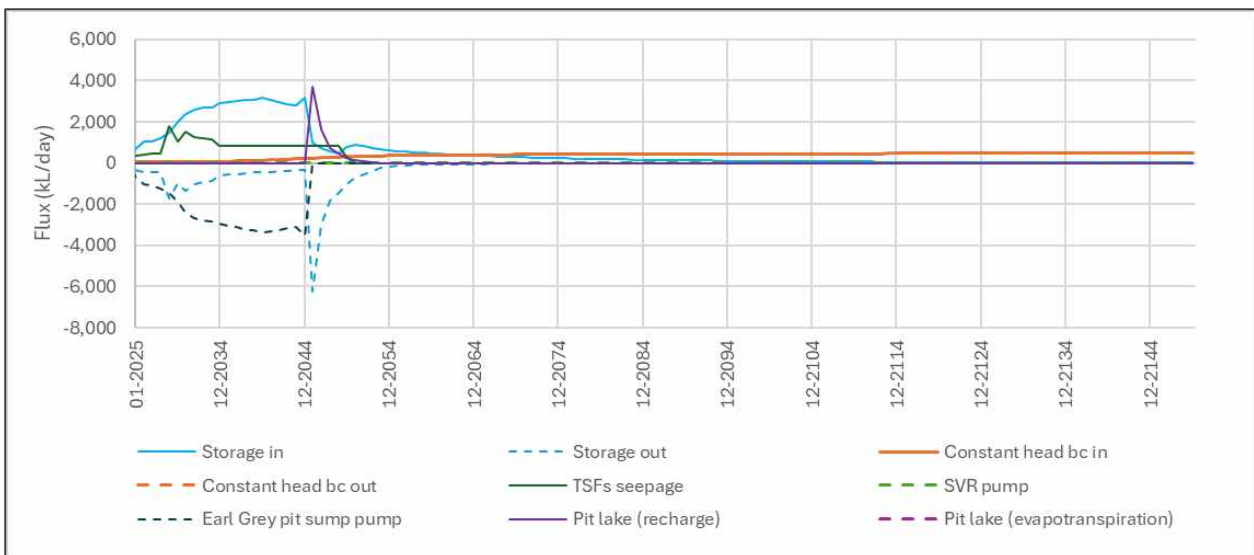


**Figure 5.2** Water balance during predictive period

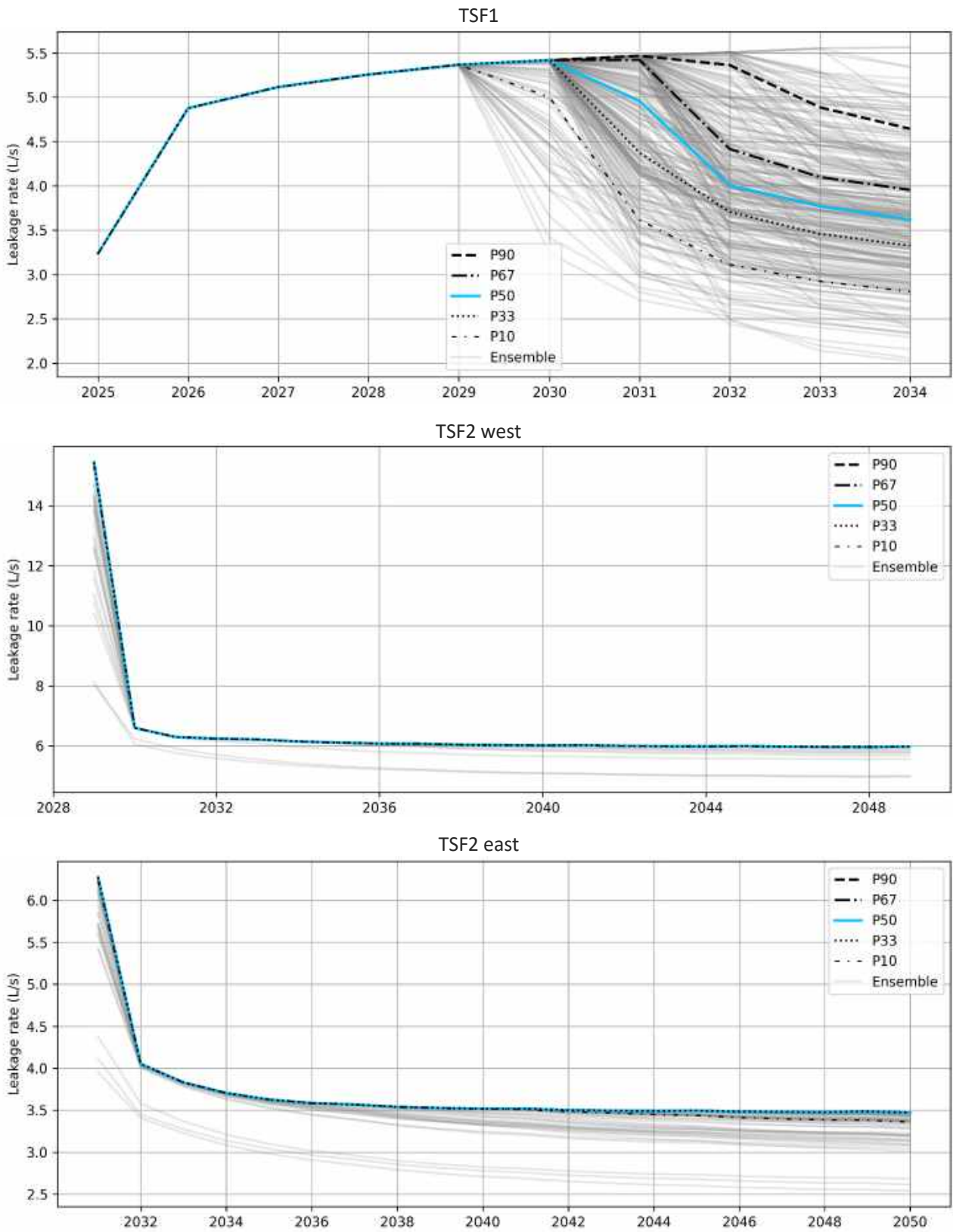
### 5.3.2 Predictive seepage from the TSFs

Figure 5.3 presents the simulated seepage rates (in L/s) from TSF1 and the newly planned TSF2 (west and east sides), based on groundwater model outputs over time. The values are presented as percentiles derived from 300 realisations, reflecting uncertainty in the system response. These seepage rates represent additional groundwater recharge inputs from the tailings storage facilities and are critical for understanding their long-term influence on the surrounding hydrogeology, particularly in terms of rising water tables and potential interactions with mining and recovery conditions.

Seepage from TSF1 is relatively consistent across the simulated period, with rates increasing modestly from 3 L/s in 2024 to a peak median value of approximately 5 L/s in 2029–2030, before gradually declining to about 4 L/s by 2045. The initial increase corresponds with tailings growth, while the decline reflects either reduced loading or stabilisation of hydraulic gradients as the facility matures.

The TSF2 exhibits a notable peak in seepage at 15 L/s in its initial year (2028), which then declines to a relatively stable range of around 6 L/s from 2033 onwards. A key factor influencing this behaviour is the presence of a thicker Saprock unit beneath TSF2 west. This unit, which overlies the Fresh rock and is itself overlain by Saprolite and Colluvium, is characterised by elevated hydraulic conductivity compared to other formations. As such, the Saprock acts as a conduit for seepage, potentially facilitating deeper and more rapid infiltration of water into the groundwater system. Over time, this may contribute to a progressive rise in the water table beneath and downgradient of TSF2 west.

In contrast, the TSF2 east shows a more gradual and consistent seepage profile. Initial seepage rates begin around 6 L/s in 2030 and decline steadily to approximately 3.5 L/s by 2049. While lower than those of the west side, the ongoing seepage may still lead to localised groundwater mounding, particularly in areas where less permeable layers limit lateral dispersion.



**Figure 5.3** Predicted seepage from the TSF1 during the operation

### 5.3.3 Predictive dewatering volumes

Figure 5.4 presents the predicted dewatering rates from the numerical groundwater model, expressed in L/s, and based on percentiles derived from 300 realisations. These values represent the volume of groundwater that must be removed from the Earl Grey pit to maintain dry conditions suitable for mining operations. The model predicts a rapid increase in dewatering demand between early 2024 and 2031, with the median (P50) rate rising from approximately 0.7 L/s in August 2024 to around 28 L/s by January 2031. This trend reflects the progressive deepening and lateral expansion of the pit. From 2031 onwards, dewatering requirements continue to increase, albeit at a slower rate, peaking near the end of the mine life. The highest median dewatering rate occurs in January 2045 at approximately 41 L/s, just after mining ceases on 31 December 2044. The P90 values – indicating more conservative (upper-bound) scenarios – reach up to 49 L/s, highlighting the potential variability and uncertainty in groundwater inflows that must be considered for operational planning.

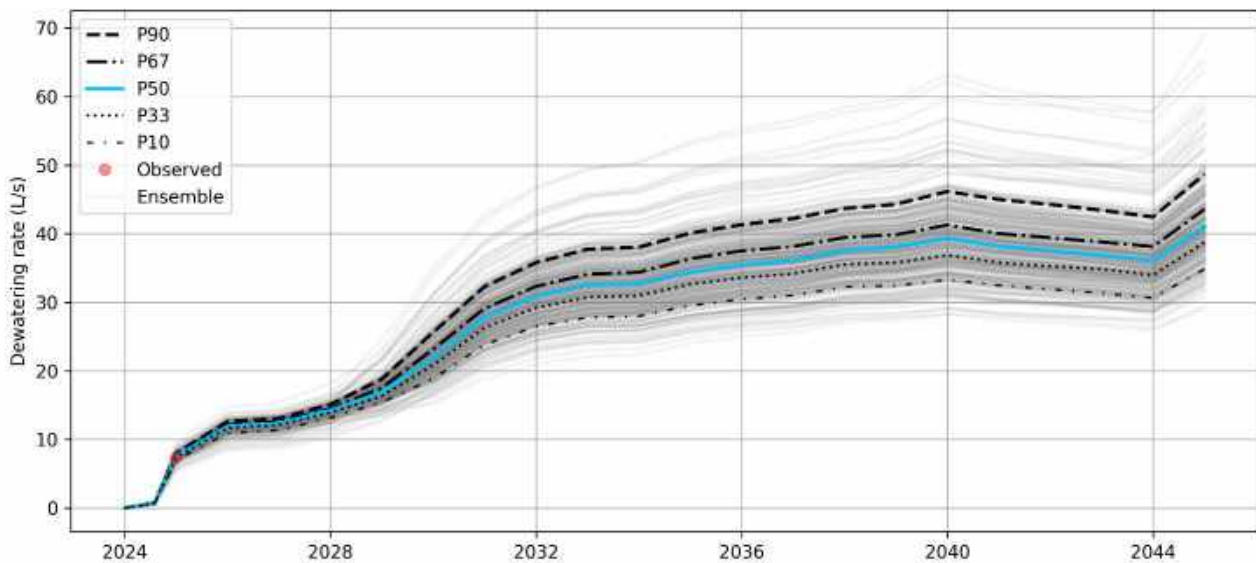


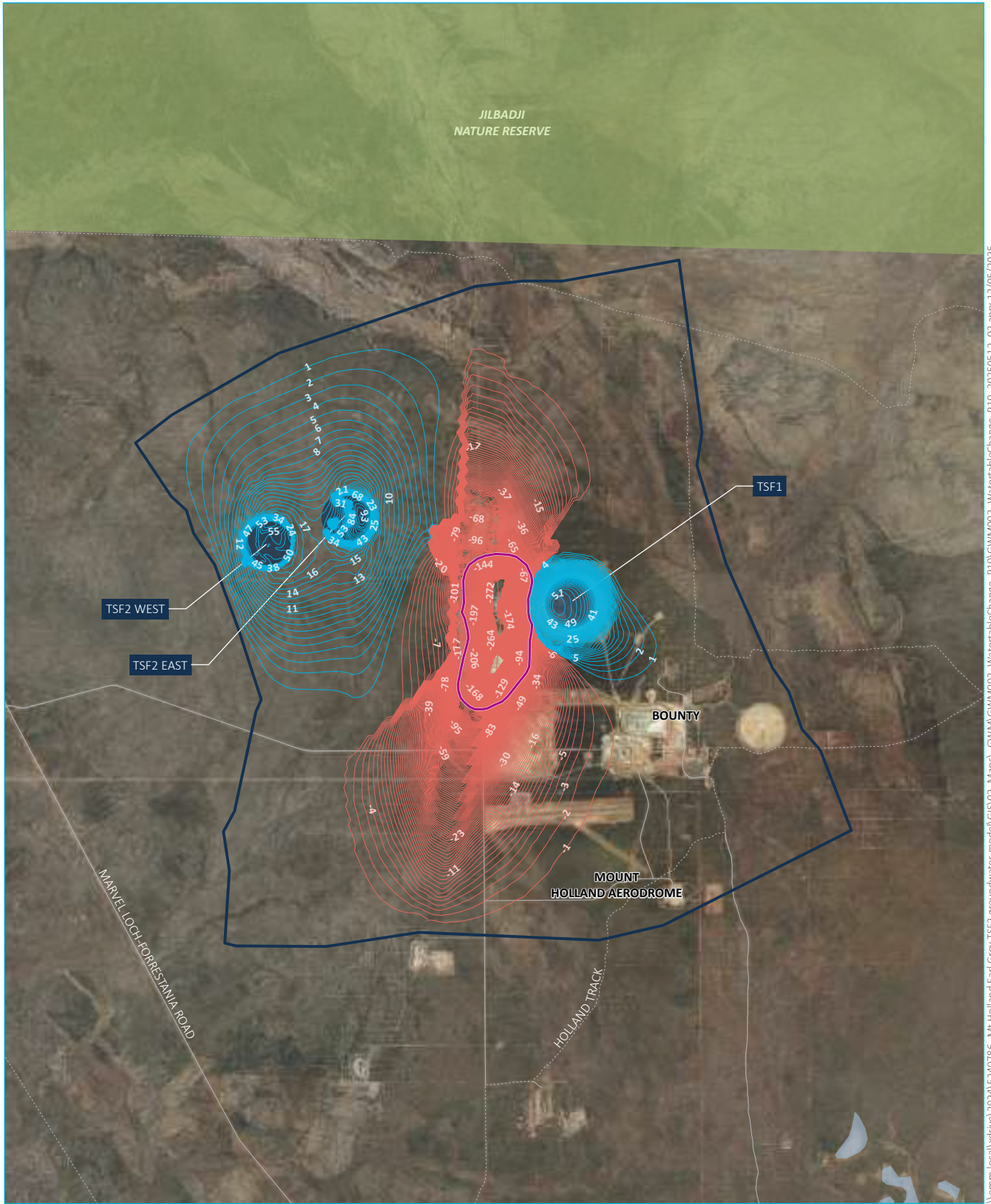
**Figure 5.4** Predicted modelled dewatering to Earl Grey

### 5.3.4 Head change at the end of operations

For the head change, the steady-state hydraulic heads were subtracted by the simulated heads at the end of the life of mine. The P10, P50 and P90 results are shown in Figure 5.5, Figure 5.6 and Figure 5.7. In all three percentile scenarios, the most prominent feature is the large, elongated cone of depression centred on the Earl Grey pit. Maximum drawdowns exceed  $-280$  m under the P90 scenario, with a substantial area of influence extending beyond 1 km in the north–south direction. Importantly, this drawdown is not symmetrical; instead, it displays a distinctly north–south elongation, which can be explained by both the hydrogeological structure and anisotropy of the model domain. As shown in Figure 4.10, a north–south trending Shear zone traverses the full length of the domain, cutting through the pit area with enhanced permeability along its axis. This Shear zone, mapped as a high-conductivity feature, has been represented as a preferential flow path, enabling more efficient groundwater movement and therefore greater drawdown propagation along its extent.

Additionally, the numerical model incorporates horizontal anisotropy, where hydraulic conductivity is higher in the north–south direction than in the east–west. This anisotropy aligns with the orientation of the Shear zone and reinforces the directional flow behaviour observed in the drawdown contours. Lateral drawdown propagation is therefore more pronounced along this structural corridor, extending up to 8 km north to south, while restricted in the perpendicular direction due to lower conductivity and the presence of less permeable lithologies such as Sapolite and fresh rock.

On the other hand, areas of positive head change—representing groundwater mounding—are clearly associated with seepage from the TSFs. TSF2 west exhibits the most substantial mounding, with values exceeding +50 m under higher percentile cases, consistent with its underlying thick Saprock unit, which has higher conductivity and greater capacity to transmit seepage into the groundwater system. TSF2 east also shows mounding of up to +60 m (mainly as its end of operation matches the end of the life of mine January 2050), while TSF1, although producing more localised mounding, is situated closest to the pit and therefore contributes to a hydraulic gradient towards the excavation. In some scenarios, particularly P90, this seepage-induced mounding appears to interact with the drawdown cone, highlighting the importance of hydraulic connectivity between the TSFs and the pit.



Source: EMM (2025); Landgate (2021, 2025); Esri (2025); GA (2009)

\\emh.local\drive\2024\E240786- Mt Holland Earle Grey TSF2 groundwater model\GIS\02\_Maps\GWM\GWM002\_WatertableChange\_P10\_20250512.aprx 12/05/2025

**KEY**

- Earl Grey pit boundary
- Model extent
- Tailings storage facility (TSF)
- Drawdown contour
- Negative potentiometric head change (m)
- Positive potentiometric head change (m)
- Existing environment
- Minor road
- Vehicular track
- Waterbody
- Reserve

Potentiometric heads change (drawdown / mounding) at the end of the operations (P10)

Covalent Lithium  
Mt Holland Earle Grey TSF2 Groundwater Model  
Figure 5.5





Source: EMM (2025); Landgate (2021, 2025); Esri (2025); GA (2009)

\\emh.local\drive\2024\E240786- Mt Holland Earle Grey TSF2 groundwater model\GIS\02\_Maps\GWM\GWM003\_WatertableChange\_P50\_20250512.aprx 12/05/2025

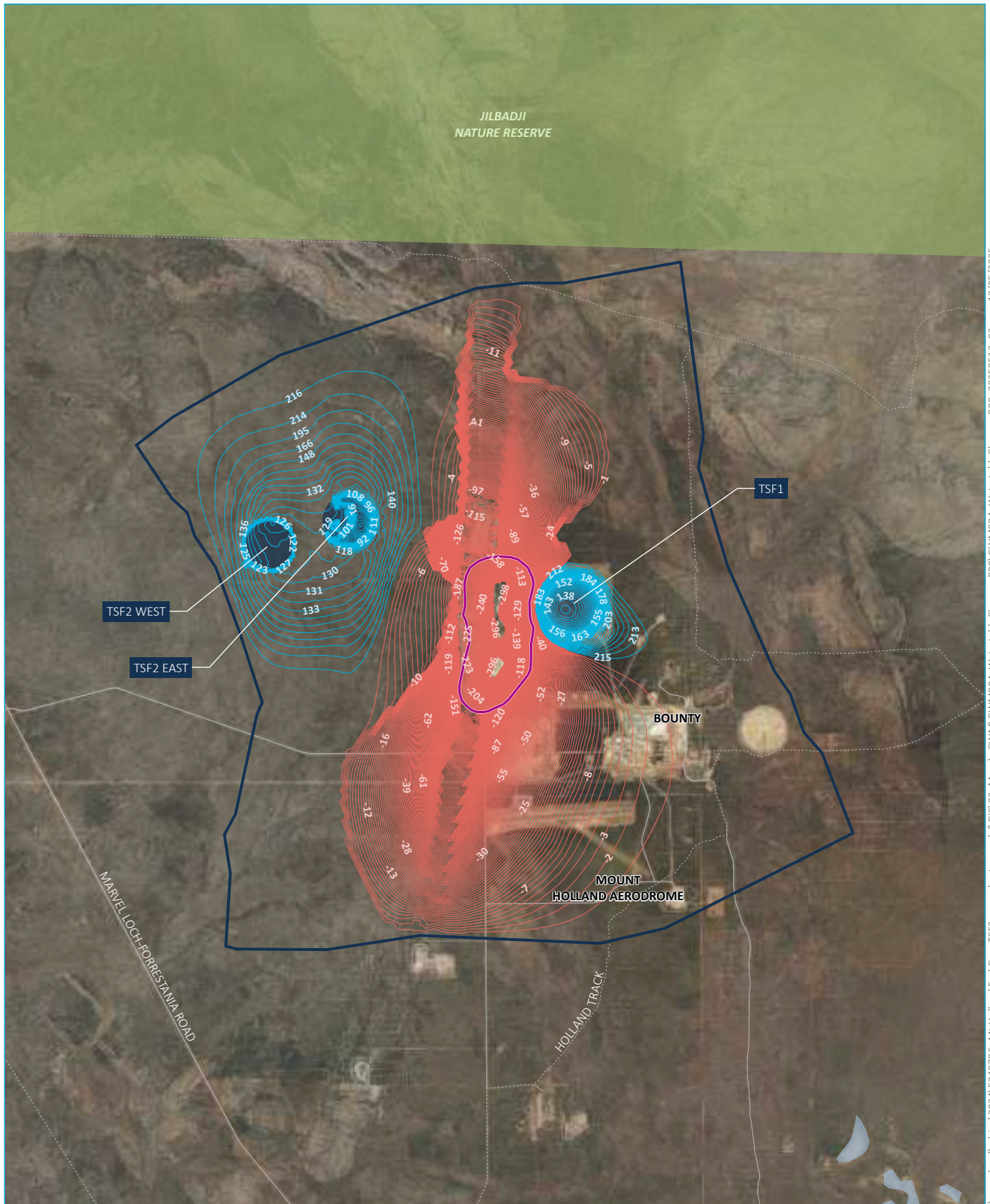
**KEY**

- Earl Grey pit boundary
- Model extent
- Tailings storage facility (TSF)
- Drawdown contour
- Negative potentiometric head change (m)
- Positive potentiometric head change (m)
- Existing environment
- Minor road
- Vehicular track
- Waterbody
- Reserve

Potentiometric heads change (drawdown / mounding) at the end of the operations (P50)

Covalent Lithium  
Mt Holland Earle Grey TSF2 Groundwater Model  
Figure 5.6





Source: EMM (2025); Landgate (2021, 2025); Esri (2025); GA (2009)



**KEY**

- Earl Grey pit boundary
- Model extent
- Tailings storage facility (TSF)
- Drawdown contour
- Negative potentiometric head change (m)
- Positive potentiometric head change (m)
- Existing environment
- Minor road
- Vehicular track
- Waterbody
- Reserve

Potentiometric heads change  
(drawdown / mounding) at the  
end of the operations (P90)

Covalent Lithium  
Mt Holland Earle Grey TSF2 Groundwater Model  
Figure 5.7



\\emm.local\drive\2024\E240786- Mt Holland Earle Grey TSF2 groundwater model\GIS\02\_Maps\GWM\GWM004\_ WatertableChange\_P90\_20250512.aprx 12/05/2025

### 5.3.5 Hydrogeological system conditions during the recovery period

Figure 5.8 presents the head change relative to steady-state conditions (P50), showing that the central drawdown cone corresponds to the location of the future pit lake remains the most prominent feature. The resulting final potentiometric surface, shown in Figure 5.9, confirms the stabilisation of the pit lake at 264 mAHD, with surrounding water levels exceeding 400 mAHD in distal areas. The resulting hydraulic gradients remain directed towards the pit, validating its long-term role as a terminal groundwater sink. Under these conditions, the lake is expected to continue capturing regional groundwater inflows passively, without the influence of active dewatering. The residual head change (see Figure 5.9) around the pit is now considerably reduced in magnitude compared to operational conditions, with maximum drawdowns approximating -110 m. However, the shape of the cone remains elongated along the north–south axis, a reflection of the north–south trending Shear zone and the anisotropic hydraulic conductivity applied in the model, which favours flow and drawdown propagation along this direction. These combined hydrogeological controls continue to influence groundwater movement even after active dewatering has ceased.

Additionally, Figure 5.9 includes forward particle paths shown as red lines, which represent the direction of groundwater movement in the long term under post-closure conditions. While many of the longest tracks converge toward the Earl Grey pit, reflecting the strong hydraulic gradient created by the pit lake, several shorter trajectories – particularly from the northwestern margins of TSF2 west and TSF2 east – diverge toward the northwestern edge of the domain. This suggests that although the pit acts as a dominant sink, some local gradients and heterogeneity in hydraulic conductivity influence flow paths near the TSFs.

In contrast, the groundwater mounding observed near TSF1, to the east of the pit, persists over time. This indicates that infiltrated water is migrating through the lower-transmissivity Saprolite and fresh rock units, resulting in a significant delay in the dissipation of seepage-induced mounding. As a result, potentiometric heads in this area remain elevated, forming a distinct mound that is clearly visible in both the head change and potentiometric surface figures.

Meanwhile, the zones formerly influenced by TSF2 west and TSF2 east, located to the west of the pit, now show near-neutral or dissipated head changes. These facilities overlay regions where the Saprock unit is thicker and more transmissive, particularly beneath TSF2 west. This stratigraphy enabled more efficient vertical and lateral dispersion of seepage during and after operations, allowing the mounded groundwater levels to equilibrate over a much shorter timescale. As a result, by the end of the recovery period, the groundwater system beneath TSF2 has returned to near pre-mining levels, and any residual hydraulic mounding has been absorbed into the regional system.



Source: EMM (2025); Landgate (2021, 2025); Esri (2025); GA (2009)

\\emmi.local\drive\2024\E240786- Mt Holland Earl Grey TSF2 groundwater model\GIS\02\_Maps\GWM\GWM005\_WatertableChange\_100yrs\_P50\_20250512\_02.aprx 12/05/2025

**KEY**

- Earl Grey pit boundary
- Model extent
- Tailings storage facility (TSF)
- Drawdown contour
- Negative potentiometric head change (m)
- Positive potentiometric head change (m)
- Existing environment
- Minor road
- Vehicular track
- Waterbody
- Reserve

Potentiometric heads change  
(drawdown / mounding)  
100 years after mine closure (P50)

Covalent Lithium  
Mt Holland Earl Grey TSF2 Groundwater Model  
Figure 5.8





Source: EMM (2025); Landgate (2021, 2025); Esri (2025); GA (2009)

**KEY**

- Earl Grey pit boundary
- Model extent
- Tailings storage facility (TSF)
- Watertable contour (mAHd)
- Particle tracking line
- Existing environment
- Minor road
- Vehicular track
- Waterbody
- Reserve

Potentiometric heads  
100 years after mine closure (P50)  
and particle tracking

Covalent Lithium  
Mt Holland Earle Grey TSF2 Groundwater Model  
Figure 5.9



\\emm.local\vdv\ve\2024\E240786- Mt Holland Earle Grey TSF2 groundwater model\GIS\02\_Maps\GWM\GWM006\_Watertable\_100yrs\_PostClosure\_P50\GWM006\_Watertable\_100yrs\_PostClosure\_P50\_20250512\_02.aprx 12/05/2025

## 6 Limitations

The following limitations have been identified:

- **Monitoring data:** While many monitoring bores have limited construction details and historical groundwater records are often inconsistent or of short duration, a subset does provide useful data for history matching. Given the 125-year predictive timeframe (25 years of operations and 100 years of recovery), ongoing and expanded monitoring will be essential to reduce uncertainty and improve confidence in long-term model predictions.
- **Spatial coverage:** The model domain is relatively small, which restricts the full representation of regional flow systems. This can artificially limit the spatial extent of drawdown and mounding due to boundary condition constraints. The constant head boundaries used at the domain edges may not fully reflect the natural hydraulic drivers at the regional scale.
- **Conceptual uncertainty:** Geological understanding is based on the Geological Survey Western Australia 1:100,000 scale interpreted bedrock geology. Hydrogeological understanding is localised to areas where drilling and temporal groundwater level monitoring have occurred. As a result, the representation of HSUs outside these zones is largely extrapolated and uncertain.
- **Simplified representation:** No vertical variation in parameter fields was applied within each HSU, and spatially invariant recharge and evapotranspiration assumptions were adopted. These simplifications are appropriate for representing regional groundwater flow patterns and ensuring model stability; however, they may not fully capture local-scale variability in hydraulic processes, particularly at the interfaces between hydrogeological units, which could influence finer-scale flow dynamics.

## 7 Summary and recommendations

The numerical groundwater model developed for the Earl Grey Lithium Project provides a framework for assessing the hydrogeological impacts of pit dewatering and tailings storage facility (TSF) seepage during operations and post-closure. Implemented using the MODFLOW-USG code through the Groundwater Vistas interface, the model benefits from the flexibility of unstructured grids, allowing for high-resolution representation of project components while reducing computational demand.

Model history matching performance for the modelled groundwater levels showed a SRMS of 0.76%, a residual mean of 0.02 m and a mean absolute error of 0.06 m, reflecting alignment with observed data given the limited and short-duration monitoring records available. Parameterisation through ensemble-based inversion allowed for uncertainty analysis, supporting more informed predictions of future behaviour under variable hydrogeological conditions.

The model simulated key processes including dewatering requirements, seepage from TSFs, and the groundwater system's long-term recovery. Predictive results show that the greatest drawdown occurs in response to pit dewatering, with a pronounced north–south elongation driven by a structurally-aligned Shear zone and horizontal anisotropy. TSF-related seepage, particularly from TSF2 west, generated mounding during operations. However, 100 years after closure, only residual mounding persists – most notably near TSF1 – where low-permeability materials inhibit dissipation. In contrast, TSF2-related mounding largely dissipated due to more transmissive underlying geology. The pit lake level stabilised at 264 mAHD, continuing to function as a terminal groundwater sink.

To reduce uncertainties and increase the reliability of future modelling and groundwater management, the following actions are recommended:

- Enrich the current hydrogeological dataset: Continue monitoring groundwater levels around TSF1 and areas where mounding has been observed. Collect detailed bore construction logs, perform long-term groundwater level monitoring, and install nested piezometers to improve vertical hydraulic head resolution.
- Expand the model domain: Increase the spatial extent of the model to mitigate the artificial influence of fixed boundary conditions. Incorporating a broader topographic and hydrological context will potentially improve simulation of drawdown and recovery dynamics.
- Improve hydrogeological conceptualisation: geological mapping beyond infrastructure footprints and revisit structural interpretations, particularly of the Shear zone, to confirm its extent and hydraulic role.
- Continue groundwater level monitoring via the dataloggers at all the recently drilled monitoring bores – MB24-01; 02; 03; 04; 05; 06; 07; 09; 10 to capture long term and seasonal water level trends and potential impacts in the TSF-2 area.
- There should be an assessment on the condition and suitability of the existing Covalent monitoring bores for the installation of similar dataloggers to provide the spatial coverage and frequency of monitoring to detect potential impacts and the data required to update the numerical groundwater model.

## References

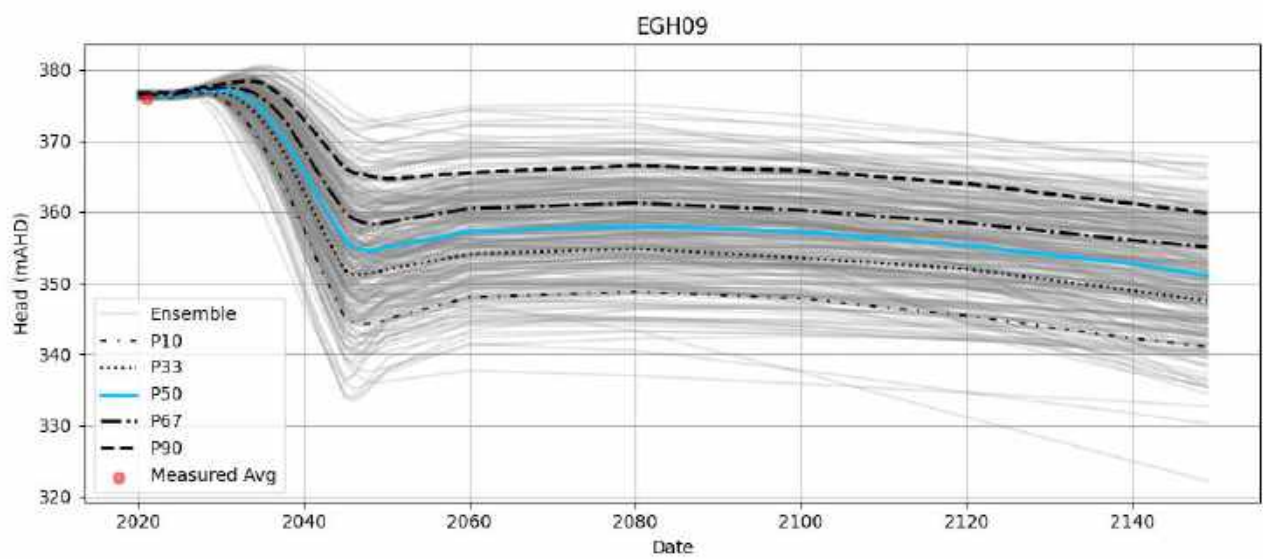
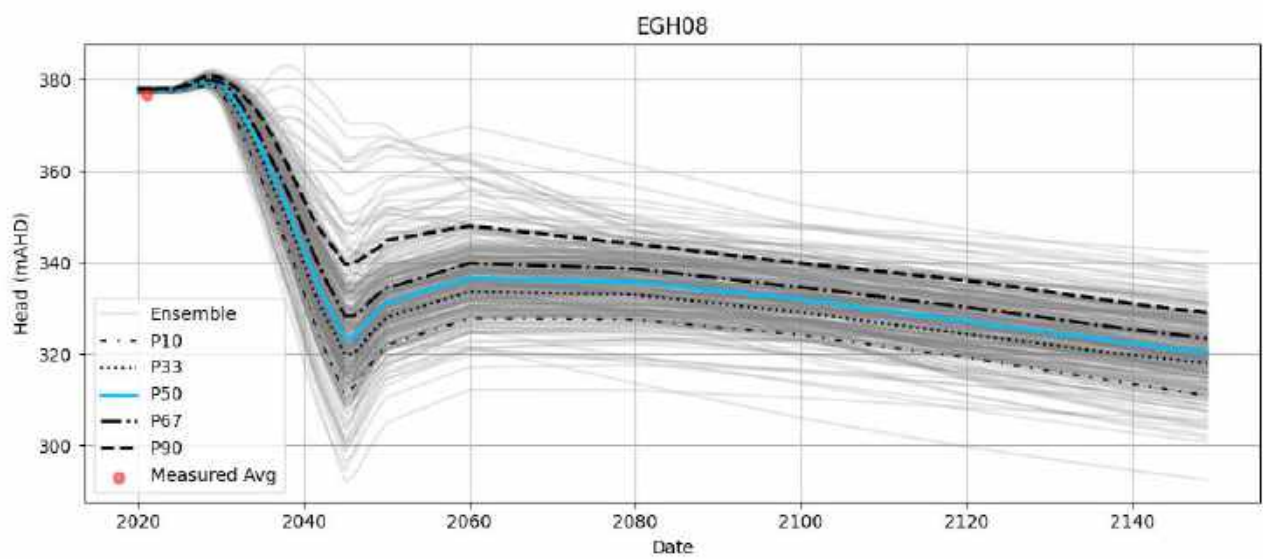
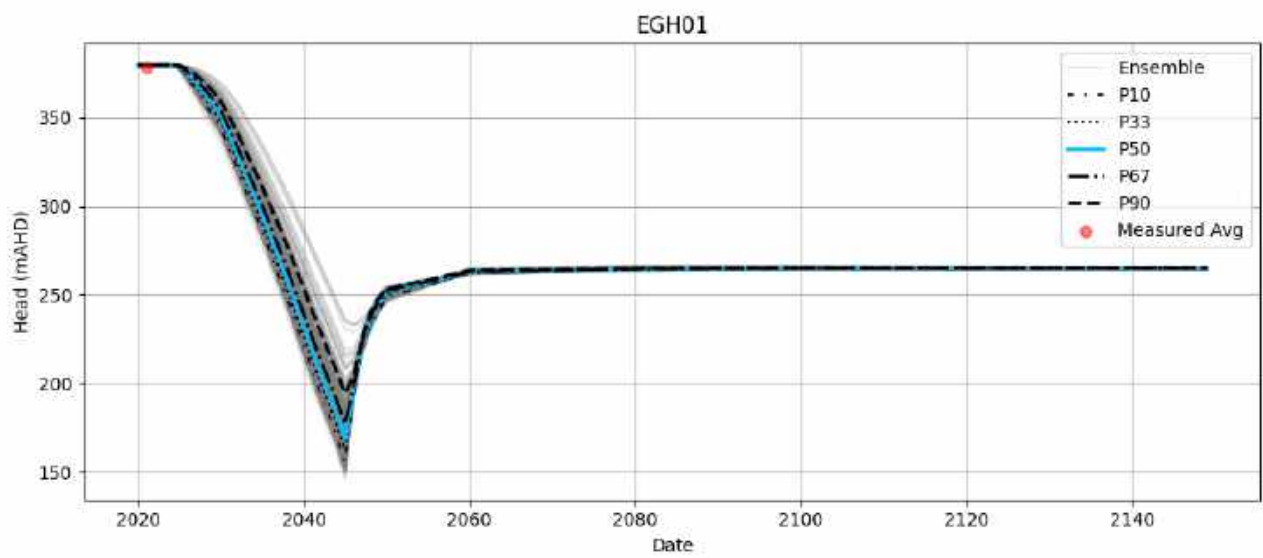
- Barnett B, Townley LR, Post V, Evans RE, Hunt RJ, Peeters L, Richardson S, Werner AD, Knapton A & Boronkay A 2012, *Australian Groundwater Modelling Guidelines*. Waterlines report series number 12. National Water Commission.
- Commander DP, Kern AM & Smith RA, 1992, Hydrogeology of the Tertiary palaeochannels in the Kalgoorlie region (Roe palaeodrainage). Western Australia Geological Survey, Record 1991/10, 56pp. Doherty J.E. 2018, PEST: Model-independent parameter estimation, 7<sup>th</sup> Edition published in 2018, Latest additions December 2024.
- Doublier MP, Thebaud N, Mole D, Wingate MTD, Kirkland CL, Romano SS, Wyche S & Duclaux G 2012, *New data on the geological evolution and gold mineralisation of the Southern Cross greenstone belt*, Geological Survey of Western Australia extended abstracts.
- Environmental Simulations Incorporated 2021, *Guide to using Groundwater Vistas version 8*, 2021.
- Golder, 2017. Western hub dewatering and water supply assessment. Hydrogeological conceptual model report. Report prepared for Fortescue Metals Group, March 2017.
- GRM, 2017. Report on Mount Holland Lithium Project hydrogeological study. Prepared for Kidman Resources Limited, December 2017.
- GRM, 2023. Earl Grey pit mine dewatering assessment report, 4 Mtpa operation. Prepared for Covalent Lithium Pty Ltd. 13 August 2023
- HydroAlgorithmics 2020, AlgoMesh 2 User Guide, August 2020.
- Jeffrey, SJ, Carter, JO, Moodie, KB and Beswick, AR, 2000. Using spatial interpolation to construct a comprehensive archive of Australian climate data, *Environmental Modelling and Software*, Vol 16/4, pp 309-330. DOI: 10.1016/S1364-8152(01)00008-1.
- Johnson SL, Commander DP & O'Boy CA, 1999, *Groundwater resources of the Northern Goldfields, Western Australia*. Water and Rivers Commission, Hydrogeological Record Series, Report HG 2, 57p.
- Keats W, 1991, *Geology and goldmines of the Bullfinch – Parker Range region, Southern Cross province, Western Australia*. Western Australia Geological Survey, Report 28, 44pp.
- Magee J, 2009, *Palaeovalley groundwater resources in arid and semi-arid Australia; A literature review*. National Water Commission, Geoscience Australia, Record 2009/3.
- Panday S., Langevin C.D., Niswonger R.G., Ibaraki M., and Hughes J.D. 2013, MODFLOW-USG version 1: *An unstructured grid version of MODFLOW for simulating groundwater flow and tightly coupled processes using a control volume finite-difference formulation*: U.S. Geological Survey Techniques and Methods, book 6, chap. A45, 66 p.
- Panday S. 2024, USG-Transport: Transport and other enhancements to MODFLOW-USG, version 2.4.0, GSI Environmental, 21 July 2024.
- Queensland DES (Department of Environment and Science), 2023. Scientific Information for Land Owners (SILO) climatic database, downloaded 8 June 2023, <https://www.longpaddock.qld.gov.au/silo/>
- Surface Water Solutions, 2023. Earl Grey Lithium Project surface water hydrology assessment. Prepared for Covalent Lithium Pty Ltd. Document Number: SWS-2023-CV-001/C. October 2023.
- White J.T., Hunt R.J., Fienen M.N., and Doherty, J.E. 2020, *Approaches to highly parameterised inversion: PEST++ version 5, a software suite for parameter estimation, uncertainty analysis, management optimization and sensitivity analysis*. U.S. Geological Survey Techniques and Methods 7C26, 52 p.
- URS, 2002. Bounty gold mine borefield aquifer review, July 2001 to June 2002. Unpublished report for Bounty Pty Ltd. August 2002.

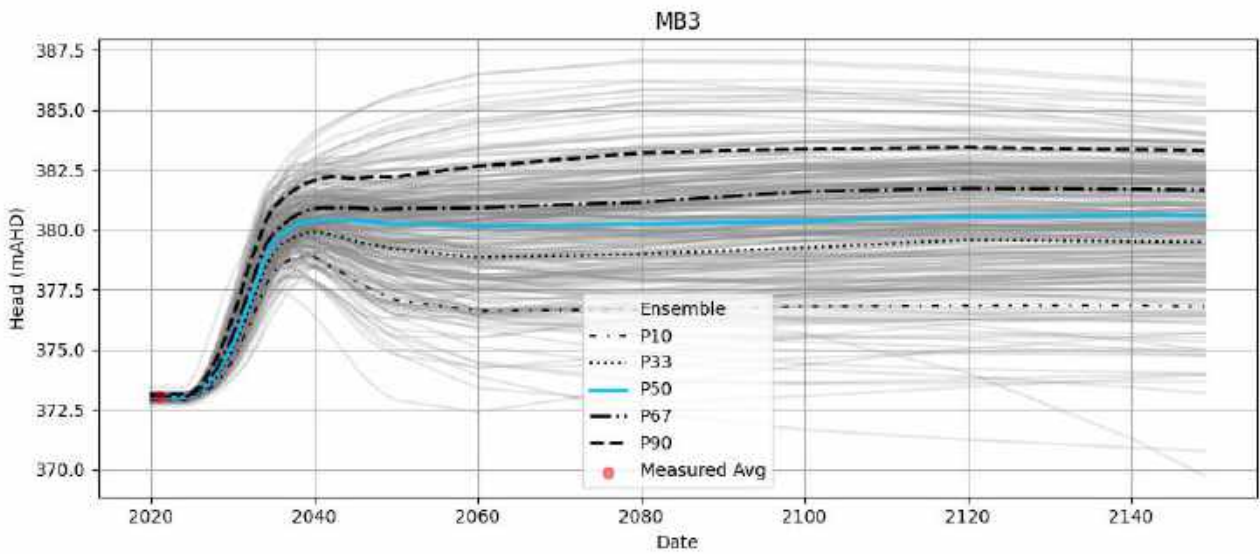
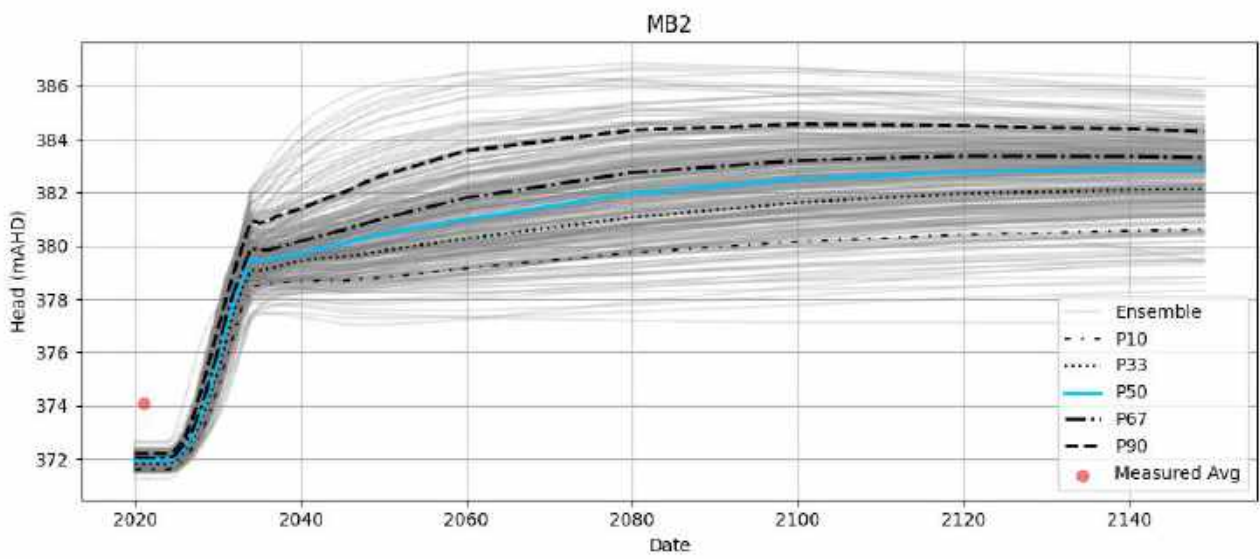
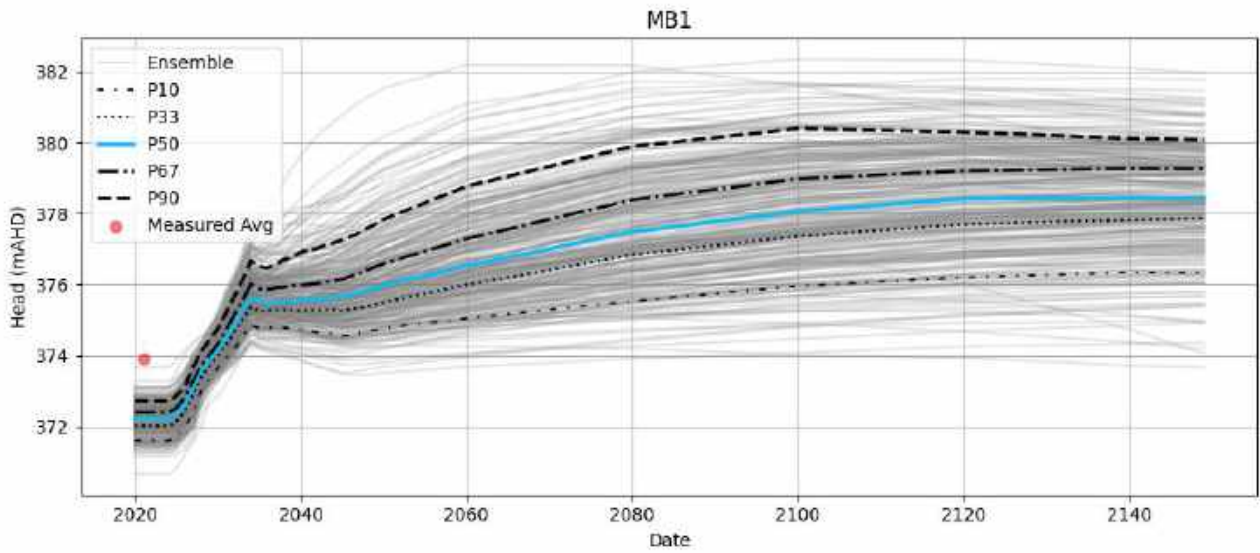
---

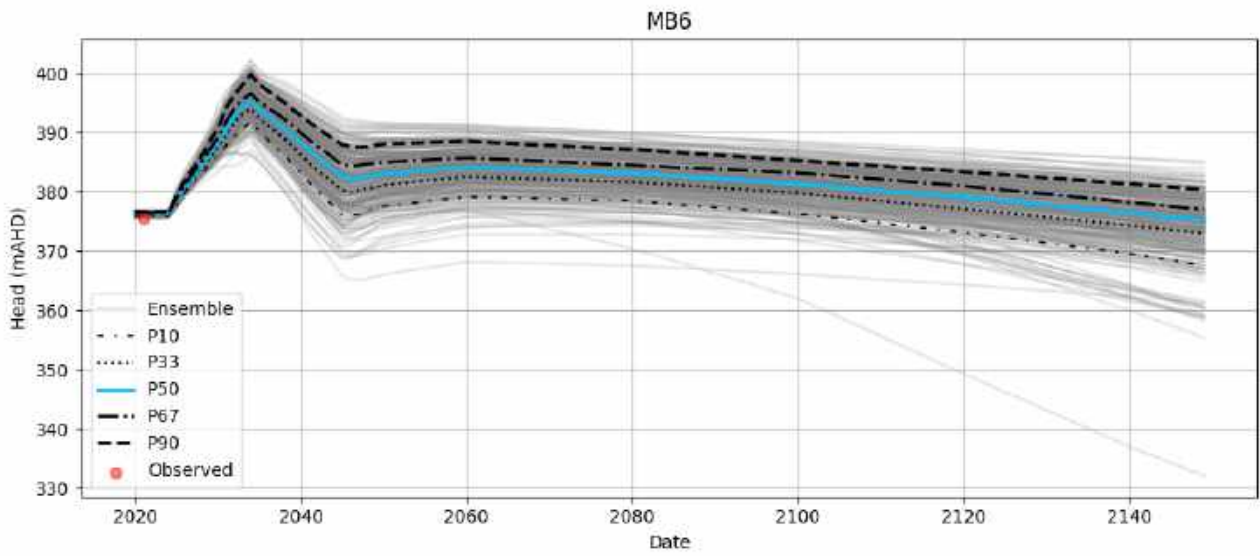
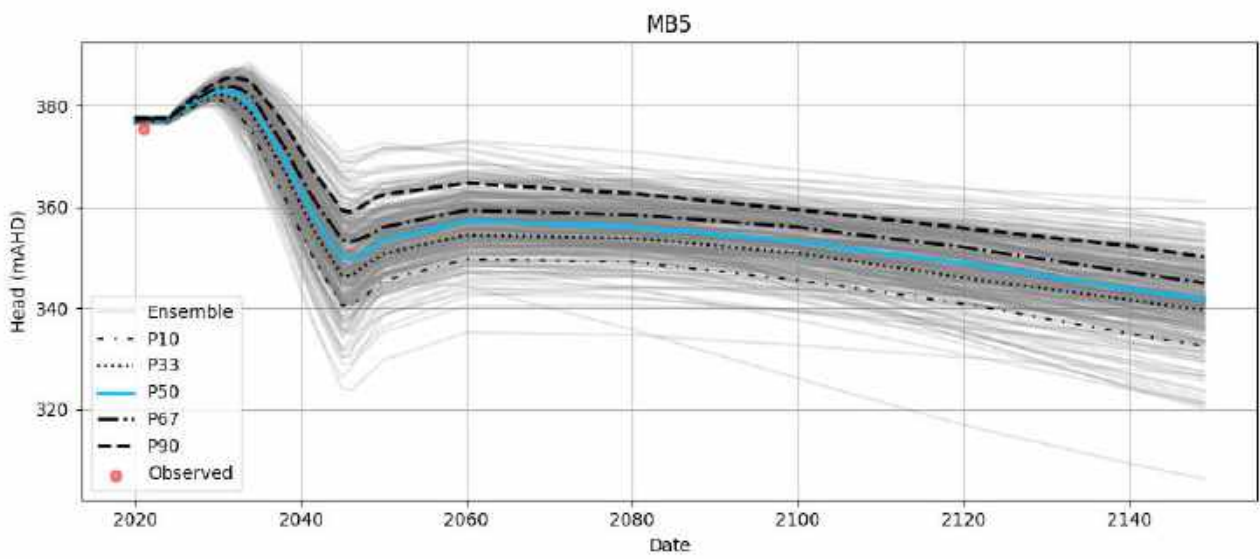
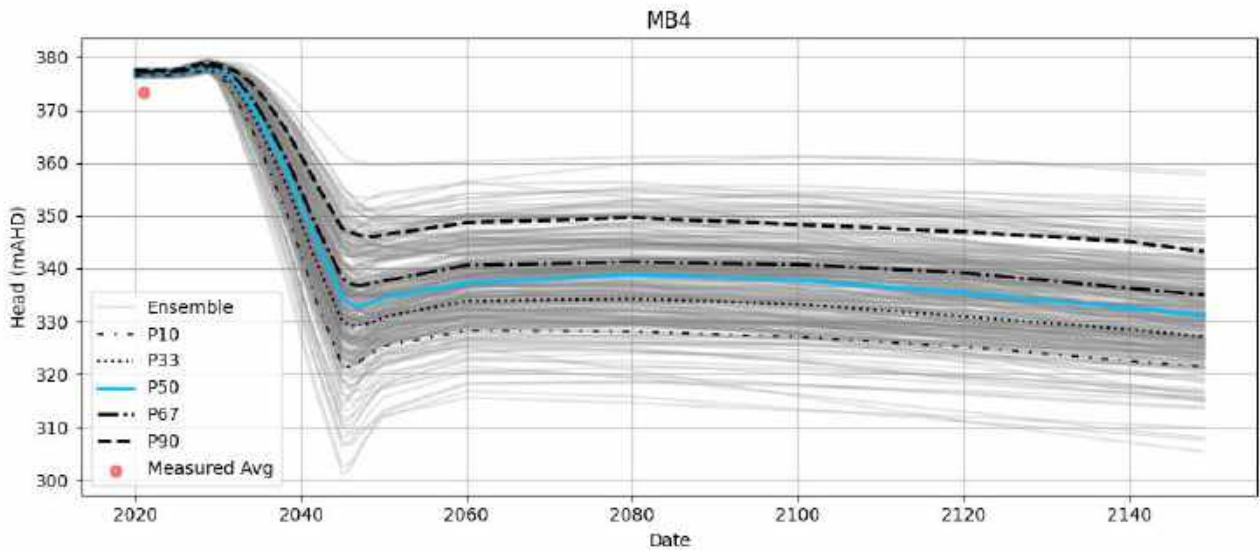
# Appendix A

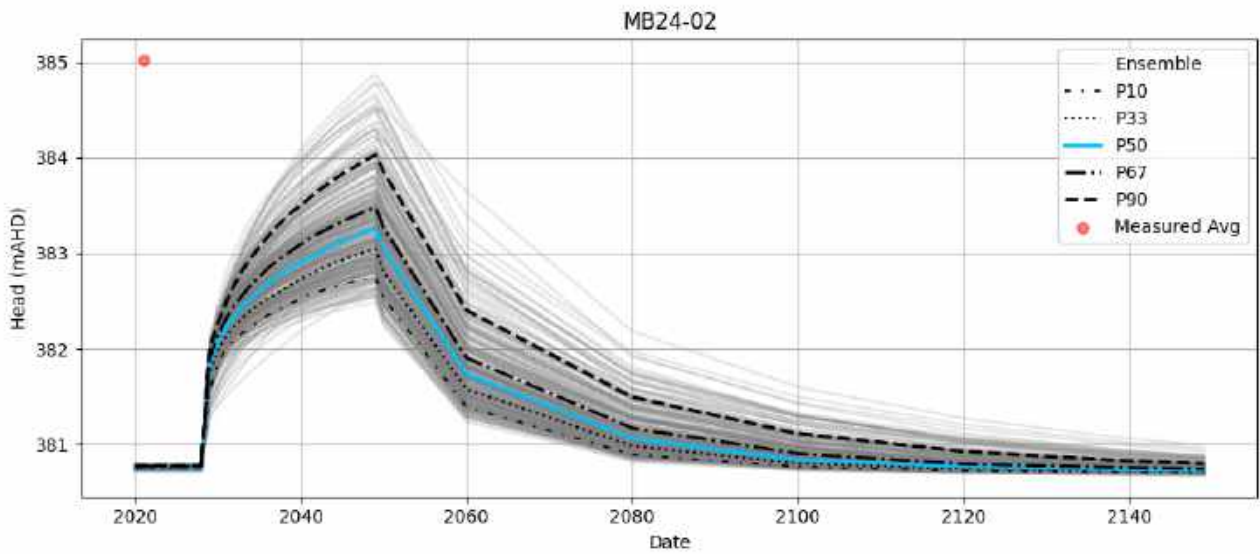
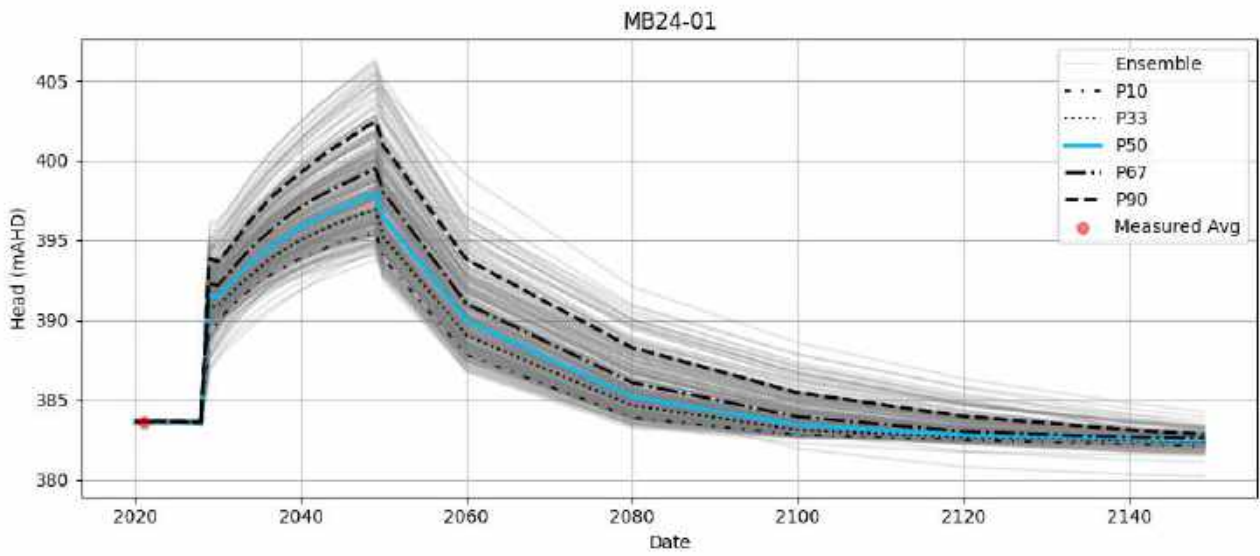
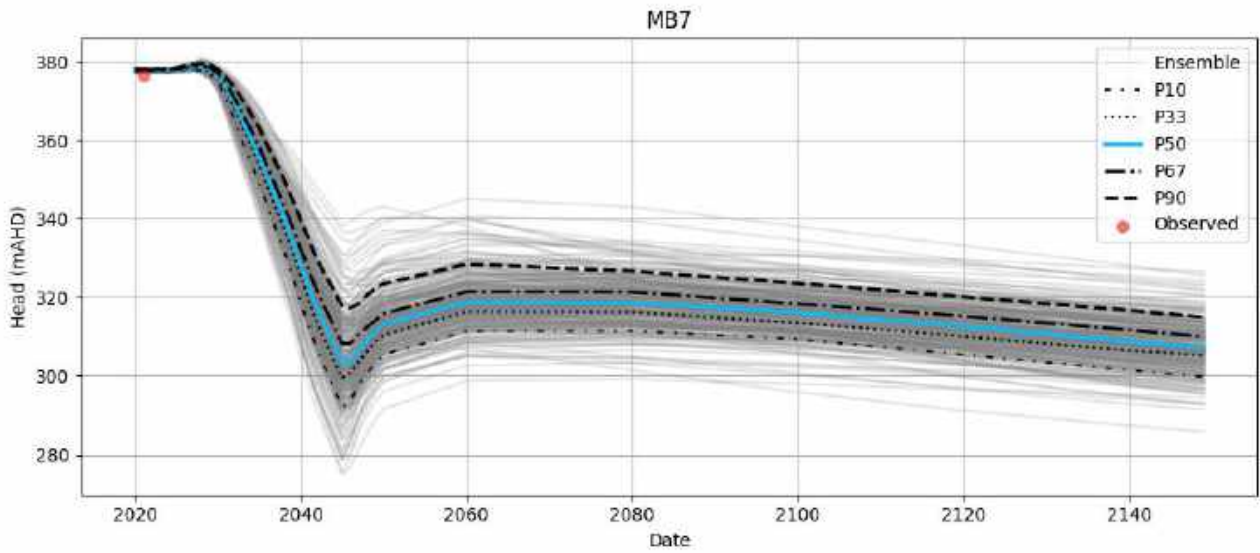
## Hydrographs

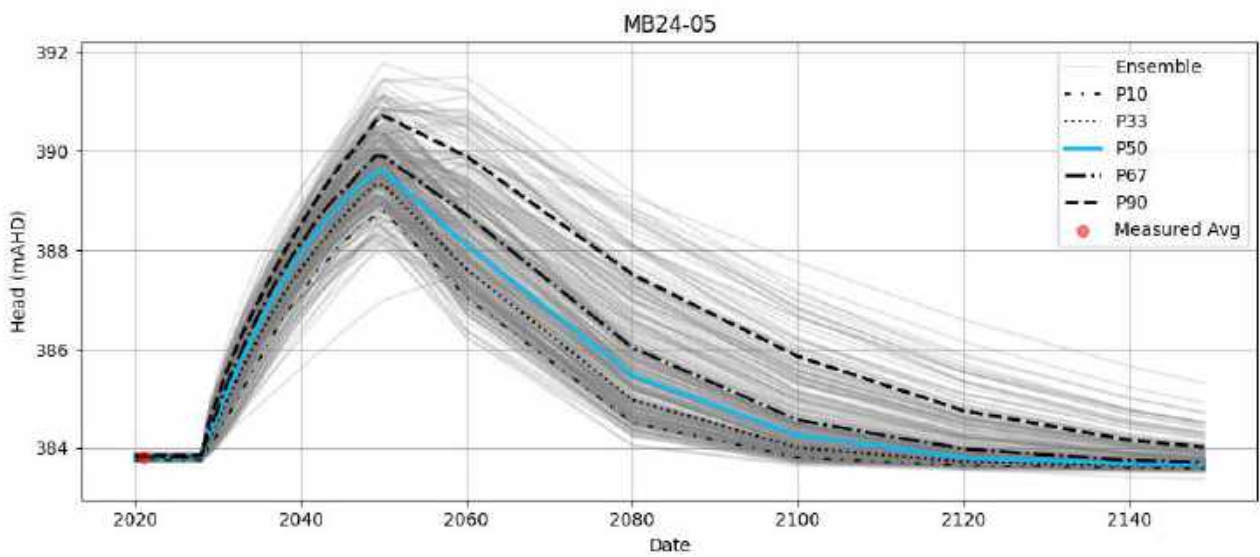
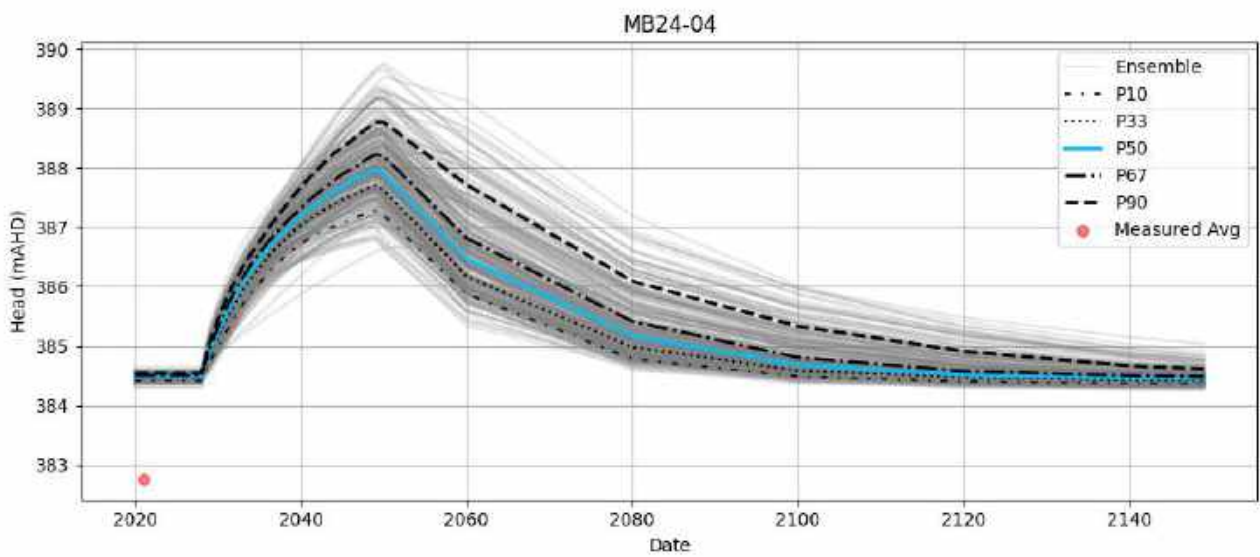
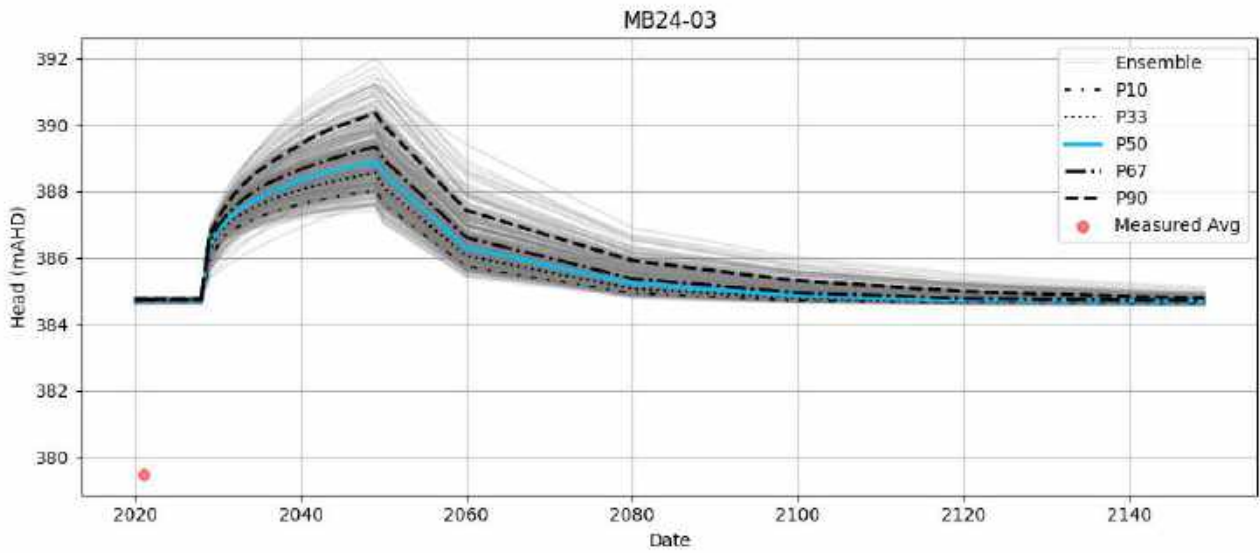
---

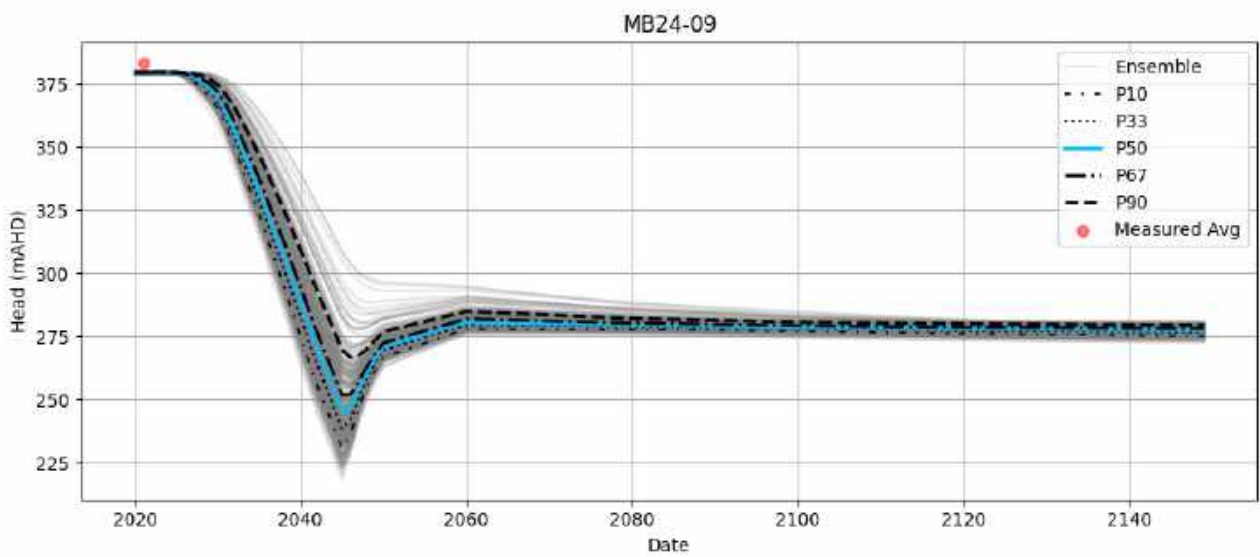
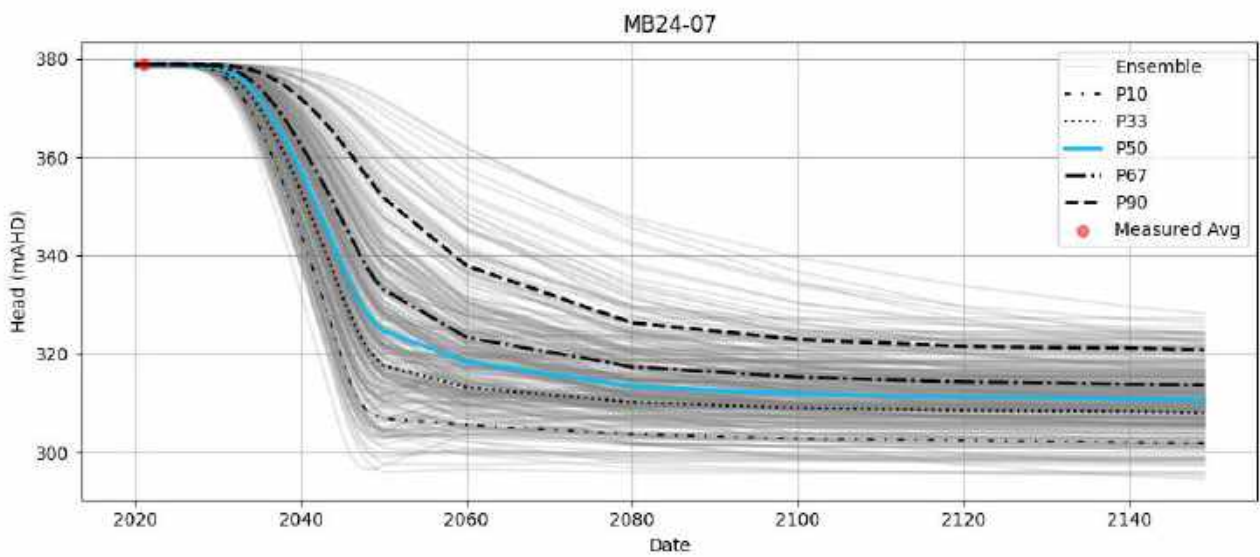
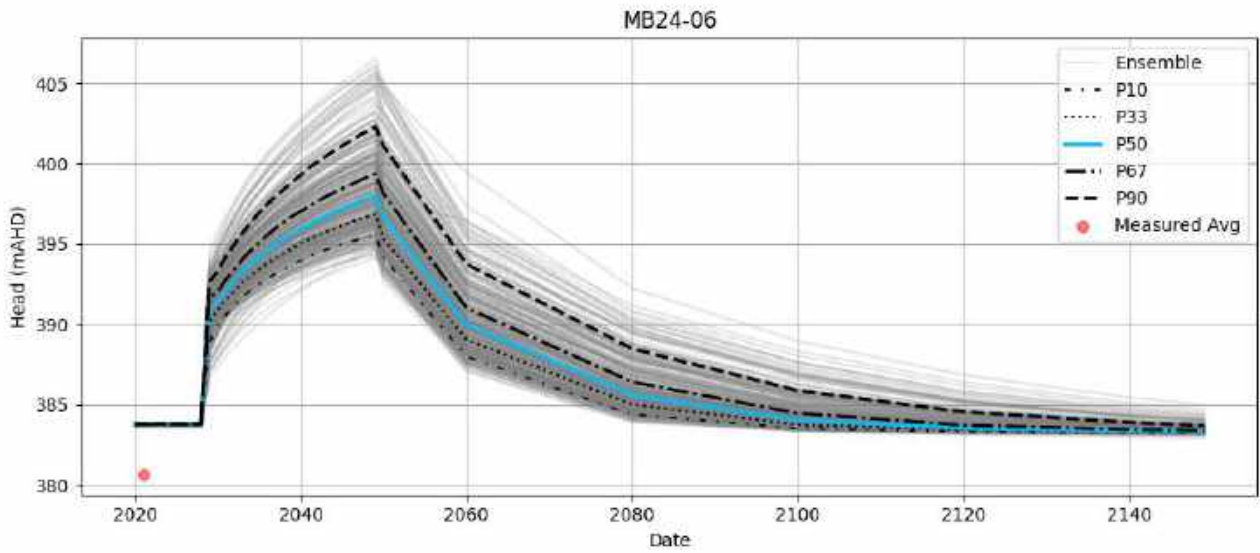




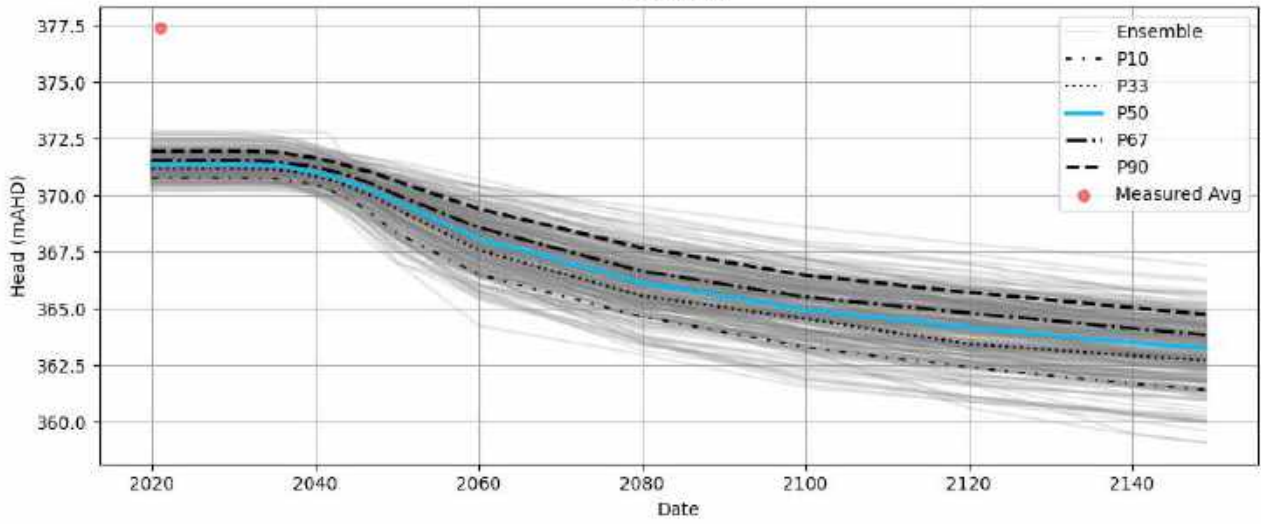








### MB24-10



## **Australia**

### **SYDNEY**

Level 10 201 Pacific Highway  
St Leonards NSW 2065  
T 02 9493 9500

### **NEWCASTLE**

Level 3 175 Scott Street  
Newcastle NSW 2300  
T 02 4907 4800

### **BRISBANE**

Level 1 87 Wickham Terrace  
Spring Hill QLD 4000  
T 07 3648 1200

### **CANBERRA**

Suite 2.04 Level 2  
15 London Circuit  
Canberra City ACT 2601

### **ADELAIDE**

Level 4 74 Pirie Street  
Adelaide SA 5000  
T 08 8232 2253

### **MELBOURNE**

Suite 9.01 Level 9  
454 Collins Street  
Melbourne VIC 3000  
T 03 9993 1900

### **PERTH**

Suite 3.03  
111 St Georges Terrace  
Perth WA 6000  
T 08 6430 4800

## **Canada**

### **TORONTO**

2345 Yonge Street Suite 300  
Toronto ON M4P 2E5  
T 647 467 1605

### **VANCOUVER**

2015 Main Street  
Vancouver BC V5T 3C2  
T 604 999 8297

### **CALGARY**

700 2nd Street SW Floor 19  
Calgary AB T2P 2W2



[linkedin.com/company/emm-consulting-pty-limited](https://www.linkedin.com/company/emm-consulting-pty-limited)



[emmconsulting.com.au](http://emmconsulting.com.au)